



CIVIL ENGINEERING STUDIES
Illinois Center for Transportation Series No. 12-022
UILU-ENG-2012-2025
ISSN: 0197-9191

THERMAL BEHAVIOR OF IDOT INTEGRAL ABUTMENT BRIDGES AND PROPOSED DESIGN MODIFICATIONS

Prepared By
Scott M. Olson
Kurt P. Holloway
Jason M. Buenker
James H. Long
James M. LaFave
University of Illinois at Urbana–Champaign

Research Report FHWA-ICT-12-022

A report of the findings of
ICT-R27-55
Instrumentation & Monitoring of Extreme Integral Abutment Bridges in Illinois

Illinois Center for Transportation

May 2013

Technical Report Documentation Page

1. Report No. FHWA-ICT-12-022		2. Government Accession No.		3. Recipient's Catalog No.	
4. Title and Subtitle Thermal Behavior of IDOT Integral Abutment Bridges and Proposed Design Modifications				5. Report Date May 2013	
				6. Performing Organization Code	
7. Author(s) Scott M. Olson, Kurt P. Holloway, Jason M. Buenker, James H. Long, and James M. LaFave				8. Performing Organization Report No. ICT-12-022 UILU-ENG-2012-2025	
9. Performing Organization Name and Address Illinois Center for Transportation Department of Civil and Environmental Engineering University of Illinois at Urbana-Champaign 205 N. Mathews , MC-250 Urbana, IL 61801				10. Work Unit No. (TRAIS)	
				11. Contract or Grant No. R27-55	
12. Sponsoring Agency Name and Address Illinois Department of Transportation Bureau of Materials and Physical Research 126 E. Ash St. Springfield, IL 62704				13. Type of Report and Period Covered	
				14. Sponsoring Agency Code	
15. Supplementary Notes					
16. Abstract The Illinois Department of Transportation (IDOT) has increasingly constructed integral abutment bridges (IABs) over the past few decades, similar to those in many other states. Because the length and skew limitations currently employed by IDOT have not necessarily been based on rigorous engineering analyses, an extensive 3-D parametric study has been performed, complemented by installation of field monitoring equipment on two recently constructed bridges, to potentially expand the use of IABs in Illinois. Some notable findings from this study include: (1) IAB configuration with extreme skew (> 60°) can perform well with proper detailing; (2) H-pile webs oriented parallel to the longitudinal axis of the bridge, regardless of skew, substantially reduces weak-axis bending; (3) compacted backfill reduces pile stresses; (4) live loads affect thermally induced pile stresses; (5) longer intermediate spans tend to increase pile stresses; and (6) time-dependent behaviors, such as concrete shrinkage, may significantly influence maximum pile stresses. Based on these findings, a more rigorously developed set of recommendations for maximum IAB lengths and skews in Illinois are proposed.					
17. Key Words integral abutment bridges, jointless bridges, design length, design skew, thermal bridge design, pile foundations			18. Distribution Statement No restrictions. This document is available to the public through the National Technical Information Service, Springfield, Virginia 22161		
19. Security Classif. (of this report) Unclassified		20. Security Classif. (of this page) Unclassified		21. No. of Pages 63 plus appendices	22. Price

ACKNOWLEDGMENTS AND DISCLAIMER

This publication is based on the results of ICT-R27-55, **Instrumentation & Monitoring of Extreme Integral Abutment Bridges in Illinois**. ICT-R27-55 was conducted in cooperation with the Illinois Center for Transportation; the Illinois Department of Transportation, Division of Highways; and the U.S. Department of Transportation, Federal Highway Administration.

The authors thank the members of the Technical Review Panel (TRP), and in particular the TRP chairperson, Mr. Gary Kowalski, and former TRP chairperson, Mr. William Kramer, for their guidance of the research and their insight into the issues related to designing, constructing, and numerically modeling integral abutment bridges. The members of the TRP included (listed alphabetically after the chair):

- Mr. Gary Kowalski (chairperson, IDOT)
- Mr. Dan Brydl (FHWA)
- Mr. Mark Gawedzinski (IDOT)
- Mr. David Greifzu (IDOT)
- Mr. Chad Hodel (WHKS)
- Mr. William Kramer (former chairperson, IDOT)
- Mr. Kevin Riechers (IDOT)
- Mr. Daniel Tobias (IDOT)

The contents of this report reflect the view of the authors, who are responsible for the facts and the accuracy of the data presented herein. The contents do not necessarily reflect the official views or policies of the Illinois Center for Transportation, the Illinois Department of Transportation, or the Federal Highway Administration. This report does not constitute a standard, specification, or regulation.

EXECUTIVE SUMMARY

The Illinois Department of Transportation (IDOT) has increasingly constructed integral abutment bridges (IABs) over the past few decades, similar to those in many other states. Throughout the United States, IABs are preferred over conventional bridge construction because they are generally cheaper and easier to construct; have lower maintenance costs because of reduced damage to bearings, expansion joints, and other conventional appurtenances; and will correspondingly enjoy longer service life spans. However, limitations on overall length and skew of IABs, as well as typical design details, vary considerably from state to state. Because the length and skew limitations currently employed by IDOT have not necessarily been based on rigorous engineering analyses, the project team has conducted an extensive 3-D parametric study, targeting typical IDOT IAB construction details and complemented by installation of field monitoring equipment on two recently constructed bridges, to potentially expand the use of IABs in Illinois. In conjunction with the parametric study, we performed an extensive literature review and corresponded with researchers and DOT officials from other states in the region for insight into other states' design and construction practices for IABs.

The 3-D parametric study focuses on identifying key interactions between the bridge superstructure, the abutment-foundation system, and the soil under thermally induced movements. This study builds on a previous effort at the University of Illinois that identified some of the key parameters influencing the overall behavior of IABs. By fully modeling a large assortment of IABs in three dimensions with varying lengths, intermediate spans, skews, pile types, and loading conditions, we obtained a more comprehensive picture of parametric influences on IAB behavior, particularly for skewed bridges.

The current 3-D numerical analyses have yielded numerous findings about the behavior of IABs subjected to extreme thermal loading. Some notable findings from these analyses are

- IABs with extreme skew of the abutments (e.g., 60°) show an additional increase in pile stresses compared with similar bridges with 40° skews, but this trend is generally not excessive. With proper detailing, even IAB configurations with extreme skew can perform well. Therefore, we recommend that IDOT not place any strict limitation on IAB skew and instead provide limitations that address the combined effects of length and skew.
- The current orientation scheme that IDOT uses for H-piles in IABs is unfavorable in skewed bridges because it permits excessive weak-axis bending. By revising the standard H-pile orientation to align all H-pile webs parallel to the longitudinal axis of the bridge, regardless of skew, substantially reduces weak-axis bending. As a result, lighter H-pile sections and/or greater IAB lengths may be possible in skewed bridges.
- The authors recommend use of compacted granular backfill behind the abutments. Except in bridges with extreme skews (beyond 45°), backfill pressures are beneficial to piles resisting thermal expansion. Furthermore, friction between the abutment and backfill plays an important role in resisting transverse abutment movements that are detrimental to pile performance in skewed bridges. Therefore, we recommend that details of drainage and other non-structural components at the abutment-backfill interface be evaluated to allow significant friction between the abutment and backfill to develop.
- Live loads affect thermally induced pile stresses by altering the amount of abutment rotation. While pile-head displacement remains virtually unchanged, the net change

in abutment rotation substantially modifies the pile-head fixity conditions. This increases pile-head loads under thermal expansion and relieves them during bridge contraction. Accordingly, thermal expansion combined with live loading is typically the critical load combination in IAB piles. Analyses also revealed that only a portion of the full HL-93 live load needs to be present to cause the majority of the change in abutment rotation. This indicates that the critical load combination likely will be reached in an extreme thermal event.

- Longer intermediate spans tend to increase pile stresses, but this effect varies with individual bridge configuration. Changes in intermediate span length are typically accompanied by changes to other parameters, such as girder cross-section and abutment height. Thus, these combined variables affect the stiffness and geometry of the IAB, and, by extension, the pile response.
- Some of our analyses corroborate other recent studies indicating that time-dependent behaviors, such as concrete shrinkage, may significantly influence maximum pile stresses for some IABs. Also, shrinkage may induce additional axial loads in the superstructure. Specifically, IABs using pre-cast, pre-stressed concrete I-beam (PPCI) girders may exhibit unusually high contraction displacements over the life of the bridge because of superstructure shrinkage. Therefore, we suggest that IDOT consider incorporating shrinkage and other significant time-dependent behaviors, such as concrete creep, pre-stress relaxation in concrete girders, and yearly increases in backfill pressure owing to cyclic compaction in any subsequent IAB research.
- Research and design practices in other states are increasingly demonstrating the effectiveness of using the plastic capacity of the foundation pile steel in IABs. Our parametric study reveals that in skewed bridges, there is a potential for substantial redistribution of loads over the pile group after the critical pile has started to yield. We recommend that IDOT reevaluate the potential benefits and risks of permitting limited plastic deformation in pile steel in its IAB design practice. Also, IDOT should incorporate some work assessing pile plasticity as a mechanism to further extend allowable IAB lengths and skews in Illinois as part of any additional IAB research programs.

As a final result of these analyses, a more rigorously developed set of recommendations for maximum IAB lengths and skews in Illinois was proposed. These recommendations apply to a wide set of commonly used H-piles and concrete-filled shell piles. When the full 3-D behavioral complexities were considered, numerous acceptable IAB length and skew combinations that did not induce stresses in the foundation piles above the steel yield stress were identified. However, to potentially expand the use of IABs to accommodate most of the applications desired by IDOT, further exploration of mechanisms that reduce pile moments may be necessary, such as allowing plastic hinging to occur in foundation pile sections. Additionally, the proposed permissible lengths and skews are based on the behavior of the piles under thermal loadings; accordingly, more evaluation of the performance of IAB abutments and superstructures is warranted to ensure that the detailing of the entire bridge system is adequate for the induced thermal loads.

TABLE OF CONTENTS

CHAPTER 1 INTRODUCTION	1
1.1 Overview	1
1.2 Problem Statement.....	2
1.3 Research Objectives and Scope.....	4
CHAPTER 2 LITERATURE REVIEW AND CURRENT STATE OF IAB PRACTICE	6
2.1 Iowa State University and Iowa DOT Research	6
2.2 University of Tennessee and Tennessee DOT Research	9
2.3 Utah Research on Pile-Head Fixity vs. Embedment	11
2.4 Recent Research on Time-Dependent Behavior in IABs.....	12
2.5 Purdue University and Indiana DOT Research	13
2.6 Review of ICT Research Report ICT-09-054 by Olson et al. (2009).....	14
CHAPTER 3 THREE-DIMENSIONAL NUMERICAL MODELING OF INTEGRAL ABUTMENT BRIDGES.....	16
3.1 Finite Element Model Construction	16
3.1.1 Model Development and Geometry	17
3.1.2 Loadings and Model Analyses.....	22
3.1.3 Model Limitations	26
3.2 Finite Element Model Behavior.....	27
3.2.1 Foundation Alignment with Primary Bridge Movements.....	28
3.2.2 Abutment Rotation and Softening of Superstructure Stiffness with Skew	29
3.2.3 Secondary Effects on Exterior Piles Caused by Transverse Thermal Behavior	31
3.3 Parametric Study Results and Discussion.....	32
3.3.1 General Trends Associated with Overall Length and Skew Variation	33
3.3.2 Concrete-Filled Shell Piles	36
3.3.3 H-Piles	39
3.3.4 Revised H-Pile Orientation	43
3.3.5 Compacted Sand Backfill	47
3.3.6 Live Loading.....	49
3.3.7 Intermediate Span Length	50
3.3.8 Time-Dependent Shrinkage Effects.....	51
3.3.9 Plasticity in Pile Steel	51

CHAPTER 4 INSTRUMENTATION AND MONITORING OF TWO ILLINOIS INTEGRAL ABUTMENT BRIDGES.....	52
4.1 General Instrumentation Scheme	52
4.2 Instruments and Data-Acquisition System Components	53
4.2.1 Vibrating Wire Strain Gages.....	53
4.2.2 Vibrating Wire Temperature Sensors	54
4.2.3 Micro-Electro-Mechanical Systems (MEMS) Tiltmeters	54
4.2.4 Linear String Potentiometers.....	54
4.2.5 MEMS Inclinerometers	54
4.2.6 Multiplexers.....	54
4.2.7 Data Loggers	54
4.3 Illinois Route 108 over Macoupin Creek.....	54
4.3.1 Bridge Details.....	54
4.3.2 Instrument Installation	55
4.3.3 Current Status.....	56
4.4 Peoria Airport Road over Kickapoo Creek and Union Pacific Railroad.....	56
4.4.1 Bridge Details.....	56
4.4.2 Instrumentation Installation	56
4.4.3 Current Status.....	57
CHAPTER 5 CONCLUSIONS AND RECOMMENDATIONS.....	58
REFERENCES	62
APPENDIX A TIME-DEPENDENT EFFECTS OF CONCRETE SHRINKAGE ON IAB BEHAVIOR.....	1
APPENDIX B EFFECTS OF PLASTIC DEFORMATION IN H-PILES ON IAB BEHAVIOR	1
B.1 Modeling of H-Pile Plasticity.....	1
B.2 Comparison of Plastic and Elastic Results	2
B.3 Incorporating Pile Plasticity in IAB Research and Design: Conclusions and Recommendations.....	9
APPENDIX C STRAIN GAGE INSTALLATION AND CALIBRATION DETAILS.....	1
C.1 Instrument Calibration	1
C.2 Strain Gage Welding Procedures.....	1
C.3 Inclinerometer Housing Installation	2
C.4 Laboratory Load Testing	2

CHAPTER 1 INTRODUCTION

1.1 OVERVIEW

Integral abutments bridges (IABs) are becoming increasingly common across the United States, including in Illinois. These bridges have been entering service in a number of states over the past few decades, and their considerable advantages are becoming more apparent. Even though many of the oldest IABs are not approaching the end of their intended useful life, state departments of transportation (DOTs) are realizing the benefits that these bridges provide in terms of lower initial construction costs, decreased maintenance costs, and longer projected service life spans.

In conventional bridges, girders sit on bearings that largely transfer only vertical load to the bridge abutments, and thermal expansion and contraction of the bridge is accommodated by expansion joints. Unfortunately, deterioration of these expansion joints, resulting from seasonal weathering (ice, road salts, and rain), traffic wear, jamming with debris, and other damage mechanisms, leads to corrosion in the bearings, girder ends, and even substructure elements of jointed bridges. In addition to repair or replacement of damaged expansion joints, corroded bearings, and other structural members, appurtenances in conventional bridges can become blocked and non-functional, inducing unintended thermal loads in the bridge, leading to further structural damage. Also, for complicated bridge geometries, typical simplifying assumptions about bridge thermal movement may inaccurately predict three-dimensional (3-D) behavior, leading to inadequate design and performance of bridge bearings and other appurtenances meant to accommodate movement (Wasserman 2011). In summary, conventional bridges with expansion joints lead to increased traffic disruption with lane shutdowns; more at-risk labor by highway workers; and of course, greater maintenance costs for state DOTs.

The chief difference between integral abutment bridges, or jointless bridges, and their conventional counterparts is the structural continuity of the bridge system. Instead of using expansion joints to accommodate thermal movements, IABs handle this directly through the transfer of thermally induced loads throughout the continuous structural system. The entire bridge moves as a unit; the superstructure with its deck and girders transfers loads to the abutments and the pile foundations. This structural continuity is achieved by the monolithic pouring of the abutment concrete with the bridge deck, the embedment (typically at least 1 ft) of the bridge girders into the abutment, and the embedment of the pile foundations into the abutment. All of these connections are semi-rigid, essentially forcing the bridge components to move together and transferring moments and horizontal forces in addition to vertical forces.

By eliminating the expansion joints, bearings, and other problematic features of jointed bridges, IABs enjoy significant comparative advantages. They are less susceptible to damage from corrosion because the continuity of the deck and abutment shields the girders, and to some extent, the substructure from harmful runoff. The lack of girder end bearings and other associated components automatically removes them as a source of design and maintenance problems, and simplifies initial construction. It is also worth noting that to achieve the flexibility needed to accommodate thermal movement in the pile foundations, IABs typically use only a single row of vertical piles, while comparable jointed bridges may use an additional row of vertical or battered piles. On average, an IAB will have fewer piles, leading to quicker, cheaper construction (Hassiotis et al. 2006). IAB construction is also usually faster and less expensive than conventional bridge construction because the formwork for the abutments is less complicated (Civjan et al. 2007), and the construction of intermediate piers typically does not require cofferdams (Hassiotis et al. 2006). Finally, with proper detailing, the structural continuity of IABs is well-suited to accommodate seismic loading (Frosch 2011). Thus, under extreme

loadings, IABs may afford greater ductility and redundancy than comparable jointed bridges. Taken together, the advantages offered by integral abutment bridge construction serve as a strong incentive to state DOTs to utilize them wherever possible.

1.2 PROBLEM STATEMENT

Like many states, the Illinois Department of Transportation (IDOT) is seeking to increase the use of jointless bridge construction to maximize the benefits described above. To confidently do this without significantly altering how IABs are constructed in Illinois, IDOT must improve its understanding of IAB behavior, particularly related to typical IAB details.

While the simple continuous construction of IABs offers the advantages described above, the coupled transfer of moments, forces, displacements, and rotations from the superstructure to the foundation and surrounding soil creates a complex soil-foundation-superstructure interaction problem. Given the 3-D nature of material behavior under thermal loading and the largely 2-D planar geometry of a bridge superstructure, IAB behavior is further complicated when considering the 3-D behavior of an entire bridge, particularly for complex bridge geometries involving high-skew angles, asymmetry, slope, or variations in soil resistance. Though significant research has been done on IABs in recent years, their behavior is not fully understood.

Historically, the use of integral bridges has grown and evolved relatively independently in individual states. Each state DOT that actively uses IABs has its own preferred design practices, restrictions on use, and typical details. Many states, including Illinois, currently rely on experience or empirical procedures to establish acceptable IAB overall lengths and skews. Some states with less IAB experience lean heavily on the provisions and details of neighboring states. These states' limitations on IAB use are typically fairly conservative (Olson et al. 2009), and thus the benefits they enjoy from integral construction may not be optimal. On the other hand, some state DOTs are leaders in IAB experience and research, and they have considerably more refined design and detailing provisions with more progressive guidelines for IAB length and skew. Because the detailing of the bridges varies in each state, the behavior of IABs also varies, and therefore specific results of research efforts using one state's typical details are not wholly transferrable to IABs in other states. Similarly, conditions and construction practices in any given state are not necessarily well-suited to adoption of another state's details.

As a result of the lack of concerted research and policy-setting efforts for IAB design in the United States, design philosophies, structural detailing, and restrictions on use of integral bridges vary considerably from state to state. No general consensus exists, even among state DOTs with leading IAB research efforts and practical experience, about best practices and limitations for integral bridge design. While new IAB research continues to shed light on general behavior and design improvements for these bridges that may be widely applicable, each state is currently faced with the challenge of optimizing its own details and improving its IAB use to maximize the benefits this type of construction offers.

Because the length and skew limitations for IABs currently used in Illinois have not been based on rigorous engineering analyses, but rely on empirical procedures that have not been recently revised, they warrant further study and evaluation. Increased knowledge of Illinois IAB behavior provides IDOT with a rational basis and greater confidence for revising current guidelines limiting the overall length and skew of these structures, thereby increasing the use of integral bridge construction in the state.

Figure 1 illustrates some of the primary features of IAB construction in Illinois, as contained in the IDOT *Bridge Manual* (2009). IDOT typically pours a pile cap over the foundation piles, embedding them 2 ft 0 in. into the concrete, then supports either pre-stressed

pre-cast concrete or steel girders on the pile cap. The girder type and size is selected based on the bridge's overall geometry and loading. Once the girders are secure, the abutment diaphragm is poured monolithically with the deck slab, surrounding the girder ends and creating a semi-rigid connection upon hardening. Note that IDOT usually corbels the back face of the abutment to facilitate end support of an approach slab.

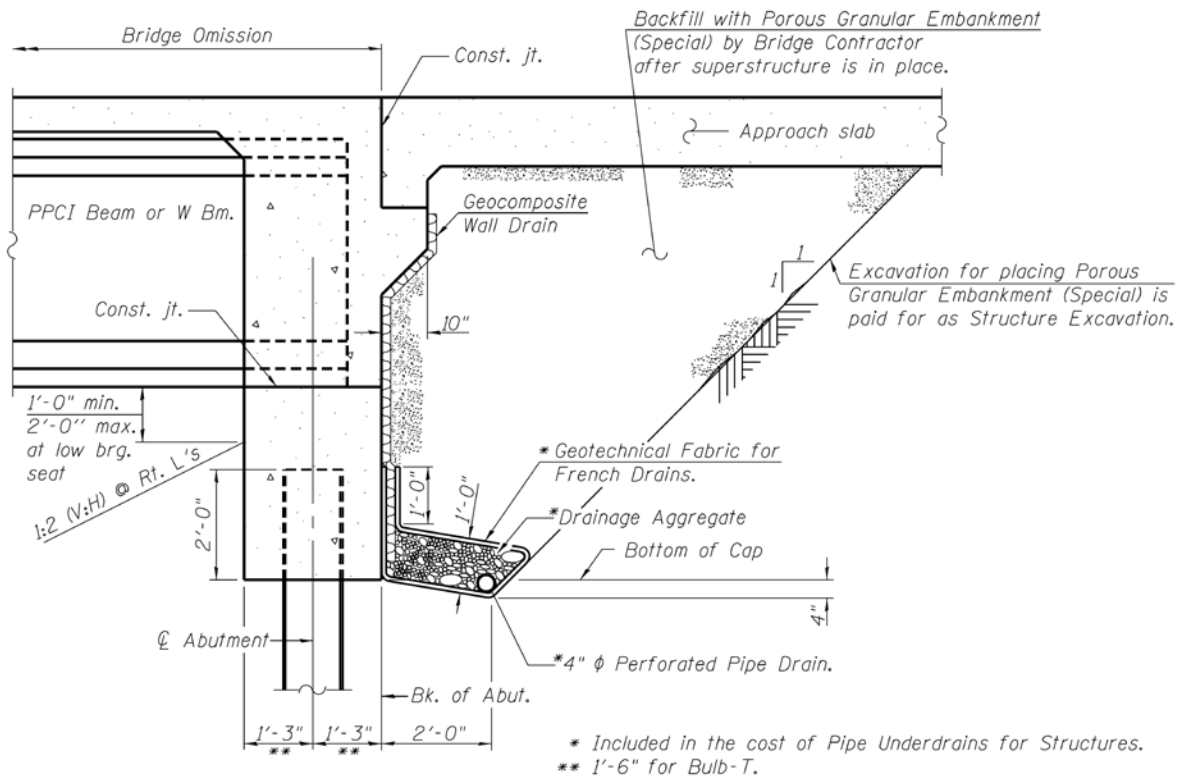


Figure 1. General IDOT integral abutment detail (adapted from IDOT *Bridge Manual*, 2009 edition).

It is appropriate to mention here a few other details about IDOT IAB construction. The two types of piles used frequently in Illinois to support IABs are steel H-piles and concrete-filled steel shell piles. The H-piles are oriented with the web of the cross-section perpendicular to the face of the abutment. Also, H-piles are typically driven into holes that are pre-drilled to a depth of 3 ft 0 in. and then a concrete encasement with welded wire reinforcement mesh is placed around them. The wire mesh extends approximately 10 in. into the bottom of the abutment. Concrete-filled shell piles have no concrete encasement, but are substantially reinforced with a spiral reinforcing cage in the top 7 ft 0 in. of the pile (the reinforcement extends 5 ft 0 in. below the bottom of the abutment). Figure 2 illustrates these typical IDOT connection details for H-piles and shell piles at the pile-abutment interface.

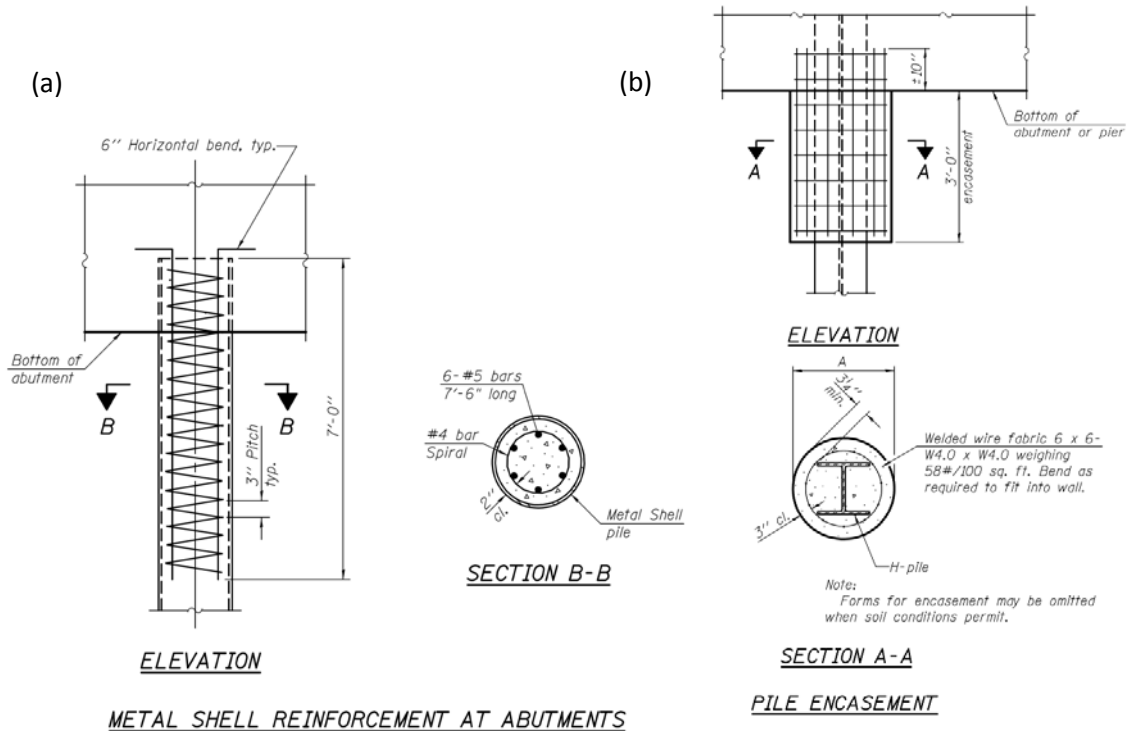


Figure 2. Typical IDOT pile-abutment connection details: (a) Concrete-filled metal shell piles, (b) H-piles (adapted from IDOT *Typical Detail Drawings* F-MS and F-HP 2010).

Finally, since publication of the 2009 edition of the *Bridge Manual*, IDOT is considering implementing a number of design revisions, some of which were recommendations from a previous study by Olson et al. (2009). If implemented, all integral abutments will be at least 3 ft 0 in. thick.

Currently, IDOT policy establishes prescriptive limits on overall length and skew for IABs, along with select parameters. To exceed these limits, bridge designers must seek approval from the Bureau of Bridges and Structures. For all IABs, the maximum permissible abutment skew is 30°. Steel girder IABs may have a maximum overall length of 310 ft, and all-concrete bridges may be up to 410 ft long. There are no explicit restrictions on the spacing of intermediate piers or the length of spans in the end bays. However, IDOT does specify that a tangent alignment must be used (curved girders are not permitted), and that the abutments and piers must be parallel (IDOT *Bridge Manual*, 2009 edition).

1.3 RESEARCH OBJECTIVES AND SCOPE

IDOT engaged the project team to perform a comprehensive numerical parametric study of IAB behavior, incorporating typical IDOT design details. Additionally, this study included instrumenting two IABs recently constructed in Illinois to facilitate long-term monitoring to eventually validate the numerical models used and provide further insight into IAB behavior. This current study builds on a previous study at the University of Illinois (Olson et al. 2009) to develop a more comprehensive, rigorous understanding of IAB behavior as a basis for growing the use of IABs in Illinois and elsewhere.

A primary focus of this study is on the behavior and loadings generated in the substructure and pile foundations of integral abutment bridges resulting from thermal expansion

and contraction. While the current study considers the whole-bridge system, we devoted special attention to the substructure and foundation because they are critical bridge components for determining feasible lengths and skews (Olson et al. 2009).

The scope of work for this project includes

- Thorough review of recent literature regarding IAB use and performance, including in-depth interviews with several regional DOT bridge officials and researchers to gain perspective on differing IAB design and research philosophies.
- Implementation of the instrumentation plan set forth in the previous ICT report (Olson et al. 2009) for two recently constructed Illinois IABs.
- Extensive 3-D numerical study of full-bridge models to examine the influence of competing and compounding parametric trends on global and localized IAB behaviors, understand current design demands and limitations, and explore methods to expand IAB use in Illinois.

CHAPTER 2 LITERATURE REVIEW AND CURRENT STATE OF IAB PRACTICE

In recent years, the body of research on integral abutment bridges has matured significantly. Building on the work of Olson et al. (2009), the authors conducted an additional review of literature concerning IABs at the outset of this project to inform and guide them as they prepared the analytical and field experiments in this project. By critically examining prior studies of integral bridges, the research team not only generated new ideas about how to build upon successful earlier work but also observed limitations and shortcomings of previous analytical and experimental programs. The research team continued to review additional relevant IAB research throughout the project to corroborate observations and preliminary results of our study as they became available and provide insight into other research avenues. These will be discussed further in later sections of this report.

Because of the wide variability in the application and detailing of integral abutment bridges and the increasing amount of research being targeted at these structures worldwide, the research team focused their effort on recent studies of integral bridges in the United States, particularly states with similar soil and climate conditions to Illinois that utilize similar construction details. Among the states with significant integral bridge research programs, differences in IAB detailing are often attributed to specific study findings. However, just as often the differences may arise because of preferences of the state bridge design agency attributed to field experience. To complement the literature search, the authors contacted leading researchers and state bridge officials to obtain their perspectives on design and detailing approaches. As a result, this study has benefited significantly from insights gained from conversations with researchers and bridge officials in the states of Iowa and Tennessee.

The following synopsis highlights important information about IAB behavior gained from our exploration of the current state of IAB literature and practice. Several topics examined here were vital in shaping our approach to the current work scope; others were helpful in interpreting our results and formulating our conclusions and recommendations to IDOT.

2.1 IOWA STATE UNIVERSITY AND IOWA DOT RESEARCH

The state of Iowa is a leader in both the use and research of IABs. As an immediate neighbor of Illinois with similar climate and soil conditions, Iowa's approach to design and detailing of IABs is relevant. Furthermore, Iowa revised its own prescriptive limitations on overall IAB length and abutment skew in 2002. These revised limits permit approximately 90% of all overhead roadway bridges in Iowa to be designed with integral abutments (Dunker and Abu-Hawash 2005). Like Illinois, Iowa relies on prescriptive limits for IAB length and skew because a significant portion (roughly 50%) of its bridges are contracted to design firms (Dunker 2011).

The relatively recent bridge policy changes by the Iowa DOT were part of the culmination of an extensive research program conducted at Iowa State University beginning in the 1980s. The final technical report by Abendroth and Greimann (2005) summarized a number of recent Iowa State studies and documents the state of practice for Iowa IABs.

Iowa's detailing of IAB foundations is markedly different from IDOT's, and is based on a wholly different design philosophy. While Illinois seeks to avoid yielding in IAB piles, Iowa relies on it. In fact, the fixed-head equivalent cantilever pile model employed in Iowa IAB analysis assumes plastic hinges form at the connection to the pile cap and at the depth of fixity, as shown in Figure 3.

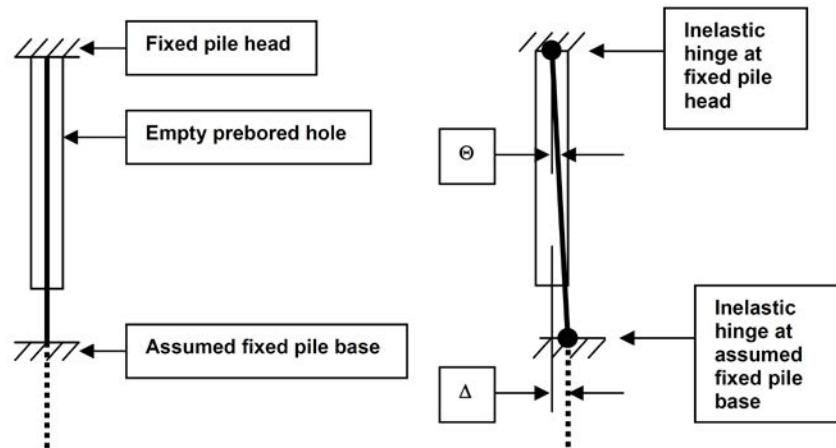


Figure 3. Fixed-head equivalent cantilever pile concept (adapted from Dunker and Abu-Hawash 2005).

Iowa IAB piles are typically driven in holes pre-drilled to a minimum depth of 10 ft and backfilled with bentonite slurry. The bentonite is assumed to provide no resistance to lateral pile movement and no local restraint to H-pile flanges. Iowa orients its H-piles with the webs parallel to the abutment longitudinal axis in bridges with skews of 30° or less. For more highly skewed bridges, the H-pile webs are perpendicular to the centerline of the roadway. In all cases, the majority of bending in the H-piles is in the weak-axis orientation. The primary objective of permitting pile plastic hinging is that once it occurs, the only additional moments induced in the piles from thermal loading are the second-order P- Δ effects of the axial loads, as shown in the illustration of the AASHTO load group I and IV conditions in Figure 4.

This hinged Iowa model relies on the assumption that the longitudinal pile strains at the hinges are treated as residual strains and therefore do not affect the pile strength. This approach substantially relieves the moment developed in the pile for a given displacement, and it provides sufficient flexibility in the structure to greatly increase the allowable IAB length compared with design based on elastic pile behavior. However, this requires that other failure (inelastic) mechanisms be considered. Specifically, when designing H-piles for IABs, Iowa considers pile fatigue and flange local buckling (Dunker and Abu-Hawash 2005). Iowa State University research has emphasized the effects of these plastic failure mechanisms, recognizing the potential for fatigue damage to reduce the flange local buckling capacity. Pile ductility under cyclic loading is a key consideration for assessing the length limits for IABs; fatigue damage reduces the inelastic rotational capacity of the pile, causing flange local buckling to occur prematurely. In short, the problem of pile capacity for Iowa IABs is approached as a beam-column interaction, with modifications to the interaction equations and special compact section criteria applied to avoid problems with flange local buckling and fatigue. The selection of a weak-axis bending orientation for H-piles is similarly driven by the desire for increased inelastic rotational capacity before the flange local buckling limit state is reached (Abendroth 2011).

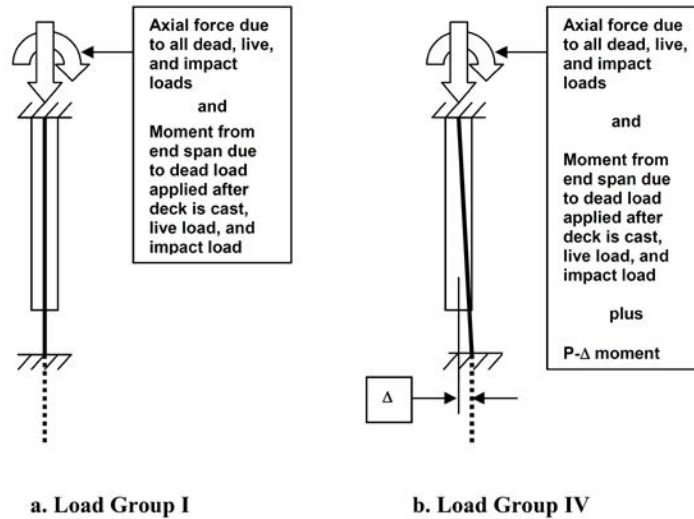


Figure 4. Loading in the fixed-head equivalent cantilever model (adapted from Dunker and Abu-Hawash 2005).

Much of the theory driving concerns about fatigue and flange local buckling affecting beam-column performance is based on a series of laboratory tests on beam-columns conducted by Lukey and Adams (1969). By pre-drilling pile holes to at least 10 ft and backfilling with these holes with bentonite, the Iowa DOT introduces a great deal of flexibility into the IAB structure, permitting longer bridges by relying on plastic hinging. However, the trade-off is a lack of confinement around the upper portion of the pile that could substantially resist the tendency of the pile flanges to buckle under combined axial and bending loads. Being limited by beam-column interaction equations that are further constrained to avoid fatigue issues, the Iowa DOT may not be fully utilizing the capacity of the piles to accommodate thermal movements.

Another important aspect of Iowa's prescriptive limits for IAB length and skew is that they are based upon a 2-D, single-pile model with conservative soil assumptions (Dunker and Abu-Hawash 2005). The 2-D Iowa model used to generate the prescriptive limits in its bridge manual incorporates the effect of differing coefficients of thermal expansion between steel and concrete materials to calculate longitudinal bridge movements. It also accounts for the primary bending stiffness of the superstructure, as determined by the girder and end span geometry, in determining the amount of rotation the abutment will undergo (Dunker 2011), but the model does not address other components of the structural stiffness in assessing the thermal movements of a bridge. In other words, Iowa's provisions do not account for 3-D thermal effects in IABs, which is the primary aspect of the current study. While Iowa does penalize permissible IAB length with increasing abutment skew, this is not based on 3-D displacements of the entire bridge but rather is driven by recognition that skew increases biaxial bending in the piles, exacerbating the tendency to exceed column stability limit states, particularly flange local buckling. Abendroth and Greimann (2005) highlight a non-linear, non-closed form relationship between permissible bridge length and skew in their final report, but this is based solely on detrimental effects to the column interaction behavior, not superstructure movement patterns.

The Iowa State research team did perform some 3-D finite element (FE) modeling of IABs that were part of their experimental monitoring program, but they did not explore parametric variations with the 3-D models. Additionally, the 3-D models only moderately agreed with the recorded field performance for the case study bridges, primarily as a result of the

complexity of IAB behavior and field conditions (Abendroth and Greimann 2005). This is a common shortcoming in many studies incorporating 3-D FE modeling of field-monitored bridges. Case studies of individual bridges using FE models often poorly capture field conditions, and little insight is gained into parametric trends in IAB behavior.

In our discussions with K. Dunker (Master Engineer, Office of Bridges and Structures, Iowa DOT) and R. Abendroth (Associate Professor, Iowa State University), both acknowledged the importance of this tendency for real IAB behavior to differ from that predicted in research or design. In fact, while Iowa's typical pavement joint details permit up to 3 in. of movement at the bridge ends, the DOT limits theoretical or design displacement of IAB piles to 1.55 in. Because experience has shown that even theoretically symmetric IABs often demonstrate tendencies to move disproportionately toward one direction once erected in the field, Iowa seeks to prevent pavement joint damage by allowing for the possibility that a given IAB may experience the vast majority of its thermal movement at one abutment end. It is possible that with enhanced accuracy in predicting 3-D asymmetric thermal movements, or pavement joints that provide greater ranges of motion, IAB lengths could be considerably increased in Iowa.

2.2 UNIVERSITY OF TENNESSEE AND TENNESSEE DOT RESEARCH

Tennessee has widely explored the versatility of IABs and has aggressively pursued integral bridge construction over the past 50 years, continually learning from previous experience to build ever-longer jointless structures. The driving force behind this concerted effort by the Tennessee Department of Transportation (TDOT) is simply expressed in a mantra voiced by the Structures Division's leadership, "The only good joint is no joint," (Burdette 2011). Edward Wasserman, Director of TDOT's Structures Division, elaborated that it is harder to achieve satisfactory performance from skewed (or even curved) conventional bridges than from continuous construction. E. Wasserman indicated that particularly for complex bridge geometries, predicting the thermal behavior is virtually impossible; the conditions in the field are more nuanced than what can be considered in design. As a result, bearings and appurtenances for conventional bridges experience more problems and damage than integral abutment bridges, even in complicated geometries. While some minor cracking may occur in IABs at interfaces caused by differential movements (e.g., at the wingwalls), TDOT expects this and is willing to accept incidental cracks as a trade-off for the significant benefits offered by integral construction. Generally, no significant cracking has been observed at major structural components of IABs such as the abutment backwall. The end result is that Tennessee designs all bridge structures with as many integral components as feasible, including not only abutments, but also intermediate piers in many cases (Wasserman 2011).

Tennessee has no explicit limits on IAB length or skew; each bridge design is unique owing to the specific site, road, and other conditions. This is manageable because Tennessee conducts over 95% of its bridge design in-house, compared with the high percentage of bridge designs contracted to design firms in other states such as Iowa and Illinois. Nevertheless, TDOT generally recognizes limits on lateral pile movement of 2 in. to 2½ in. and 1 in. in either direction for H-piles and concrete friction piles, respectively. However, these limits on pile movement do not strictly translate into prescriptive limitations or even guidelines for integral bridges. This is due to TDOT's recognition of the complexity of IAB behavior; by acknowledging this in design, a far greater number of their bridges can be built integrally. Innovative IAB design that pushes the limits of traditional applications requires an element of design freedom, which is more easily managed in TDOT's in-house design context (Wasserman 2011).

While the climate and soil conditions in Tennessee differ from those in Illinois, the typical details used in TDOT IABs are relatively close to IDOT's. Tennessee does not pre-drill holes for its piles; the embankment soil surrounds the piles throughout their depth, up to the pile cap. This

is structurally similar to Illinois construction, where (at most) a short concrete encasement is poured around the top of H-piles. Unlike Iowa, which primarily uses a weak-axis, H-pile orientation, Tennessee orients the webs of its H-piles parallel to the longitudinal axis of the IAB, regardless of skew. TDOT prefers this orientation because, within the elastic range, it generates lower maximum H-pile stresses at a given thermal displacement and may reduce potential for localized concrete crushing within the abutment at the pile/abutment interface, compared with a weak-axis orientation. However, like Iowa, Tennessee expects significant plasticity at the pile-abutment interface during an extreme thermal cycle and accounts for it in design (Wasserman 2011). This is a key difference in IAB design approach from the current IDOT standard to prevent yielding in pile steel.

In recent years, Tennessee sought to formally corroborate its experience-led growth in IAB use with research. As a result, the University of Tennessee at Knoxville conducted a significant research program incorporating numerous full-scale tests of both H-piles and concrete friction piles, the two most commonly used IAB piles in the state. The University of Tennessee studies, led by Edwin Burdette, were completed in two phases. The initial study, completed in December 1999 (Burdette et al. 1999), focused on H-piles, while the second study, published in 2003 (Burdette et al. 2003), addressed concrete friction piles. Together, these studies verified the performance of the pile and abutment details being used across Tennessee, and propelled further innovation in IAB design. Burdette noted that generally, in H-piles, failure occurred because of cracking in the abutment and a loss of integrity at the abutment-pile interface, while with concrete friction piles, the 12 in. of embedment into the abutment was able to generate the full strength of the pile, which failed first (Burdette 2011).

Both studies incorporated a series of full-scale field load tests, verified by numerical analyses, simulating piles supporting IABs under varying soil conditions. A combination of axial and lateral load was slowly applied to the piles to mimic seasonal thermal cycles until failure resulted. Because Illinois chiefly uses H-piles in its IABs, the results of the first study are more relevant to Illinois. Some key findings of the H-pile load tests were

- The axial load carrying capacity of the H-piles was virtually unchanged under extreme lateral loadings, and traditional beam-column interaction equations such as those in AASHTO and AISC do not apply to H-piles confined by soil. The vertical support behavior of piles exceeds that predicted by such equations. The piles in the study were able to develop plastic bending moments under axial load up to and in excess of the theoretical strong-axis cross-sectional maximum capacity of the steel without any loss of stability. Despite yielding and even local buckling of the compression flanges in some of the H-piles, the surrounding soil provided enough confinement to prevent any reduction in column stability and vertical load capacity. No column buckling failure modes are possible; this sharply contrasts with the assumptions used in design of Iowa IABs.
- While tests with 1-ft pile embedment showed complete adequacy for the levels of displacement desired by TDOT, a test on a pile with 2-ft embedment into the abutment demonstrated significantly enhanced capacity for lateral deflection under axial load without any loss of structural integrity (up to 4.3 in. in very stiff clay) (Burdette et al. 1999). It is notable that the test abutments were intentionally restrained from rotating during the tests; this was done to represent the rotational fixity applied to the abutment by the IAB superstructure. Because the abutments were restrained, the pile-abutment interface results are essentially for a fixed-head condition (Burdette 2011). The Burdette et al. (1999) results are therefore conservative compared with real IABs that experience a limited amount of abutment rotation and a corresponding reduction in pile-head fixity.

The results from Burdette et al. (1999) are of particular interest to Illinois because current IDOT standards and length limitations could benefit from this research. Burdette et al. (1999) strongly implied that the 2-ft pile embedment typically employed by IDOT would maintain integrity for H-piles deformed well into the plastic range with no loss in column stability. The stability in the region of maximum pile moments (the top of the pile) may be even more confidently assured by the presence of the 3-ft concrete encasement of each H-pile below the top of the pile cap. The pile cannot behave in a normal beam-column interaction manner because it is confined.

Furthermore, Tennessee has refined its design methodology to capitalize on the research of Burdette et al. (1999). A 2-ft embedment is now commonly used in TDOT IABs to avoid localized cracking at the abutment-pile interface and permit larger maximum lateral pile displacements. The strong evidence against typical column interaction behavior in IAB H-piles affirmed TDOT's continued use of these piles with their webs parallel to the direction of the roadway, maximizing the proportion of strong-axis bending. According to E. Wasserman (2011), strong-axis bending promotes lower internal bearing stresses of the pile tip against the abutment concrete, permits more pile movement before the initiation of yielding (leading to fewer thermal cycles that induce yield), and a smaller proportion of the member above the yield stress at a given displacement. Finally, Tennessee is only marginally concerned about fatigue in IAB piles, as several IAB foundations that have been exhumed have shown no evidence of fatigue damage (Wasserman 2011).

As an anecdote to describe IAB performance, E. Burdette (2011) described the 1,175-ft, curved, sloped bridge of State Route 50 over Happy Hollow Creek as follows, "it just seems to breathe." This phrase provides a fitting description of the ability of IABs to shift and respond to external stimuli throughout the structural body, rather than in separate, isolated member responses. As observed later in the numerical analyses performed for this study, this ability of IABs to perform well through whole-structure response is strongly 3-D, and as illustrated by TDOT experience, the benefits of integral construction are enhanced when plasticity is selectively permitted in the structure.

2.3 UTAH RESEARCH ON PILE-HEAD FIXITY VS. EMBEDMENT

A recent study from the state of Utah (Rollins and Stenlund 2010) addressed the extent of pile-head fixity in the pile-abutment connection. Rollins and Stenlund (2010) focused on how variations in embedment depth and connecting steel reinforcement in concrete-filled shell piles influenced the degree of fixity at the pile-pile cap interface. Rollins and Stenlund (2010) performed numerical analysis and full-scale tests of four 2-pile groups with different amounts of rebar and pile embedment depths to explore the relationship of the connection detail to lateral load response.

Their findings strongly indicated that even concrete-filled shell pile connections with embedments as shallow as 6 in., which are widely regarded as pinned in design, demonstrate significant fixity so long as they have a reinforcing cage spanning the interface between the pile and the cap. Such connections can develop moments of at least 40% to 60% of the moment capacity of the pile, and this estimate may be conservative owing to the fact that axial pile pullout failure occurred in the shallow-embedment test specimens prior to connection failure. An analysis based simply on embedment length to establish connection capacity is inadequate even for shallow embedments when significant reinforcement exists; under established connection shear and moment capacity equations, both of the shallow-embedment specimens should have experienced connection failure before the termination of the test. However, this did not occur. Significant moments developed in both the 6 in. and 12 in. embedment specimens.

This observation demonstrates that it is difficult to design an embedded pile connection that is truly pinned (Rollins and Stenlund 2010).

Rollins and Stenlund (2010) also tested a shell pile with a 24-in. embedment without any reinforcing steel across the pile-pile cap interface. This specimen showed better load-deflection performance than reinforced shallower connections and did not experience any signs of connection failure during the lateral load test. With sufficient embedment, a concrete-filled shell pile connection can develop the full moment capacity of the pile, even without reinforcement (Rollins and Stenlund 2010).

Overall, Rollins and Stenlund (2010) illustrated that for the analysis of Illinois IABs, a truly fixed interface is an appropriate representation of the pile-to-abutment connection, particularly because IDOT's shell pile detail incorporates a 24-in. embedment with significant reinforcement. Combined with results from Burdette et al. (1999), this strongly suggests that IDOT's H-pile details provide a fixed interface (i.e., a fixed-head pile condition). Thus, the primary question of IAB pile capacity is more related to the actual loads developed at the top of the pile under the fixed interface, rather than the interface itself.

2.4 RECENT RESEARCH ON TIME-DEPENDENT BEHAVIOR IN IABS

Awareness of time-dependent behaviors and their potential effects on IAB performance has increased in recent years. Studies have identified two main time-dependent behaviors in IABs: (1) backfill soils behind the abutments may be prone to time-dependent changes in their resistance with cyclic load; and (2) concrete components of an IAB superstructure are prone to substantial shrinkage effects (Hassiotis and Xiong 2007; Fennema et al. 2005; and Kim and Laman 2010).

Hassiotis and Xiong (2007) performed a 4-year field study monitoring an IAB in New Jersey. The researchers observed that the backfill pressures behind the abutments regularly increased with yearly thermal cycles. The majority of this increase occurs as a result of densification of the backfill under seasonal and daily abutment movements during the first few years after an IAB enters service. During the study, Hassiotis and Xiong (2007) observed that the passive soil pressure buildup substantially slowed after the initial period of increase and appeared to reach a steady state of behavior.

Another potentially important time-dependent behavior present in IABs is the shrinkage of their concrete components, particularly in the superstructure (Fennema et al. 2005, Kim and Laman 2010). Though virtually all IABs in Illinois experience shrinkage of the cast-in-place bridge deck, substantial shrinkage may also occur in PPCI girders when used for IABs. Shrinkage has a significant effect on IAB behavior because the continuity of the system causes the shrinking components to impose forces and displacements on the remainder of the structure.

Recent studies led by Pennsylvania State University (Fennema et al. 2005; Kim and Laman 2010) used a combination of field monitoring and numerical modeling to explore long-term IAB behaviors. In addition to noting the presence of increasing backfill pressures behind abutments, Penn State researchers (Fennema et al. 2005; Kim and Laman 2010) explored the combined effects of concrete creep and shrinkage along with PPCI girder pre-stress relaxation in several Pennsylvania IABs. Both studies illustrated that contraction of the abutments and piles are significantly higher because of long-term creep and shrinkage. Fennema et al. (2005) and Kim and Laman (2010) also monitored superstructure performance. Both backfill pressures and concrete creep and shrinkage were observed to induce large axial compressive stresses in the bridge girders and deck; the backfill exerts axial loads on the superstructure resisting thermal expansion, and concrete shortening induces compressive stresses on the girders and

deck that are largest during maximum seasonal contraction. As a result of the significant axial loadings developed in IAB girders by time-dependent effects, both studies recommended incorporating these loadings into girder design. While a number of monitoring and numerical studies have explored time-dependent IAB behavior, Kim and Laman (2010) performed calibrated numerical simulation of one of the monitored bridges to predict its long-term behavior throughout the expected bridge life, a period of 75 years. This analysis indicated a sharp drop in the rate of increase in thermal displacements caused by time-dependent behaviors after the first 30 years (Kim and Laman 2010). However, as IABs grow longer and geometrically more complex, the potential increases for long-term behaviors to significantly impact not only the pile foundations, but also the design of the superstructure.

2.5 PURDUE UNIVERSITY AND INDIANA DOT RESEARCH

Recent and ongoing investigations at Purdue University, led by Robert Frosch (Frosch 2011), have shed light on a number of aspects of IAB behavior of interest to this study. IABs in neighboring Indiana are constructed very similarly to those in Illinois and are typically founded on concrete-filled shell piles and H-piles, similar to IDOT bridges. However, Indiana orients its H-piles for weak-axis bending in the direction of longitudinal bridge movement.

With regard to time-dependent behaviors, in addition to noting an increase in backfill pressures to a steady state level during the first few years of an IAB's service, Frosch (2011) found that Indiana IABs experience a significant "ratcheting" behavior in the thermal displacements caused by concrete shrinkage, particularly in the first several years after construction. Frosch (2011) instrumented two Indiana IABs, constructed with PPCI girders and differing geometries, and monitored them for periods of 4 and 7 years, respectively. They observed that the seasonal magnitude of thermal expansion and contraction cycles remained roughly the same, but the abutment movements ratcheted inward toward the center of the bridge. This inward movement of the abutments resulted in markedly higher contraction displacements of the foundation piles from their original position each year. The ratcheting appeared to slow with time, particularly in the bridge monitored for 7 years, strongly indicating that shrinkage, primarily of the cast-in-place deck, was driving the observed contraction. Analytical models of the bridges incorporating deck shrinkage closely correlated with the observed field responses. Owing to the net inward movement of the abutments, Frosch (personal communication) identified the contraction load case as critical for IAB design.

Purdue researchers (Frosch 2011) also built a large-scale, highly skewed (45°) IAB model at their laboratory to conduct additional testing on the effects of skew on bridge displacements. The quarter-scale test bridge incorporated two abutment ends connected by a series of load actuators. The actuators simulated the thermal expansion and contraction of the superstructure. The model deformations showed significant 3-D effects in the movement of the abutments, piles, and superstructure. The skewed abutments translated in both the transverse and longitudinal directions, and rotated significantly in the horizontal plane in addition to the expected vertical rotations. The critical lateral displacement demand on the piles was observed to occur in the acute corners of the skewed bridge for both simulated expansion and contraction cases (Frosch 2011). These results support the findings of this study (as described in later sections) that skewed IABs demonstrate complex 3-D global deformation patterns, contributing to uneven loading of the foundation piles.

Another phase of Frosch's research (2011) involved a numerical parametric study of factors that most affected IAB pile displacements. Skew was found to cause a significant increase in both critical longitudinal and transverse displacements, and skews above 30° were penalized with respect to permissible IAB length by Frosch (2011). Interestingly, pile orientation,

section, and soil spring resistance played a negligible role in determining pile displacements (Frosch 2011). These results imply that the superstructure dominates the pile response.

Similar to Rollins and Stenlund (2010), Frosch (2011) also tested abutment-pile connections in the laboratory and found that increased embedment (i.e., 24 in. versus 15 in.) improves load-deformation performance. Additionally, Frosch (2011) tested an H-pile with spiral confining reinforcement surrounding the embedded portion and found that this configuration improved the ability of the pile to maintain lateral load capacity at all lateral displacements measured in the test, instead of the declining lateral resistance observed in piles without confinement. The laboratory tests indicated pile-head displacements on the order of 2 in. could be incurred in IABs without damage, and up to 4 in. of displacement was possible while remaining within an “acceptable” damage limit. Indiana permits plasticity in pile steel to increase acceptable IAB lengths considerably (the lengths nearly doubled) from previous provisions. This is partly because axial load capacity was undiminished even after yielding in the pile connection tests, and weak-axis orientation makes the pile performance primarily displacement-driven because of hinging. Still longer bridges (up to 1,000 ft) are recommended as feasible with H-piles if spiral confinement is used (Frosch 2011).

While the Purdue pile-abutment connection tests primarily focused on Indiana’s weak-axis orientation, Frosch also tested an HP8x36 in a strong-axis orientation with a 15-in. embedment. The pile responded more stiffly than its corresponding weak-axis counterpart, and the connection deteriorated at lower displacements under the higher lateral load. However, the mechanism that initiated concrete cracking was local buckling of the H-pile flanges (Frosch 2011). Because the laboratory connection tests were conducted in the open air without the benefits of soil confinement, flange local buckling may have occurred prematurely, compared with a field load test of an equivalent pile. Additionally, deeper pile embedment may further reduce the tendency of connection performance to deteriorate at lower lateral displacements in the strong-axis orientation, as corroborated by the full-scale strong-axis field load tests conducted by Burdette et al. (1999).

The substantial amount of research at Purdue targeting the behavior of IAB piles in neighboring Indiana strongly indicates that this current 3-D parametric study of Illinois IABs is warranted. Based on Indiana’s experience, further research by Illinois, with appropriate design and detailing adjustment, may allow significant expansion of IAB use in Illinois.

2.6 REVIEW OF ICT RESEARCH REPORT ICT-09-054 BY OLSON ET AL. (2009)

The foundation for the current parametric study of Illinois IAB behavior was the 2009 study conducted by Olson et al. (2009). The earlier study identified the primary parameters affecting the performance of IAB substructures and foundations, proposed design modifications, and described potential field instrumentation and monitoring for Illinois IABs.

The scope of work completed by Olson et al. (2009) included (1) a literature review; (2) a targeted survey of regional DOTs that employ IABs to understand their experience with the superstructure and substructure design and construction, as well as the maintenance and performance record of IABs in Illinois; (3) 2-D geotechnical and structural modeling of IABs based on IDOT designs to understand key parameters in addition to length and skew affecting basic IAB behavior and serve as benchmarks for 3-D analyses; (4) 3-D numerical modeling of various IAB geometries and configurations to assess the importance of 3-D effects on parametric variation in behavior, particularly in skewed bridges; and (5) development of preliminary instrumentation plans for measuring the performance of Illinois IABs.

Key findings from the earlier University of Illinois study highlighted some of the dominant factors influencing IAB behavior and demonstrated the need for additional research. Olson et al.

(2009) guided many of the modeling assumptions employed in the current parametric study, and helped eliminate parametric variations that had been previously shown to be insignificant. The primary conclusions of Olson et al. (2009) are summarized here for context:

- For the range of soil conditions modeled, the foundation soil type had only a secondary effect on the abutment and pile foundation performance. In many practical applications, variations in soil resistance can be neglected in assessing pile behavior under thermal loading.
- Use of steel versus concrete girders (within the limited number of girder types and sizes considered) caused only minor variation in the performance of the abutments and piles. Thus, for predicting pile loads, the type of girder was a secondary factor. While the coefficient of thermal expansion of concrete is lower than steel, causing smaller displacements for a given temperature change, the flexural stiffness of the PPCI girders considered was higher than that of the steel girders. Higher girder stiffness exerted more rotational restraint on the abutment for a given displacement, which caused greater moments and stresses in the piles.
- Compacted granular backfill was recommended for use behind the abutment backwalls based on the following results: (1) the buildup of passive pressure on the abutments caused by the presence of backfill soil has little impact on pile foundation behavior; (2) orienting IAB wingwalls parallel to the bridge deck (as opposed to parallel to the abutment backwall) had no significant effect on abutment or foundation performance and did not reduce the settlement of uncompacted backfill; and (3) use of uncompacted backfill reduces the vertical support of the approach slab and induces greater stresses and moments in the slab.
- A number of options were proposed to reduce bending moment transmitted to IAB piles, which may permit further relaxation of length and skew limitations in Illinois.
- Parametric limitations of IAB length and skew based on IDOT detailing were suggested. In conforming with IDOT's request that pile steel stresses be limited to the yield stress, the permissible length and skew combinations were somewhat limited, even compared with current IDOT standards, for smaller pile types.
- In some bridges, the moments developed at the cold joint between the abutment and pile cap or the girder-abutment connection may exceed the capacity of these connections. If yielding or hinging at either of these interfaces occurs, some relief in loads transmitted to the piles may occur.

Results from Olson et al. (2009) prompted IDOT to further explore 3-D parametric investigation of IAB foundation behavior. The 2-D parametric study and limited 3-D modeling performed in the 2009 study revealed the potential benefits of whole-bridge 3-D FE modeling. Once the primary variables influencing Illinois IAB behavior were identified by Olson et al. (2009), a targeted, more comprehensive 3-D modeling program was deemed feasible to capture complexities of trends in permissible IAB lengths and skews not possible with more basic 2-D parametric investigation. Some of the results published by Olson et al. (2009) have since been refuted by the more extensive and refined 3-D modeling performed for this study, but the vast majority of the behaviors observed in the 2009 parametric study were confirmed and further defined by the current work.

CHAPTER 3 THREE-DIMENSIONAL NUMERICAL MODELING OF INTEGRAL ABUTMENT BRIDGES

3.1 FINITE ELEMENT MODEL CONSTRUCTION

The project team performed an extensive analytical study of integral abutment bridges as the primary means of generating the substructure and foundation data, results, and recommendations for design modification. Modeling and analyzing entire bridge structures in 3-D is more labor- and time-intensive than using simplified 2-D approximations; but this level of detail is appropriate and more accurate, given the complex behavior of integral abutment bridges. The project team's prior experience in studying substructure and soil-interaction behavior of IABs has shown that even for bridges without skew, significant 3-D effects exist because of the 3-D nature of thermal material behavior and the plate-like 2-D area of the bridge deck. When considering skew, 3-D behaviors become more pronounced. 3-D analyses are inherently more rigorous in terms of modeling and computation time; however, the project team primarily modeled bridges in 3-D to develop the most complete understanding of the highly coupled, interdependent behavior of these structures.

To understand the factors that most affect IAB behavior and how these interact with one another as bridge parameters change, a thorough parametric study was performed, involving a number of bridge models to account for variations in each parameter considered. Our parametric study involved a large number of bridge models to capture the variations and trends in IAB behavior as given aspects of bridge design were adjusted. Through the parametric study, the complexity of competing behaviors caused by the interaction of multiple design parameters was discovered, which may lead to optimization of design details for the substructure and further insights into its relationship to the superstructure behavior.

Based on IDOT direction and the findings from Olson et al. (2009), the authors focused this study on the following parameters that had previously been shown to significantly influence IAB behavior:

- Overall bridge length
- Abutment skew
- Span between intermediate supports
- Pile type and size
- Live loading

As the study results developed, we conducted additional analyses on other model subsets to explore some parameters beyond the basic scope established by IDOT:

- H-pile orientation
- Abutment-backfill type and compaction
- Strength of the soil surrounding the piles
- Girder size and type (pre-stressed concrete vs. steel)
- Time-dependent behavior of concrete, including shrinkage
- Abutment depth

To explore these parameters, this study included the creating, analyzing, and interpreting of hundreds of 3-D integral abutment bridge models. These models are described below.

3.1.1 Model Development and Geometry

The authors used the popular commercial structural analysis software package SAP2000 (CSI Software 2009) to create the 3-D FE models of each bridge. Olson et al. (2009) successfully used SAP2000 for a limited number of 3-D models, and they observed very reasonable approximations of IAB behavior. Because this study also focuses on the global IAB behavior, and in particular the loads developed in the substructure and foundation, the team felt that continuing to use SAP2000 would be sufficiently accurate and would allow direct comparison to the results from Olson et al. (2009).

Each bridge model was constructed from a number of different element types and material properties, and incorporates sequential non-linear load cases and non-linear boundary elements to capture the non-linear response of the structure to the complex load history. Figure 5 shows the primary features of our 3-D FE models.

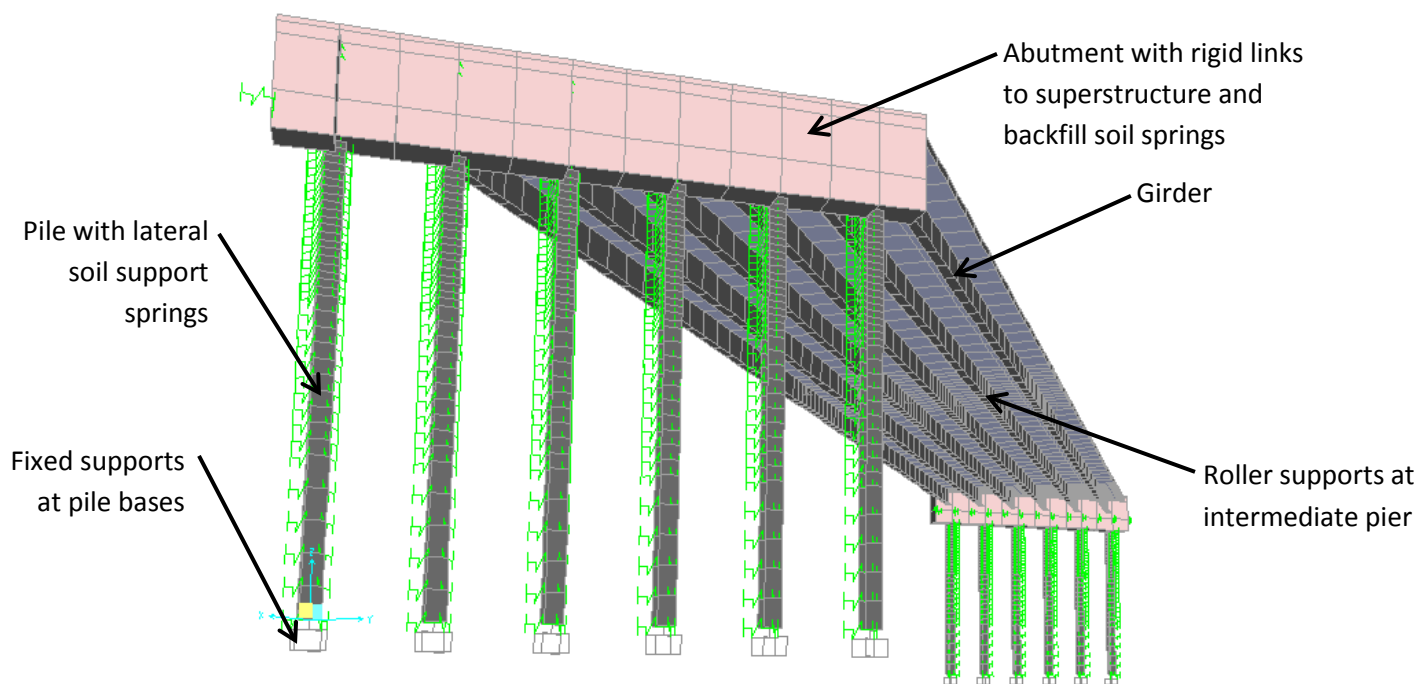


Figure 5. Isometric rendering of 2 x 100 ft span, 40° skew, HP 14x117 bridge FE model.

3.1.1.1 Deck, Girders, and Abutments

The model superstructure represents typical IAB design practices in Illinois. The bridge is modeled with an 8-in. cast-in-place concrete deck acting compositely with steel girders. The steel girders pass continuously over rolling intermediate supports and terminate integrally into the cast-in-place abutments. The specific steel girders selected for the models are representative of IDOT integral bridge construction; for shorter 100-ft spans up to an overall

length of 200 ft, W36x170 girders were used. The authors used W36x194 girders for bridge lengths from 400 to 600 ft with 100-ft spans. For 200-ft intermediate span bridges of any length, we selected plate girders with 6 ft, 4 in. deep webs. The 9/16-in. girder webs joined 18-in. wide, 1½-in. thick flanges above intermediate supports, which reduced to ¾-in. thickness in positive moment regions. All girders were assigned a yield stress (F_y) of 50 ksi.

To model the superstructure system, we used thin-shell elements of 4,000-psi concrete for the bridge deck. The deck elements were defined by a horizontal plane of nodes at the concrete deck centerline. The girders were modeled using frame elements that were coincident with the deck nodes. To appropriately model girder stiffness, the frame elements were inserted with the top flange as the reference point and a joint offset of 4 in. at each end to allow for the concrete deck. The concrete abutments ($f'_c = 4,000$ psi) were modeled using thick-shell elements defined by a vertical plane of nodes.

We modeled the interface between superstructure and the abutments to allow for accurate distribution of load throughout the bridge during the non-linear load case sequences. At locations where the girders connected to the abutments, rotational releases at the girder ends remained in place until after the dead load was applied, reflecting the pinned behavior of the girder end bearings on the pile caps under the weight of the fresh concrete deck until the abutment concrete hardens and joint fixity is achieved. Additionally, the deck elements closest to the abutments were not inserted until after the dead load was applied, to avoid transfer of dead load moments to the abutments through the slab. Vertical rigid links were used to transfer the load from the deck-elevation nodes to the abutment elements at the elevation of the elastic neutral axis of the composite girder-deck system. While this is not strictly accurate for the dead load case, it is of little consequence because no moments are transferred until after fixity is achieved. Once abutment-superstructure fixity occurs, this approach accurately simulates the transfer of moments from the superstructure to the abutments during the thermal and live loading cases of interest. Finally, in skewed bridges with 200-ft intermediate spans (and other select cases), an additional set of rigid links connect the remaining “free” deck nodes (those that are not coincident with a girder element) to nearby nodes at the top of the abutment. This was done to more accurately represent the connectivity of the deck, which is poured monolithically with the abutments, when the global torsional and transverse stiffness components of the superstructure play a significant role in the bridge behavior.

Figure 6 schematically illustrates the composite superstructure in the FE model. The basic scope of this study included only steel girders because Olson et al. (2009) indicated that pile stresses were negligibly affected by girder type; however, some model subsets with pre-stressed pre-cast concrete I-beam (PPCI) girders were analyzed to explore time-dependent effects. In FE models utilizing PPCI girders, the ends of the frame elements representing the girders are free to rotate at the intermediate supports as well as the abutments during the dead load case; this more accurately reflects the simply supported condition of the pre-cast members before the deck and continuity diaphragms have hardened.

3.1.1.2 Pile Foundations

The current study considered two types of driven piles: concrete-filled steel shells and steel H-piles. In the 3-D models, the piles were represented by a series of frame elements with nodes at elevations corresponding to non-linear soil support locations. The ends of the frame elements have no releases, reflecting the continuity of the structural piles.

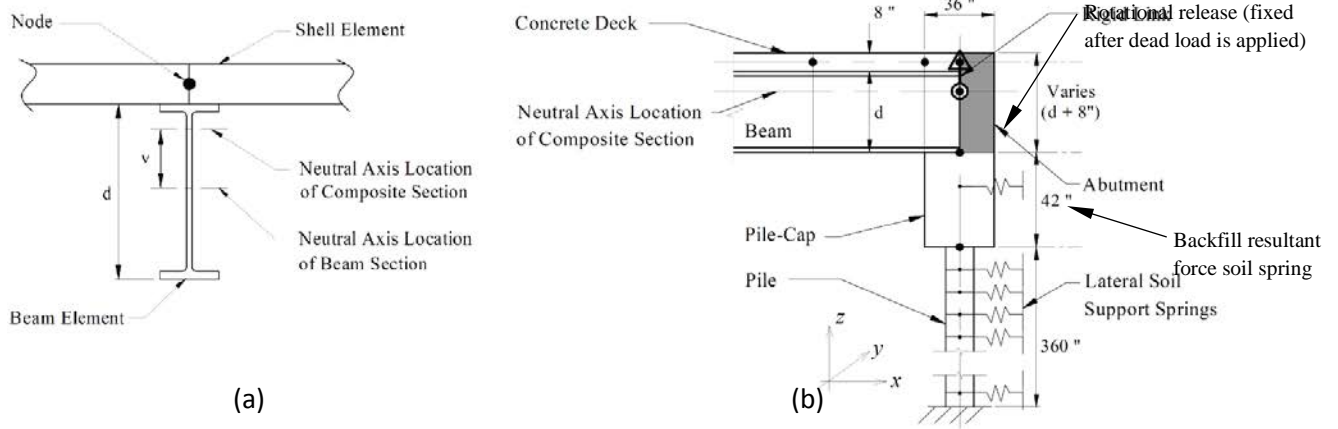


Figure 6. Details of FE model construction: (a) composite cross-section representation; (b) superstructure-abutment-foundation connection (adapted from Olson et al. 2009).

The composite cross-sectional properties of the shell piles were computed using SAP2000. The 4,000-psi concrete used in the shell piles was transformed to an equivalent steel area for stiffness calculations. However, a stiffness reduction (in the form of a factor applied to the moment of inertia in SAP2000) from this initial value was needed to account for cracking of the concrete prior to first yield in the shell pile steel. (Note: $F_y = 45$ ksi in the shell piles, a typical value in Illinois.) To determine an appropriate reduction in the composite stiffness, the project team used a non-linear analysis of each shell pile section of interest in LPILE Plus 5.0 (Ensoft 2005) to generate a curve of composite stiffness (EI) vs. moment at axial loads roughly corresponding to the bridge dead loads in both the long and short span configurations. Figure 7 presents one of these plots.

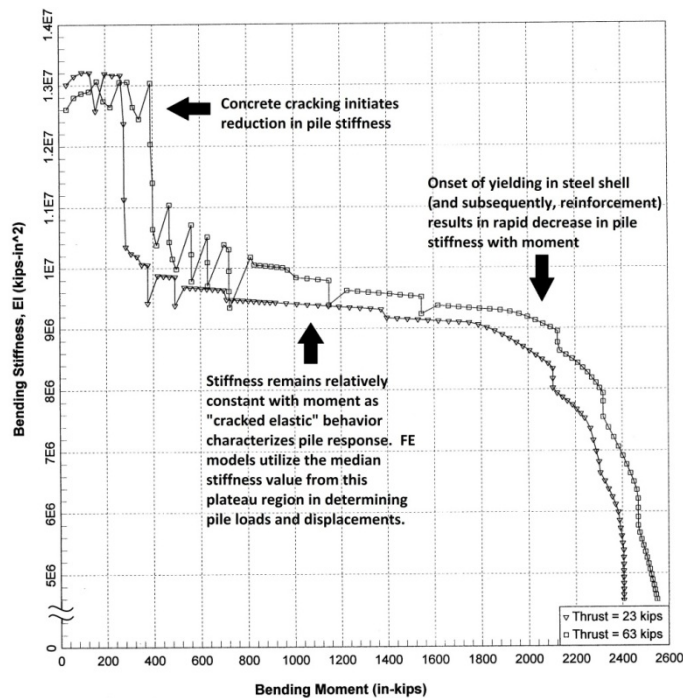


Figure 7. LPILE results for concrete-filled MS14x0.25: Bending stiffness vs. bending moment under varying axial force.

From this relationship, we determined that concrete cracking occurs under relatively low thermal loading, i.e., likely during a typical thermal cycle prior to an extreme temperature change, and that further deterioration of pile stiffness was negligible until significant steel yielding occurs. IDOT identified the initiation of yielding in the piles as the upper limit for integral bridge performance. Therefore, the stiffness of the shell piles could be considered to be relatively constant for the bridges modeled here. Accordingly, we chose to utilize a stiffness reduction factor in SAP roughly corresponding to the median stiffness in the plateau region of the EI vs. M curve generated from LPILE for analysis purposes.

3.1.1.3 Soil Resistance at Piles

We modeled the resistance of the soil surrounding the piles with a series of non-linear elastic springs, spaced every 6 in. in the top 10 ft of the pile below the pile cap, 12 in. for the next 10 ft, and 24 in. for the remainder of the piles. For simplicity, at a depth of 30 ft below the pile cap, the piles terminate at fixed supports. The length of the pile to its fixed support is sufficient to permit the variable depth-to-fixity for any given IAB configuration to be implicitly modeled by the lateral soil springs. Vertical skin friction and end bearing of the piles was neglected because lateral movements are the object of this study. The piles are assumed to have adequate vertical support.

The project team constructed the soil springs in the SAP2000 models using non-linear analyses performed in LPILE Plus 5.0 for a medium-stiff clay (representative of site conditions often encountered in Illinois). The clay was assigned a unit weight of 120 pcf and an undrained shear strength (s_u) of 1,500 psf. To determine the lateral load-deflection (p-y) response, we used the Reese model for stiff clay without free water available in LPILE Plus 5.0. LPILE default values for the strain factor (ϵ_{50}) were used.

This study considered only the single soil described here because Olson et al. (2009) observed that IAB foundation performance was relatively insensitive to reasonable variations in soil type and strength. Load-deflection (p-y) curves were generated for all variations of abutment height, pile diameter (or width), and pile type used in the study. Specifically, variations in abutment height with girder size, differences in IDOT connection detailing between H-piles and shell piles, the axial pile load (which is a function of span length), and pile diameter all affect the p-y curves with depth. We initially performed computations with separate p-y curves for different pile types, diameters, and intermediate span lengths. However, these analyses illustrated that the effect on pile stresses was negligible, consistent with the conclusion from Olson et al. (2009) that soil resistance has a minor effect on IAB pile behavior. Therefore, for the majority of the analyses, we used p-y curves computed for 12-in. diameter shell piles.

Soil springs were oriented in two directions, parallel and perpendicular to the longitudinal axis of the bridge. Soil resistance parallel to the bridge length for outward pile movement (i.e., during thermal expansion) was generally higher than for pile movements in the inward or transverse directions. This accounts for the greater surcharge pressure and confinement provided by the soil behind the abutment, compared with the sloping apron of soil in front of the abutment (toward the interior of the bridge).

In skewed bridges, despite the fact that the orientation of the abutment relative to the longitudinal bridge axis (and thus the soil geometry) changes, the project team maintained a constant global orientation of the soil springs along the piles for modeling simplicity. Olson et al. (2009) had previously explored varying the soil spring alignment and concluded that the difference in the loads and displacements induced in the piles was negligible.

3.1.1.4 Backfill Pressure

Again, the need for an accurate but simple, repeatable modeling approach guided the project team in its modeling of the resistance of the abutment-backfill soils. Therefore, we explored the effect of a typical compacted sand backfill behind the abutments. We assumed a unit weight of 120 pcf for the sandy backfill and assigned it a passive pressure coefficient (K_p) of 6. Similar to the pile springs, we modeled the backfill resistance to abutment movement with a group of multi-directional springs. However, we determined that in the case of the backfill, it would be sufficiently accurate to use a single horizontal row of springs supporting the abutment elements, located at the elevation of the force resultant of the triangular backfill pressure distribution, to capture the important effects on global bridge behavior. Some trial models incorporating more detailed representations of the backfill soil resistance indicated no significant difference in pile loading. Therefore, we used this simple representation for most of the FE models.

The creation of the backfill soil support springs in SAP2000 addressed several aspects of the backfill behavior. First, we oriented the backfill springs perpendicular to the face of the abutment. We assumed a simple linear increase in soil pressure with abutment movement (during bridge expansion) up to a displacement of 1 in., when the limiting passive pressure was reached. For skewed bridges, the authors added a backfill spring-resistance component parallel to the longitudinal axis of the abutment to account for frictional resistance between the abutment and the backfill. The exact magnitude of friction developed between the abutment and the backfill could vary considerably in the field depending on the interface materials (e.g., geotextile/geocomposite drain, foam, bare concrete, etc.) and how they are attached to the concrete. For the FE models, the authors judged that the frictional forces would orient the soil pressure resultant at an angle of 15° from the component perpendicular to the abutment face. In the case of inward abutment movement (thermal contraction), no soil resistance from the backfill was applied to the abutment, including the frictional components.

These backfill pressure models are not strictly accurate because they neglect the at-rest pressure acting on the abutment when it is in the undeformed configuration and do not capture the slight decrease in soil pressure with thermal contraction (to the active earth pressure condition). However, they are a good approximation of the more significant effects of passive pressure and abutment-backfill friction that occur during thermal expansion of an IAB and comply with the SAP2000 requirement for such spring supports that at zero displacement, the spring applies zero load.

3.1.1.5 Sequential Geometric Change with Load Application

IABs are structurally continuous at the completion of construction; but prior to this, they experience a number of geometric and loading changes. To accurately capture the behavior of IABs under thermal loadings, the project team sought to replicate the important sequential changes in bridge geometry and pair them with the appropriate application of loads.

To do this in SAP2000, we used the Staged Construction module of the program to create a sequential load case. This allowed the sequential addition and removal of structural components and loadings, and the ability to incorporate time-dependent effects in some models. At the conclusion of the Staged Construction load case, SAP2000 recorded the full stiffness, displacement, and force arrays for the model as a starting point for subsequent non-linear thermal load cases.

For a typical Illinois IAB, the girders are placed on the pile caps and intermediate piers, and then the concrete deck and abutments are poured monolithically. Because the fresh concrete has virtually no strength, the self-weight dead load of the structure is supported by the girders alone, and those girders, while continuous over the intermediate piers, are free to rotate

at the abutments (except for PPCI members, which are simply supported at the intermediate supports as well). Furthermore, while no moments are transferred to the pile foundations, axial load is transferred, and the superstructure undergoes significant bending deformation. To replicate this behavior in the 3-D FE bridge models, we initially placed rotational releases on the ends of the girders and delayed the installation of the rows of deck elements adjacent to the abutment until after the self-weight dead load was applied. Once the bridge had accommodated the dead load, the girder releases were fixed and the end elements of the deck were inserted to achieve structural continuity. Concurrently, the stiffness reduction factor was applied to models using concrete-filled shell piles, reflecting prior cracking during a non-critical thermal cycle. Following these sequential changes, thermal and live loading sequences were applied.

Though not explicitly required, we performed a set of analyses for steel girder and PPCI bridges that incorporated the time-dependent effects of concrete shrinkage in the Staged Construction load case. Shrinkage was accounted for at the end of the sequential load case, prior to thermal loading. Additionally, in the subset of PPCI bridges, we established continuity of the girders over the intermediate supports only after the dead loads were applied, reflecting the simply supported condition of the pre-cast girders at the time the cast-in-place deck and continuity diaphragms are poured.

3.1.2 Loadings and Model Analyses

IABs are subjected to the same loading conditions as conventional bridges; however, the continuous structural nature of these bridges means that the sequence and interaction of the various loads have a significant effect on the response of the bridge as a whole, compared with the relatively linear and isolated behaviors observed in conventional bridges. The loadings applied to the bridge models in this study all represent nominal service conditions, i.e., no factors are applied. IDOT requested this approach to load modeling in order to obtain accurate predictions of IAB behavior under service conditions. Further details of the loads are provided in the following sections.

3.1.2.1 Thermal Load Range

Because they have no expansion joints, IABs primarily accommodate thermal expansion and contraction of the superstructure through displacements and rotations of the abutments and pile foundations. With IDOT guidance, and per the guidelines set forth in the 2009 IDOT *Bridge Manual*, the research team applied a thermal loading range of +80°F to -80°F from an arbitrary “neutral” temperature. While this 160°F range nominally covers the LRFD and LFD design temperature range (-30°F to 130°F) cited in the *Bridge Manual*, in reality, construction of IABs in Illinois is completed under varying temperature conditions. Thus, we recognize that while the design temperature range is meant to be conservative, it is not unrealistic that an IAB whose abutments and deck set and cure in colder or warmer conditions than the 50°F reference temperature might see a temperature change of 80°F in service under an extreme thermal cycle.

Additionally, the FE models allow the concrete abutment elements to change temperature with the bridge superstructure. While Olson et al. (2009) held the temperature of the abutments constant while the deck and girders changed, we conducted some basic thermal analyses using the program HTTonedt (Ribando and O’Leary 1998) and determined that this assumption is not entirely valid. Although the massive concrete abutments of IABs are partially insulated from the ambient air on two sides by the backfill soil and do lag behind temperature changes in the superstructure, this thermal lag is certainly not seasonal and may be substantially eliminated in a matter of hours at a constant temperature. Because the critical thermal events we are considering in the study may occur over many hours or even days, it is

likely more accurate to assume the abutment changes temperature with the superstructure rather than remaining constant. More detailed analyses may reveal that modeling some abutment thermal lag is realistic, and that a thermal gradient exists between the exposed and buried portions of the abutment. Also, some of our preliminary models and results from Olson et al. (2009) suggest that such thermal variation within IABs may induce additional bending in the abutments, causing some secondary effects on the foundation piles, but such effects are likely inconsequential for most IABs.

3.1.2.2 Dead Loads

The dead load considered in this study was simply the self-weight of the bridge structure. Superimposed dead loading, while present for real bridges, depends on the roadway wearing surface material and thickness and other appurtenances added to a completed bridge. Also, any superimposed dead loads on an IAB are applied after fixity of the superstructure is achieved and thus cause a response in the structure similar to a small, uniformly distributed lived load. For these reasons, the research team decided that representing surcharge gravity loading with a live load case would be adequate, and superimposed dead loads were neglected for simplicity.

3.1.2.3 Live Loads

Because the primary application for IABs in the United States and Illinois has been for automobile traffic (as opposed to railroad, pedestrian, or other uses), the logical live loading of interest to IDOT and the project team in this study was the AASHTO HL-93 vehicular traffic loading. For the 36-ft-wide, two-lane highway bridges considered in this study, with relatively long intermediate spans of 100 to 200 ft, the HS-20 truck was the critical design vehicle. An HS-20 truck concentrated-load configuration was applied to each lane at the center of one end span in each bridge model (adjacent to the abutment and foundation). In addition to the HS-20 truck loading, a uniform design lane live load of 64 psf was applied over the width of both driving lanes in the same end span of the bridge.

The researchers chose to load only the end span because of the continuity of the bridge superstructure; such a patterned loading was deemed realistic under service conditions and provided the greatest effect in abutment and pile foundations. By loading the whole bridge, significant moment relief of the end span would occur, alleviating some of the effect of the live load surcharge on the piles.

3.1.2.4 Time-Dependent Effects

Recent IAB research has emphasized the significance of time-dependent behaviors in bridges (Fennema et al. 2005; Hassiotis and Xiong 2007; Kim and Laman 2010; Frosch 2011). Of particular interest is the shrinkage of the cast-in-place concrete deck frequently used for Illinois IABs, as well as shrinkage of PPCI girders. Though not initially part of the project scope, concrete shrinkage effects on a subset of bridge models were explored. We considered both bridges with steel girders and with PPCI girders for comparison.

To model shrinkage of concrete members, we defined member-specific, time-dependent material properties in SAP2000. The shrinkage calculations were based on the CEB-FIP 90 approach programmed into SAP2000. We determined the hypothetical size, h , of the deck, abutments, and PPCI girders, when applicable, from the ratio of surface area to volume. We employed the SAP 2000 default value of 5 for the shrinkage coefficient (B_{sc}). The starting age for our cast-in-place members was zero; and for bridges with PPCI girders, the girders were aged 30 days, an estimate of the elapsed time from casting at the pre-casting plant to installation at the IAB site. Because IDOT typically requires pre-cast members in multi-span structures to be aged for 45 days prior to installation, our models permit a modest amount of

additional shrinkage in the PPCI girders, making estimates of corresponding effects conservative. Though annual averages for atmospheric conditions vary somewhat throughout the state, we used the statewide annual average relative humidity of 73% for shrinkage calculations. Based on our shrinkage model, roughly 90% of the total shrinkage occurred in 22 years, which is only a fraction of the design life span of a typical IAB. As such, we thought it reasonable to use this amount of aging in our models; the most extreme thermal loading cycle for a given bridge could easily occur after most shrinkage has occurred.

3.1.2.5 Load Cases and Sequences

The creation of a sequential load case using the Staged Construction module of SAP2000 was discussed previously; this section places that discussion in context and elaborates on the sequence of non-linear load cases used to determine the structural response of the IAB throughout its load history.

As previously described, the Staged Construction feature of SAP 2000 allowed sequential geometric revisions, application of static loads such as the dead load, and time-dependent material changes. SAP2000 records the results and the state of the structure at the conclusion of this initial non-linear static load case, permitting it to be used as the starting point for multiple subsequent load cases. At the conclusion of the Staged Construction load case, the model represents the state of the IAB after the completion of construction and any aging, without any live load, just prior to the beginning of a critical thermal loading.

We used the state of the bridge at the conclusion of the Staged Construction case as the initial state for two non-linear time-history load cases applying the thermal loading, representing the warming and cooling of the bridge through the temperature range. Each non-linear thermal load case employed direct time integration via the Hilbert-Hughes-Taylor (HHT) scheme, with $\gamma = 0.5$, $\beta = 0.25$, and $\alpha = 0$. (Note when $\alpha = 0$, the HHT integration reduces to the classic Newmark method.) The 80°F temperature change was applied as a ramp function over 80 timesteps of 0.1 seconds, and the results for the structure were recorded after the equilibrium convergence of each timestep. By using 80 timesteps, the structural behavior was recorded at 1°F increments. Additionally, the relatively slow 8-second application of the load essentially eliminated dynamic effects in the bridge while permitting any non-linearities of the structural response to be recorded. The state and results of the model were saved at the conclusion of each load case, as they were at the conclusion of the non-linear Staged Construction case, to permit subsequent analyses of other load cases to be initiated from the deformed configuration.

The project team applied live loads to the bridges after the conclusion of the thermal load cases, reflecting a load history sequence mimicking real behavior. The live load cases were also non-linear time-histories following a similar quasi-static ramp function approach to the full load; however, we used a series of 50 timesteps at 1 second intervals to apply these gravity loads, permitting more Newton-Rhapson iterations per step to ensure convergence.

Figure 8 schematically illustrates the load history applied to each bridge model in SAP 2000. At the conclusion of all analyses, SAP2000 provides a substantial record of the response of the structural model for post-processing and review; including the bridge response to the application of dead loads and any time-dependent effects, the history of its deformation under thermal expansion and contraction, and then under subsequent live loading. Together, the battery of analyses run for each bridge configuration considered in our study allowed a thorough examination of the parametric trends in IAB behavior.

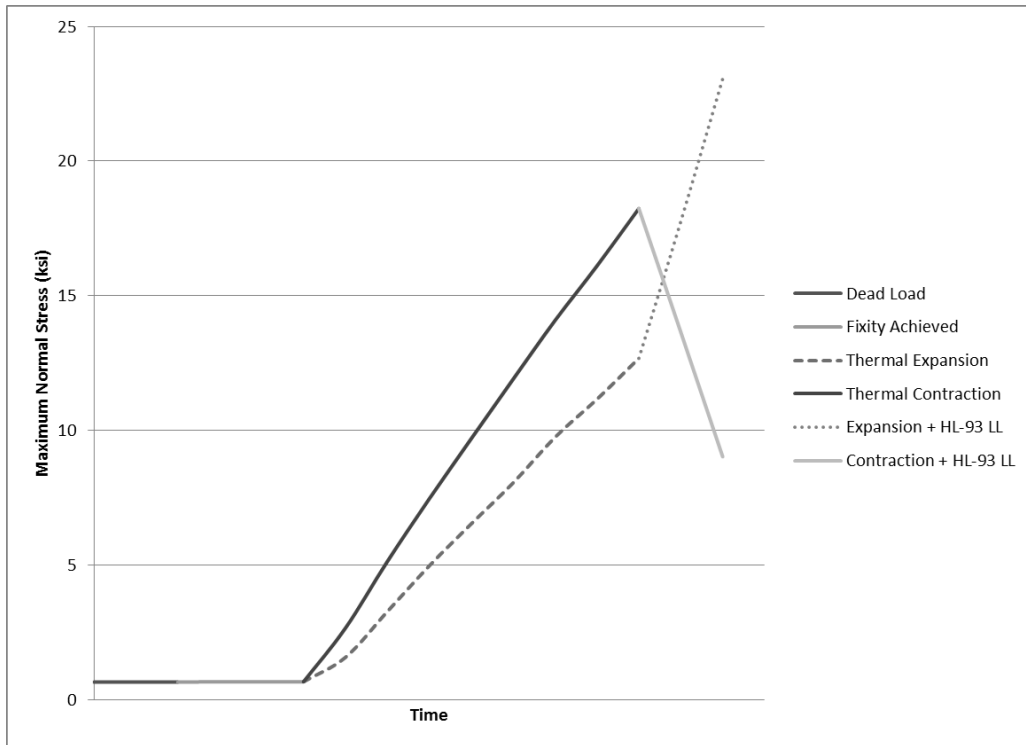


Figure 8. 4 x 100 ft. spans, HP 14x117, 0°-skew bridge: Center pile load history.

3.1.2.6 Summary of Analyses

The parameters affecting IAB behavior explored in this study were described in Section 3.1. Table 1 summarizes the final set of bridge configurations analyzed by the research team. Unless noted otherwise in the table, all models were analyzed for the same medium-stiff clay embankment soil with compacted granular backfill behind the abutments, and dead and live loads were applied in combination with thermal expansion and contraction cycles. Also, the project team elected not to solve all FE models for all pile sections in cases where we anticipated the pile stresses to be well beyond the linear-elastic range of the steel because such results are not meaningful for assessment of allowable bridge lengths by the first-yield criterion. However, in some cases, we analyzed models beyond steel yield for the purpose of illustrating general trends in IAB behavior that occur when piles remain linear elastic. Such configurations are included in Table 1.

Table 1. Summary of 3-D FE IAB Model Configurations Analyzed in Parametric Study

Pile Section	Overall Length (feet)	Intermediate Span (feet)	Girder Section	Skew (Degrees)	Other Conditions/Notes	No. of Models Analyzed
HP10x42	100	100	W36x170	0/20/40/60		4
	200	100	W36x170	0/20/40/60		4
	400	100	W36x194	0/20/40/60		4
	400	200	76" Web PL Girder	0/20/40/60		4
	600	100	W36x194	0/60	IDOT, Strong, and Weak-Axis Alternate Orientations	5
	600	100	W36x194	0/60	Pile Plasticity (IDOT, Strong, and Weak-Axis Orientations)	5
	600	200	76" Web PL Girder	0/20/40/60		4
HP12x74	100	100	W36x170	0/20/40/60		4
	200	100	W36x170	0/20/40/60		4
	400	100	W36x194	0/20/40/60		4
	400	200	76" Web PL Girder	0/20/40/60		4
	600	100	W36x194	0/20		2
	600	200	76" Web PL Girder	0/20/40/60		4
HP14x89	100	100	W36x170	0/20/40/60		4
	200	100	W36x170	0/20/40/60		4
	400	100	W36x194	0/20/40/60		4
	400	100	W36x194	0/40	Concrete Shrinkage Effect Test	2
	400	100	54" PPCI Beams	0/40	Concrete Shrinkage Effect Test	4
	400	200	76" Web PL Girder	0/20/40/60		4
	600	100	W36x194	0/20/40/60		4
	600	200	76" Web PL Girder	0/20/40/60		4
HP14x117	100	100	W36x170	0/20/40/60	IDOT, Strong, and Weak-Axis Alternate Orientations	11
	200	100	W36x170	0/20/40/60	IDOT and Weak-Axis Alternate Orientations	8
	400	100	W36x194	0/20/40/60	IDOT, Strong, and Weak-Axis Alternate Orientations	11
	400	200	76" Web PL Girder	0/20/40/60		4
	600	100	W36x194	0/20/40/60	IDOT and Strong-Axis Alternate Orientations	6
	600	200	76" Web PL Girder	0/20/40/60		4
	1200	100	W36x194	0		1
	1600	100	W36x194	0		1
MS12x0.179	100	100	W36x170	0/20/40/60		4
	200	100	W36x170	0/20/40/60		4
	400	100	W36x194	0/20/40/60		4
	400	200	76" Web PL Girder	0/20/40/60		4
	600	100	W36x194	0		1
	600	200	76" Web PL Girder	0		1
MS12x0.25	100	100	W36x170	0/20/40/60		4
	200	100	W36x170	0/20/40/60		4
	400	100	W36x194	0/20/40/60		4
	400	200	76" Web PL Girder	0/20/40/60		4
MS14x0.25	100	100	W36x170	0/20/40/60		4
	200	100	W36x170	0/20/40/60		4
	400	100	W36x194	0/20/40/60	Models w/ and w/out Backfill Run	8
	400	200	76" Web PL Girder	0/20/40/60		4
	600	100	W36x194	0		1
MS14x0.312	100	100	W36x170	0/20/40/60		4
	200	100	W36x170	0/20/40/60		4
	400	100	W36x194	0/20/40/60		4
	400	200	76" Web PL Girder	0/20/40/60		4
	600	100	W36x194	0		1
TOTAL						200

3.1.3 Model Limitations

The models were intended to accurately capture the essential elements of Illinois IAB behavior under thermal loadings and service conditions, but they are limited in scope, detail, and accuracy. Many of these limitations can be attributed to the assumptions, approximations, and other engineering judgments made by the authors, as described below.

3.1.3.1 Elastic Behavior of Models

One important limitation of the 3-D models used in this study is that they are primarily based on elastic material behavior. While the load history and soil behaviors in the models are non-linear, the SAP2000 approximations of the bridge structure rely on a fundamental assumption that the steel and concrete materials remain within their linear-elastic ranges. Even in the case of the shell piles, where the pile stiffness was adjusted to reflect concrete cracking, the analysis proceeded assuming that the shell piles remained in the “cracked elastic” range. The linear-elastic material behavior assumption is generally reasonable, considering that the loadings considered are representative of nominal service conditions. As a result, any results indicating significant yielding of the steel or concrete contain significant error.

Because the stiffness of the structural components remains constant in the SAP 2000 models, no load redistribution with yielding occurs, and the resulting loads and displacements for components beyond first yield of the material become increasingly inaccurate under increasing load. Additionally, owing to the relatively coarse FE mesh and level of detail in our entire bridge models, certain locations in the superstructure are subjected to stress concentrations and localized yielding that is largely fictitious. As a result, the models of this study are not well-suited for examining connection details and interfaces in the superstructure. Because IDOT was interested in first yield in the pile steel as a limiting criterion for establishing valid IAB configurations, the linear-elastic models were considered reasonable.

3.1.3.2 Idealized Integral Abutment Bridges vs. Real Bridges

Many of the modeling techniques used in this parametric study required approximation of true IAB behavior. The authors sought to carefully represent and capture the important aspects of IAB geometry, loading, and response in the models. Additionally, for computational efficiency, the SAP 2000 models were analyzed without explicitly accounting for geometric non-linearities. Given that second-order P- Δ bending effects in the foundation piles are relatively small compared with the first-order loads induced by thermal loadings, the authors judged this to be a reasonable simplification to our analyses. However, because the models are defined by a large number of relatively short/small elements, significant global deformations of the structure away from lines of axial actions (e.g., thermal expansion displacements or compressive forces) cause second-order effects to be implicitly recorded in the non-linear load history.

In addition to the limitations described above, the models represent idealized IAB configurations. Real IABs incorporate numerous additional geometric complexities not modeled here, often from necessity. For example, the bridge models in this study are perfectly level and highly symmetric. Site conditions and roadway plans for real bridge designs often require deviations from idealized geometries. For instance, many bridges of significant length may encounter substantial variation in soil properties from one foundation to another. Also, many bridges are constructed on a slope along the bridge longitudinal axis. Furthermore, to promote drainage and for other traffic considerations, the decks of all bridges are not flat but have some cross slope transverse to the road centerline. Finally, site constraints may require that the bridge geometry be asymmetric with respect to intermediate pier spacing, abutment orientation (not currently permitted by IDOT), or a number of other variables.

As a result, the idealized bridges analyzed in this study can only be viewed as indicative of general trends and patterns in IAB behavior; the response of a similar but distinct real bridge design may differ from its idealized equivalent.

3.2 Finite Element Model Behavior

The FE models in this study represent somewhat idealized but realistic Illinois IABs. While the models, constructed and loaded as previously described, are a mathematical

approximation of a complex physical system, their response to the applied loadings yields an accurate prediction of the performance of the physical bridge. Thus, the FE models provide a conceptual framework for understanding the expected responses of IABs in the field. The following sections describe the effects of influential structural mechanisms on the performance of the pile foundation system.

3.2.1 Foundation Alignment with Primary Bridge Movements

Though thermal expansion and contraction of IAB materials occurs in 3-D, it is dominated by the 2-D planar geometry of the concrete bridge deck. To a large extent, the thermal loading problem for an IAB may be viewed as a displacement-controlled loading; the abutments and pile foundations, while generating some resistance, basically move with the superstructure. Generally, the relatively long, narrow bridge deck induces displacements of the abutments parallel to the longitudinal axis of the bridge. Because the magnitude of the movement of the abutments and foundations in this direction is dictated by the superstructure, the resistance induced in the pile foundations under this displacement load is strongly affected by the stiffness of the abutment-foundation system. In other words, the loads generated in the foundation piles, both individually and as a group, are affected by their alignment relative to this primary direction of motion.

In the non-linear analyses conducted by the project team, the relationship between foundation system stiffness, thermally imposed displacements, and resulting loads in the piles is continually shifting as the temperature change increases. The stiffness of the abutment-pile foundation system in its current deformed state attracts a corresponding amount of load in the abutment and piles. At each step in the non-linear analysis, the current resistance from the foundation affects the subsequent additional movement of the bridge superstructure, which favors the path of least resistance. Thus, the non-linear FE response to the thermal load case captures a secondary load and displacement redistribution effect; as thermal load increases, the accumulating resistance of the foundation to the 3-D thermal movement of the bridge alters subsequent additional displacements and loads generated throughout the structure.

3.2.1.1 Relative Orientation of Pile Group

From a global-stiffness perspective, the overall orientation of the pile group relative to the bridge longitudinal axis (i.e., the abutment skew) has the largest effect on the resistance to thermal movement mobilized in the foundation. Bridges with zero or minimal skew essentially mobilize the sum of the stiffnesses of each individual pile to lateral movement to resist thermal loading; there is relatively little interaction between the piles in the group. However, as bridge skew increases, the pile group orientation becomes closer to the primary direction of the thermally induced abutment movement. As this happens, the high flexural stiffness of the concrete abutment/pile cap facilitates intense group action in the piles. The entire abutment-foundation system behaves similarly to a moment-resisting frame in resisting the component of the thermal displacements along the longitudinal axis of the abutment. Therefore, the stiffness of the highly skewed bridge's foundation is much greater than the summation of the stiffness in each pile. Under primarily displacement-controlled loading (both expansion and contraction), piles in highly skewed bridges develop higher loads, on average, than piles in low-skew bridges. Additionally, the bridge skew and pile group action introduces a significant gradient in the distribution of resistance among the individual piles.

3.2.1.2 H-Pile Section Orientation

For steel H-piles, the most common pile type employed in Illinois IABs, the foundation response to thermally induced movements is also directly influenced by the orientation of the pile relative to the bridge longitudinal axis. Because the H-pile sections considered in our study

all possess a significantly higher strong-axis moment of inertia compared with their weak-axis value, the load the piles attract under a given displacement is linked with the orientation of the pile relative to the resultant direction. Figure 9 illustrates the standard IDOT orientation for H-piles in Illinois IABs.

Because the pile web is oriented perpendicular to the abutment face, the overall stiffness of the foundation response to thermal movement generally decreases with increasing skew. Therefore, in general, less resistance is developed in the H-piles in high-skew bridges than if the stiffness were uniform in any direction (e.g., in shell piles). However, the maximum stresses in the H-pile steel tend to increase more dramatically with skew. This occurs because the highly skewed H-piles experience a large component of the resultant bending moment in the weak-axis direction, inducing high stresses at the flange tips. This behavior is undesirable for the “first yield” performance criterion, as discussed in Section 3.3.4.

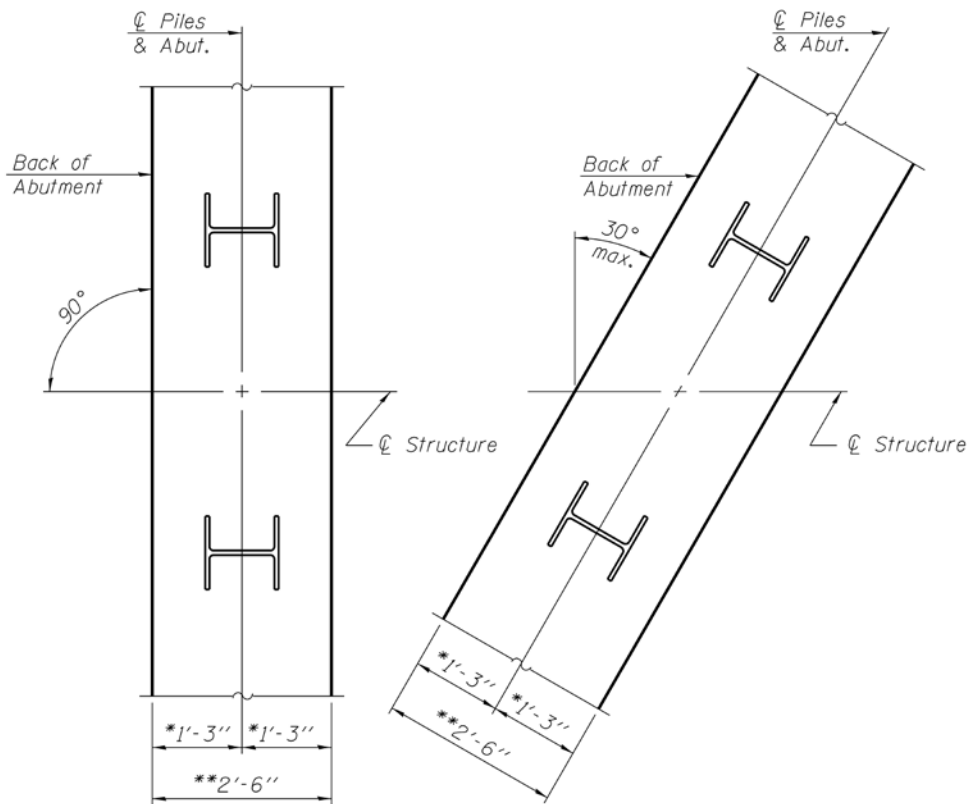


Figure 9. Standard IDOT integral abutment bridge H-pile orientation plan (adapted from IDOT *Bridge Manual*, 2009 edition).

3.2.2 Abutment Rotation and Softening of Superstructure Stiffness with Skew

For piles subjected to an imposed lateral displacement, the distribution of moment with depth is dictated by the pile-head restraint (i.e., free head versus fixed head). In a free-head condition, zero moment develops at the pile head and the maximum moment occurs at some depth below the top of the pile. In contrast, the maximum moment during lateral loading typically occurs at the pile head when the head is fixed. Therefore, the response of IAB piles to thermal displacement is strongly affected by abutment rotation. Generally, the greater the abutment rotation, the more the pile loadings resemble free-head conditions. Because the thermal

displacement is only marginally affected by the resistance developed in the piles (i.e., the piles are essentially displacement-controlled), when abutment rotation is minimal, pile response more closely resembles fixed-head conditions. Our study indicates that most IAB configurations experience pile-restraint conditions closer to fixed head than free head, meaning that the resultant moment typically is greatest at the pile-pile cap interface.

Abutment rotation is the key influence on pile-head restraint because the continuity between the piles and abutments prevents significant moment relief at that interface. The concrete pile cap and abutment are stiff compared with the piles; and in our study, the connection between the pile and abutment elements was approximated as rigid. While in reality, there is some flexibility at the pile-pile cap interface, particularly for shallow pile embedment (e.g., 6 in. to 12 in.) (Rollins and Stenlund 2010), modeling the pile-abutment connection as rigid is adequate to capture the development of piles loads in Illinois IABs which employ an embedment of 24 in.

More important in influencing pile-head fixity and load distribution is the flexibility of the interface between the superstructure and the abutment. This interface largely dictates the rotation of the abutment about its longitudinal axis during thermal displacement, as well as under any additional gravity surcharge loading (e.g., live load). When the girders and deck restrain abutment rotation about its longitudinal axis, the abutment remains nearly vertical during thermal expansion or contraction of the bridge deck. Because the semi-rigid abutment is nearly vertical, the thermal movement of the superstructure must be almost fully accommodated at the pile heads, and the pile-head condition is nearly fixed. In contrast, a more flexible superstructure permits substantial rotation of the abutment, and some of the thermal deck displacement is accommodated by abutment rotation. In this case, the pile heads are closer to a free-head condition, and the moments are less severe. Figure 10 illustrates the difference in pile response during thermal expansion with differing superstructure stiffness.

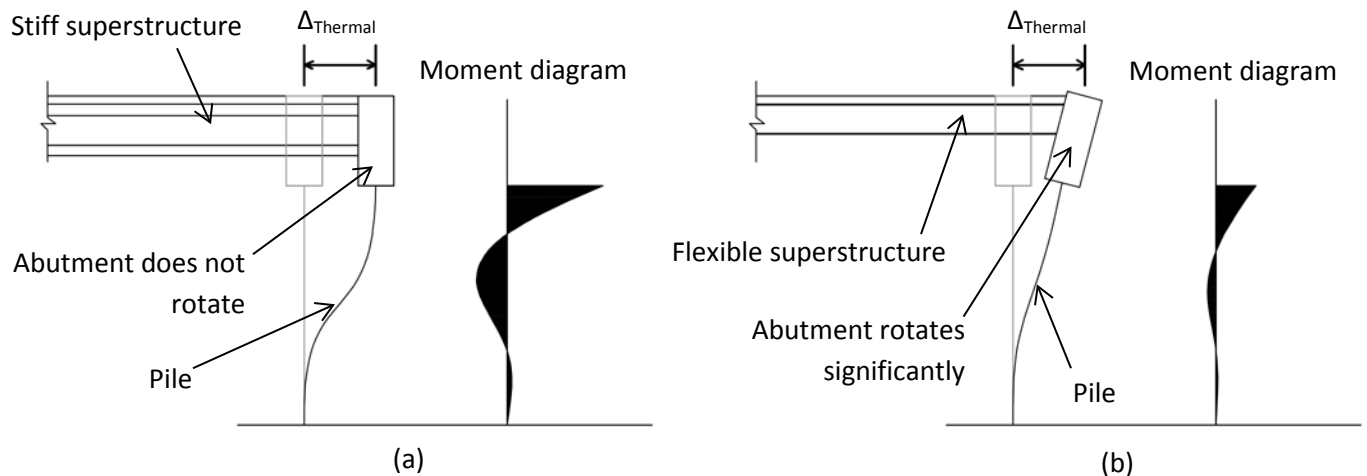


Figure 10. Effect of superstructure stiffness on pile-head fixity conditions: (a) stiff superstructure restraining abutment rotation, (b) flexible superstructure permitting substantial rotation of the abutment.

Several parameters influence restraint to rotation provided by the superstructure. For typical IABs, the most important parameters are intermediate span geometry, girder type, and bridge skew. The lengths of the intermediate spans, particularly the end bays, affect abutment

rotation because for a given composite superstructure cross-section, longer spans increase the flexibility of the structure. When considering the global stiffness of the entire bridge cross-section, the girder type strongly affects the ability of the superstructure to resist abutment rotation. For zero- or low-skew bridges, abutment rotation primarily depends on the strong-axis bending properties of the girders. However, in significantly skewed bridges, other properties of the superstructure can greatly influence the rotational stiffness of the abutment. These additional properties include the global torsional and transverse bending stiffnesses of the superstructure. For example, as skew increases in bridges of an otherwise constant configuration (i.e., girder type, span length, deck thickness), a secondary softening effect exists in the rate of pile load increase. This occurs because skewed abutments increasingly rotate about the torsional and weak bending axes of the girders, reducing the global resistance to this motion. Even though the length of the deck-abutment interface increases with skew, this is not enough to offset the reduction in abutment restraint corresponding to the larger effect of the torsional and transverse bending components in the girders. The overall increase in abutment rotation effectively reduces the fixity at the pile heads, thereby reducing the pile loads. This softening effect is most prevalent in long-span plate girder bridges, which show the greatest disparity between the global primary bending stiffness and transverse and torsional stiffnesses.

Finally, the overall abutment height, essentially dictated by the girder depth, also influences the thermal displacement imposed on the piles. For a given abutment rotation, larger distances between the concrete deck and the pile heads result in a greater portion of the thermal movement being accommodated by abutment rotation. This, in turn, reduces the loads on the piles during expansion and contraction. In summary, we note that greater global restraint to abutment rotation results in higher pile stresses.

3.2.3 Secondary Effects on Exterior Piles Caused by Transverse Thermal Behavior

One prominent aspect of IAB behavior observed in our 3-D parametric study is the presence of localized secondary effects in the pile response. Specifically, the 3-D models capture the transverse expansion and contraction of the bridge, revealing significant displacement, rotation, and loading gradients across the width of the bridge. These gradients dramatically affect the exterior piles.

When the bridge experiences thermal loading, it expands or contracts in all directions. The movements that most affect the piles are those dictated by the shape of the planar concrete deck. Even in a zero-skew bridge, significant transverse (to the longitudinal axis) movement of the deck and abutment occurs, adding a secondary directional component to the primarily longitudinal movement of the piles. This transverse movement is largest in the exterior piles, and often the additional bending resistance generated here makes the stresses in these piles critical for design.

Transverse thermal behavior becomes significantly more complicated for skewed bridges. Near the ends of a skewed bridge, the total cross-sectional width of the deck begins to decrease linearly (toward the acute corner), resulting in decreasing transverse thermal movement. As one approaches the acute corner of a skewed bridge, the imaginary line of zero-transverse thermal movement shifts from the centerline of the roadway to the acute corner. Because the abutment also changes temperature, only the piles are available to resist the transverse thermal movement of the deck. Although this also occurs in non-skewed bridges, points located along both edges of the slab are equidistant from the pile supports (i.e., the amount of resistance provided by the piles to transverse thermal movement is equal). However, in a skewed bridge, the restraint provided by the piles in the transverse direction is not equal on both sides of the bridge. The side of the slab adjacent to the abutment encounters greater stiffness to transverse movement than the exposed side. Thus, the transfer of transverse

thermal load to the piles at a given cross-section of the bridge becomes a function of the transverse bending stiffness at that section. Approaching the acute corner, the transverse stiffness drops considerably, and the distance along the exposed side of the slab to the abutment (which semi-rigidly transfers load to the piles) becomes negligible. Figure 11 conceptually illustrates how skew affects the transverse stiffness at the end of the bridge to resist thermal loading.

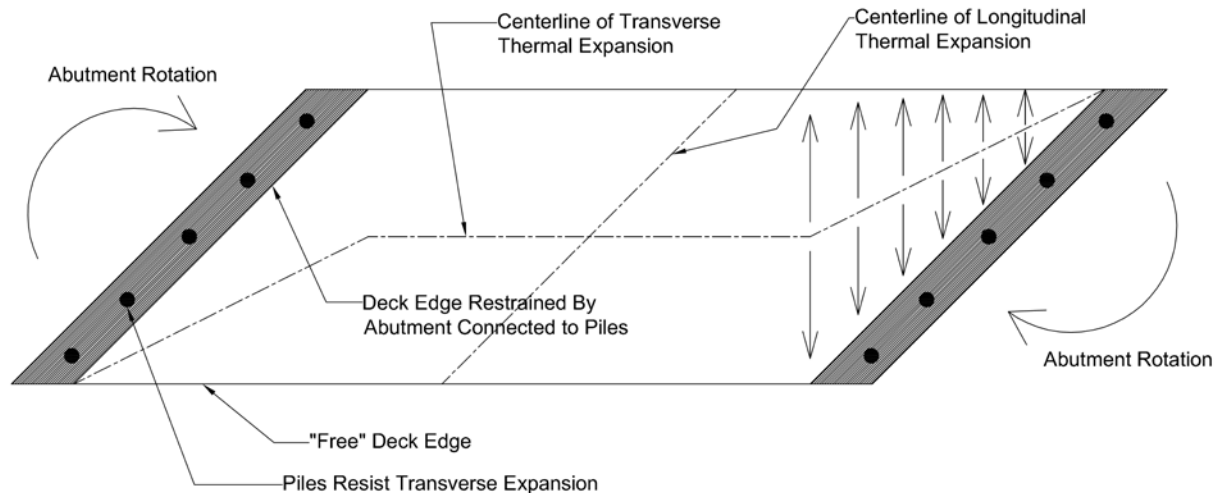


Figure 11. Plan illustrating the effect of transverse thermal expansion on acute corner piles in 45°-skewed IAB.

Though this qualitative variable-stiffness explanation is not comprehensive, it sheds some light on the complexities of thermal response in skewed IABs. In this study, behaviors associated with transverse thermal mechanisms include a gradient in the transverse bending of the superstructure, rotation of the abutments in the horizontal plane, global rotation of the superstructure in the horizontal plane, and as anticipated, a gradient in the amount of transverse pile movement.

In summary, transverse thermal movement in skewed IABs causes load to concentrate in the acute corner piles, typically making this the critical location where pile steel yield first occurs. The nature of the load, rotation, and displacement gradients across the pile group is influenced by other parameters.

3.3 Parametric Study Results and Discussion

The results of our 3-D parametric study generally indicate that a majority of bridge geometries frequently used by IDOT may be constructed integrally using piles currently employed by the state. However, pile performance varies, depending on the size and type used; in many bridge configurations modeled, only a heavy H-pile would remain below the steel yield stress under imposed service loadings. Given IDOT's performance criterion that stresses in the pile steel should remain below yield, the parametric study results show that concrete-filled shell piles are generally limited to shorter IABs, and H-piles are a better alternative when additional length is required. All bridge foundation and geometric configurations show a dramatic variation in pile stress with skew; the effects of skew are especially pronounced in IABs founded on H-piles.

In addition to better defining the current limits of pile performance in IABs utilizing IDOT details, our parametric study revealed a number of interesting and influential mechanisms that drive IAB behavior. Many of these behaviors display strong 3-D characteristics. Beyond the significant impact of abutment skew on the 3-D models, we also noticed a number of other parameters that strongly affect IAB performance, including: H-pile orientation, the presence of compacted backfill behind the abutments, live load effects, the intermediate span length and girder design (as it relates to the superstructure stiffness), and concrete shrinkage in IABs with PPCI girders. Although stresses above the yield stress for the pile steel are not strictly accurate because linear-elastic behavior was assumed in the material models, they still reveal trends in IAB behavior that occur in other bridge configurations.

3.3.1 General Trends Associated with Overall Length and Skew Variation

Pile stresses in Illinois IABs tend to be higher for a given bridge length as abutment skew increases. This increase is non-linear, and some slowing of the rate of increase can occur in the critical pile at moderate abutment skews of 20° to 40°. The extent of non-linearity appears to be driven by two primary factors:

- the stiffness of the superstructure and its influence on rotation of the abutment, which dictates the extent of pile-head fixity; and
- the stiffness of the pile foundation response, which depends on both individual and group mechanisms, affecting the amount of resistance developed to the imposed displacements.

In our 3-D bridge models, these two behaviors are influenced to some extent by virtually all of the bridge design parameters, and so pile response variation with skew does not scale across bridges of varying overall length, intermediate span, pile type and size, and girder design.

Typically, the largest loads in skewed bridges are carried by the piles closest to the acute corners of the superstructure, and the corresponding gradients across the pile group tend to increase with skew, consistent with findings by Frosch (2011). While certain norms of IAB behavior exist in bridges with significant skew, unusual or extreme design configurations can deviate from these trends when parametric influences are competing. This means that in real IABs with asymmetries related to soil, layout, slope, or other parameters, beneficial or detrimental behaviors outside the idealized norms may occur that require consideration for effective design. However, the general trends serve as a reference for comparison to detailed analyses of more complex IAB geometries.

In IABs founded on shell piles, after some softening at moderate skews, pile moments often increase more rapidly as skew increases to 60° because the group response is stiffer and more frame-like against the longitudinal movement of the bridge, as illustrated in Figure 12. Figure 13 highlights how shell pile moments change with IAB length. Although minor variations exist, generally speaking, pile moments increase roughly linearly with bridge length above the minimum 100-ft length considered in this study (so long as the pile steel remains linear elastic). It is likely that more significant non-linear load increase occurs in short bridges because the thermal displacements at these lengths correspond with the most non-linear portion of the soil resistance P-Y curves.

Conversely, in H-pile bridges, the softening of the stress increase continues to extreme skews, as seen in Figure 14. Because the stiffness of the individual pile responses continues to decrease as they become increasingly bent about their weak axes, the H-piles attract less additional moment, offsetting the group behavior effect observed in shell piles. Further evidence of this is displayed in Figure 15, which illustrates the relatively constant magnitudes of bending

loads induced in the H-piles as skew increases. Finally, Figure 16 illustrates a linear trend in H-pile stress with IAB length, similar to that seen in the shell pile cases. This observation suggests that, with proper engineering judgment, some linear extrapolation beyond the parametric study results can be used to estimate maximum allowable bridge lengths, provided the data used for the extrapolation are not well outside the linear-elastic regime of the materials.

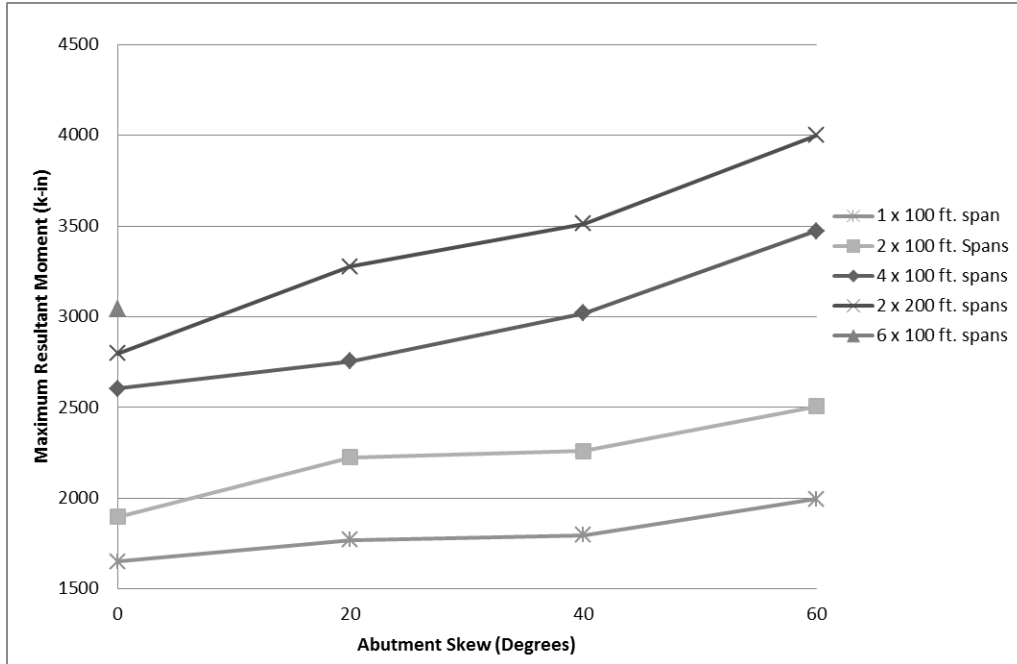


Figure 12. Maximum moments in MS14x0.312 piles vs. skew for bridges of varying length.

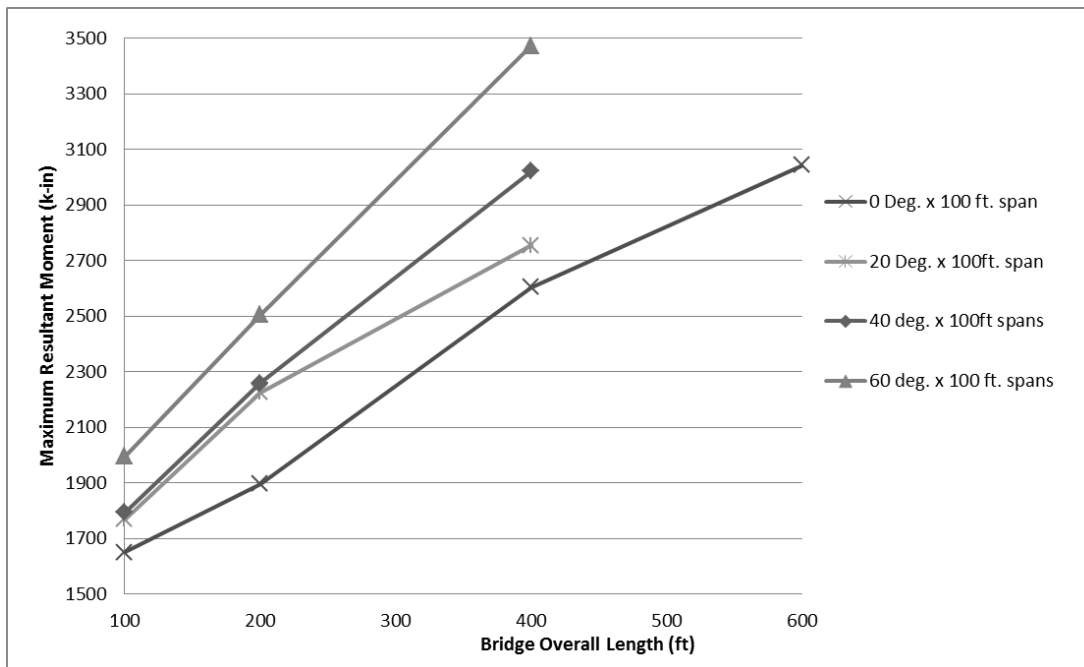


Figure 13. Maximum moments in MS14x0.312 piles vs. length for bridges of varying skew.

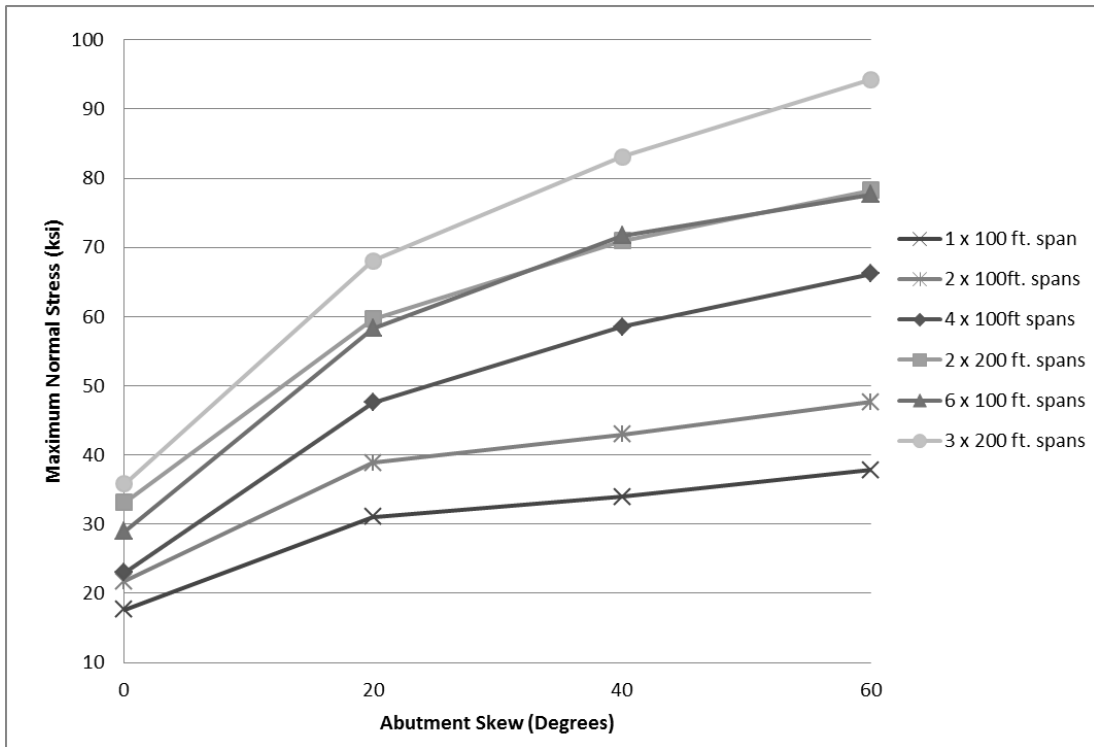


Figure 14. Maximum normal stress in HP14x117 piles vs. skew for bridges of varying length.

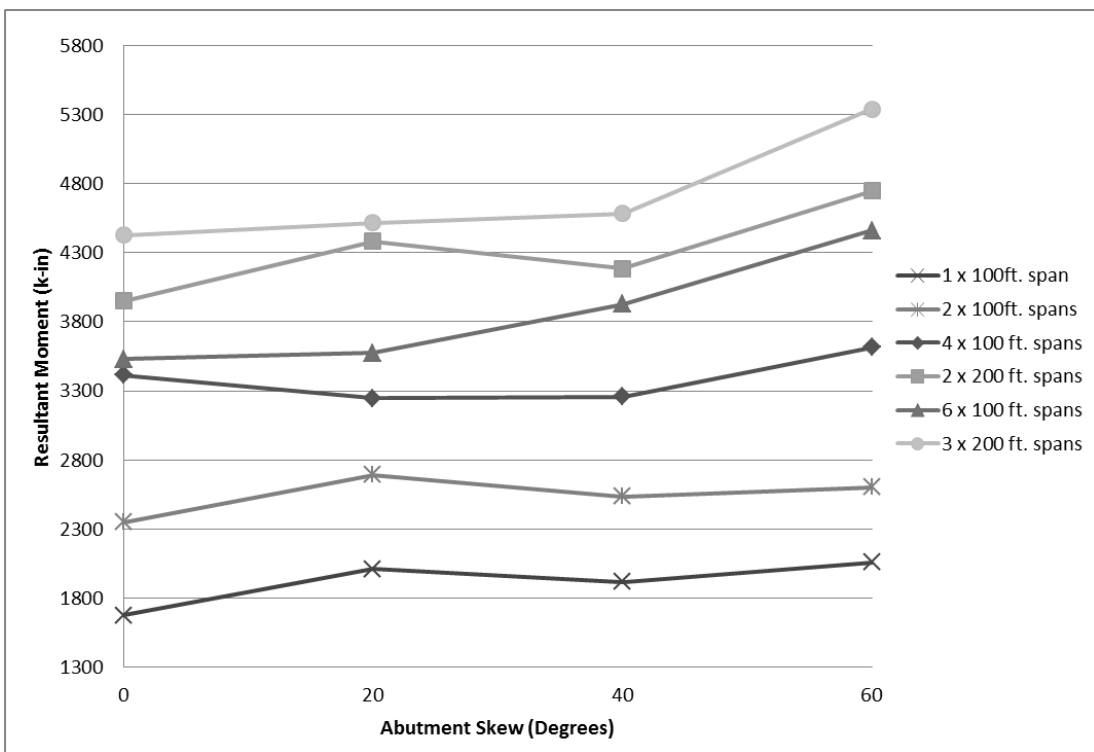


Figure 15. Maximum moment in HP14x117 piles vs. skew for bridges of varying length.

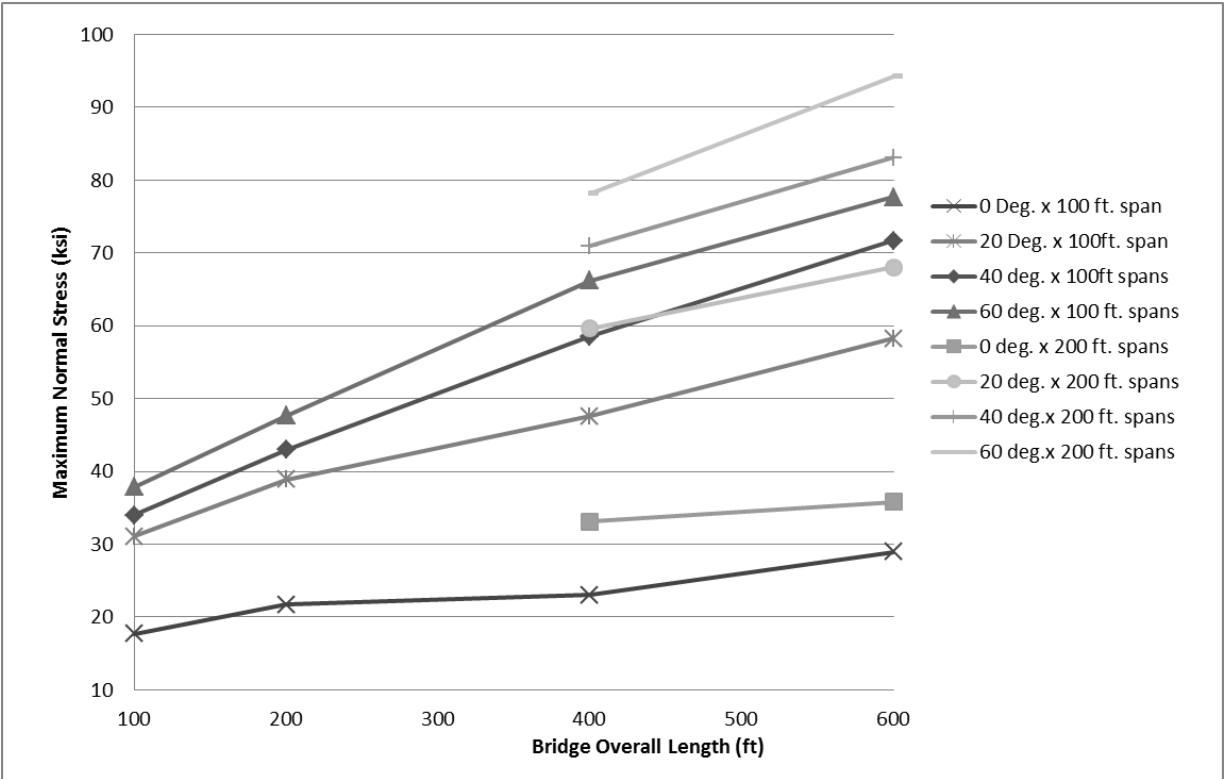


Figure 16. Maximum normal stress in HP14x117 piles vs. length for bridges of varying skew.

3.3.2 Concrete-Filled Shell Piles

Figures 17 through 20 present permissible length and skew combinations for concrete-filled shell piles. Each figure includes estimated stresses from the analyzed bridge models (which typically correspond to stresses below first yield of the steel), as well as the linear extrapolation of the analytical results to the length at which steel yielding would initiate. In some cases, none of the parametric analyses conducted at a given skew were allowable by strictly applying the limit of first yield; but if the stresses in the piles were reasonably close to the linear range, we linearly interpolated the analytical results to estimate a shorter, acceptable length.

Reflecting current IDOT *Bridge Manual* guidelines, the parametric study clearly indicates that use of concrete-filled shell piles should remain limited to shorter IABs. However, the results also show that other than for the smallest common shell pile (MS12x0.179”), the current IDOT restrictions are conservative, particularly in bridges with low skew. For example, at skews up to 40°, MS14x0.312 piles should perform satisfactorily for IABs exceeding 350 ft in length. Considering that the analytical length limitations correspond to the onset of yield at the extreme tensile fiber of the steel, the results suggest that less conservative length and skew limitations could be adopted by IDOT, provided the shell piles used have adequate diameter and wall thicknesses.

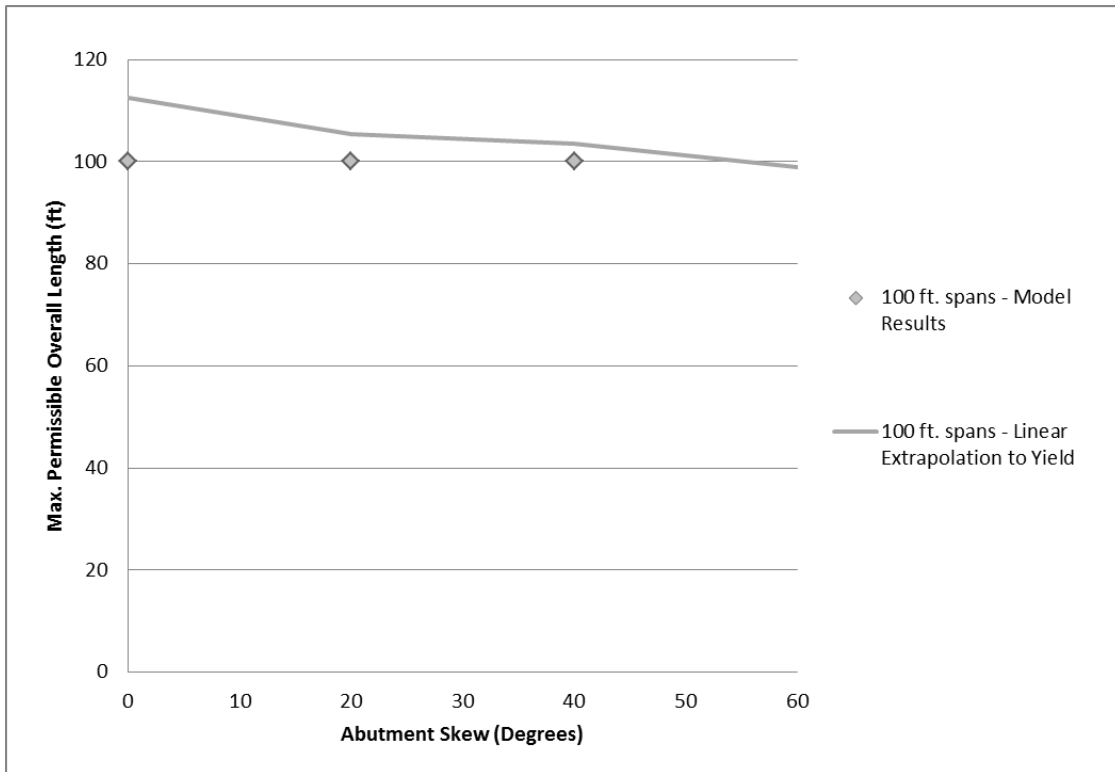


Figure 17. MS 12x0.179: Permissible IDOT IAB lengths vs. skew.

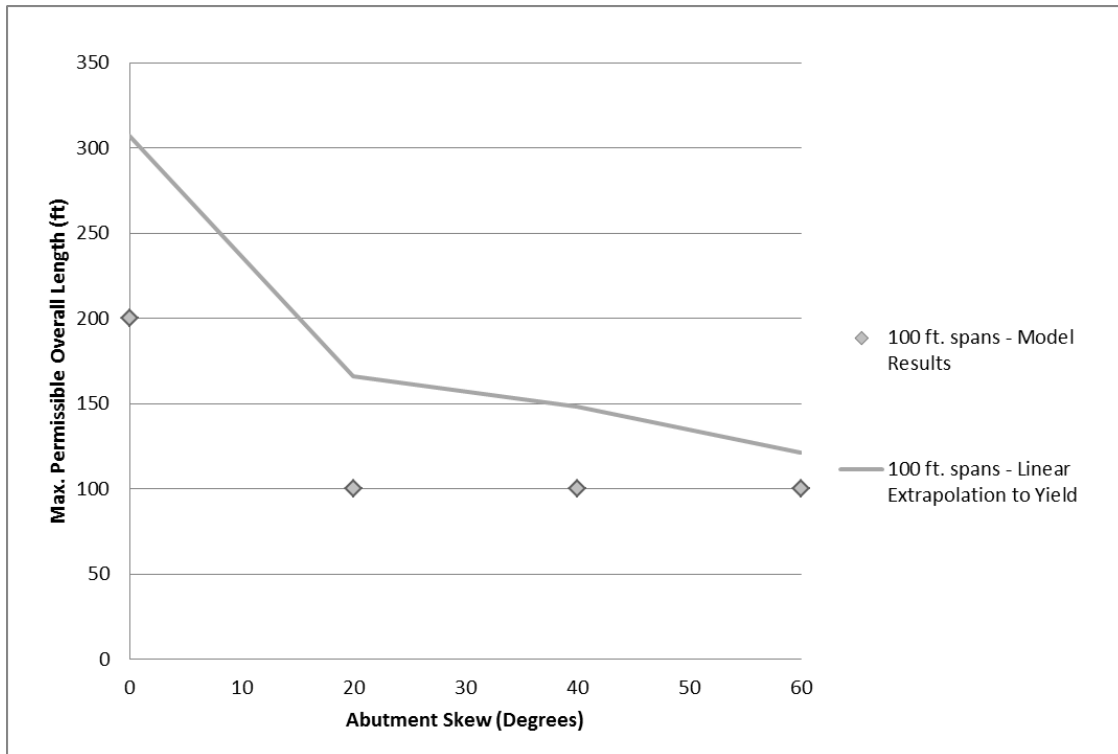


Figure 18. MS 12x0.25: Permissible IDOT IAB lengths vs. skew.

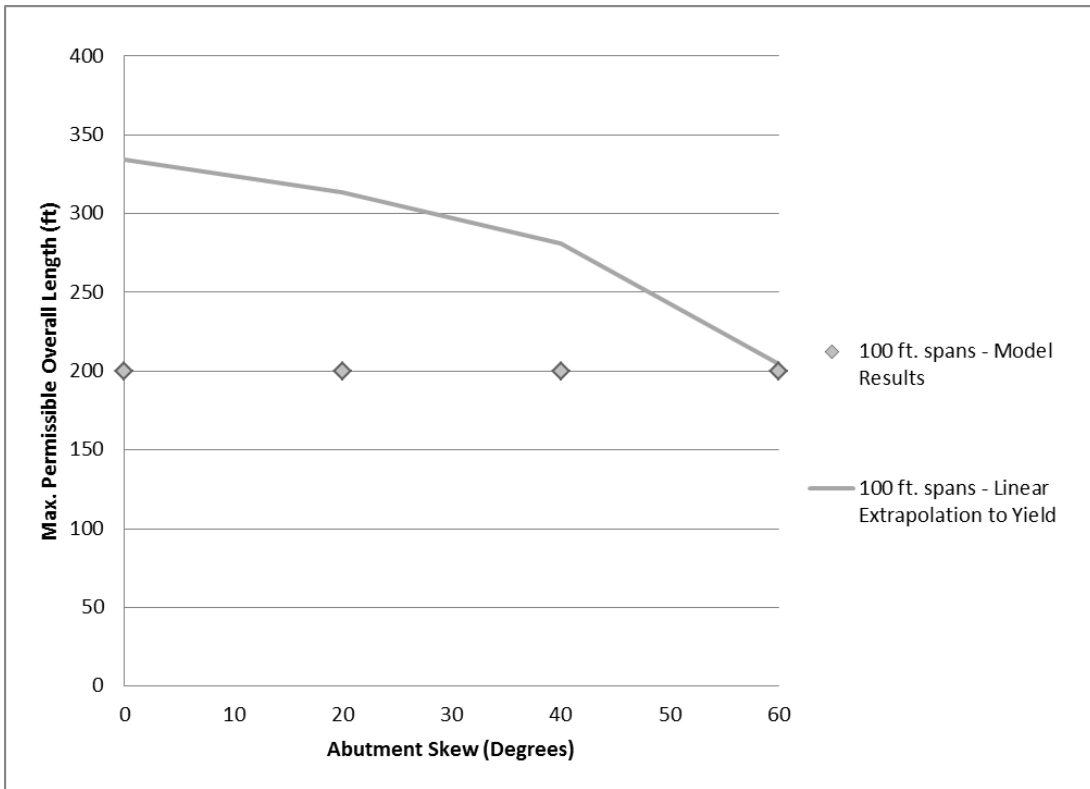


Figure 19. MS 14x0.25: Permissible IDOT IAB lengths vs. skew.

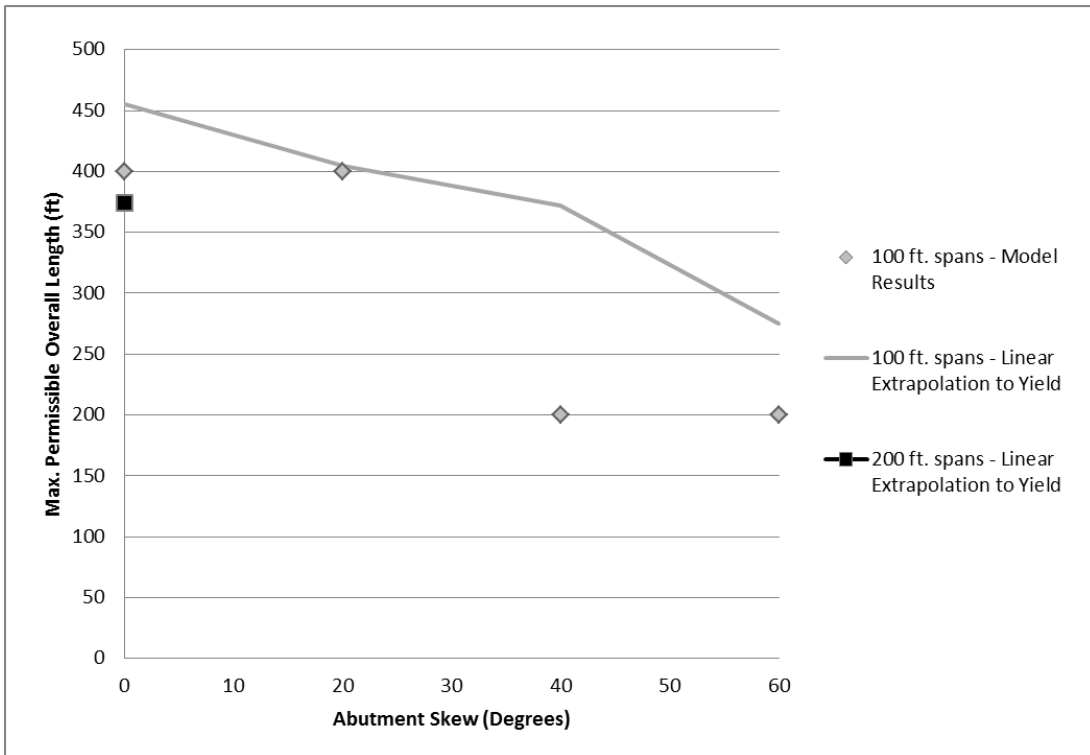


Figure 20. MS 14x0.312: Permissible IDOT IAB lengths vs. skew.

3.3.3 H-Piles

Figures 21 through 24 illustrate permissible maximum allowable lengths and skews for H-pile founded IABs, with supporting FE model results. Generally speaking, H-pile IABs can be longer than equivalent shell pile-supported IABs at lower skews. However, bending about the weak axis in significantly skewed bridges quickly causes stresses to increase at the tips of the pile flanges, initiating localized yielding of the section at drastically lower bridge lengths. Also, the introduction of skew begins to cause movements of the abutments in the transverse direction (i.e., perpendicular to the bridge longitudinal axis). These movements add to the weak-axis bending component in the piles. In fact, greater lengths can be achieved with 14 in. shell piles at skews in excess of 20°. As previously discussed, there are strong indications that this undesirable drop in H-pile performance with skew is linked to IDOT's standard orientation detail.

For H-pile IABs without skew, the lack of a large weak-axis bending component permits the H-piles to remain in the linear-elastic range at lengths several times those of even moderately skewed bridges. Also, the predicted maximum allowable length for HP14x117 piles in a straight IAB exceeds IDOT's current limitation on steel IAB superstructure length (310 ft) by more than a factor of 4. While this strongly indicates the conservatism of IDOT's current prescriptive length limits, it also compels further discussion of the mechanisms permitting such beneficial pile behavior to occur.

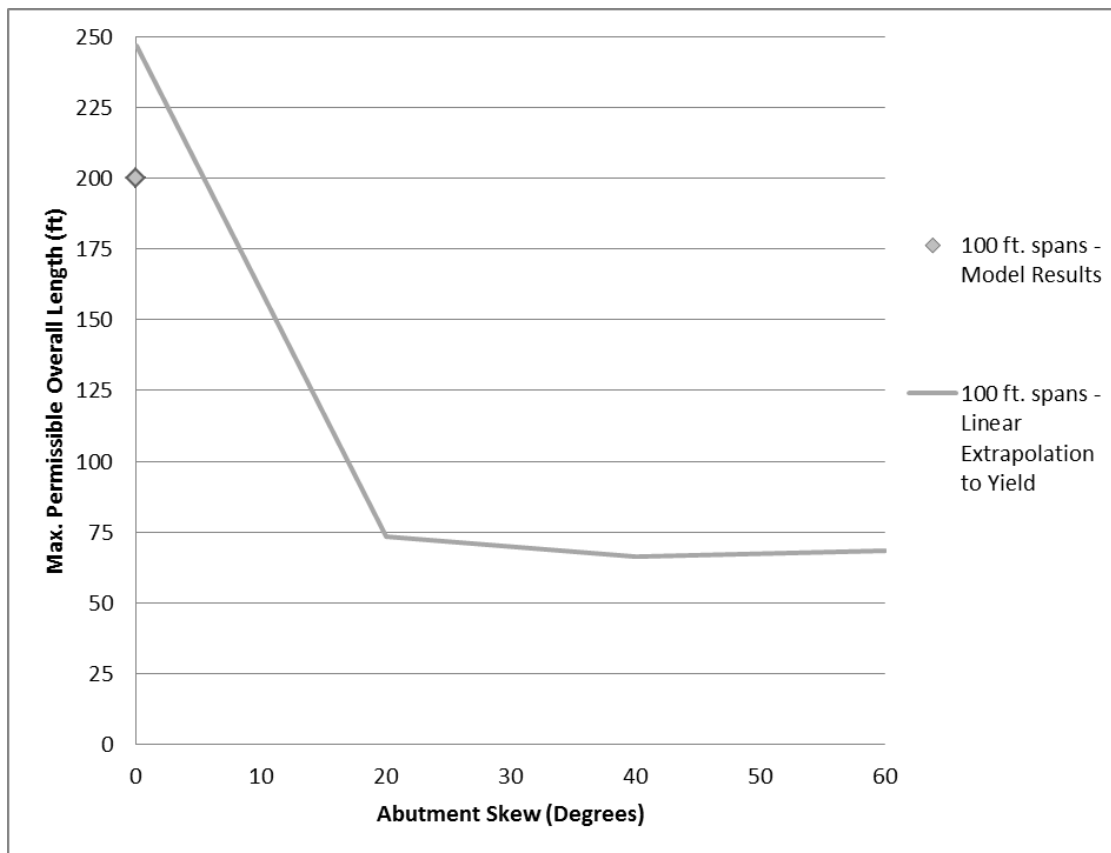


Figure 21. HP 10x42: Permissible IDOT IAB lengths vs. skew.

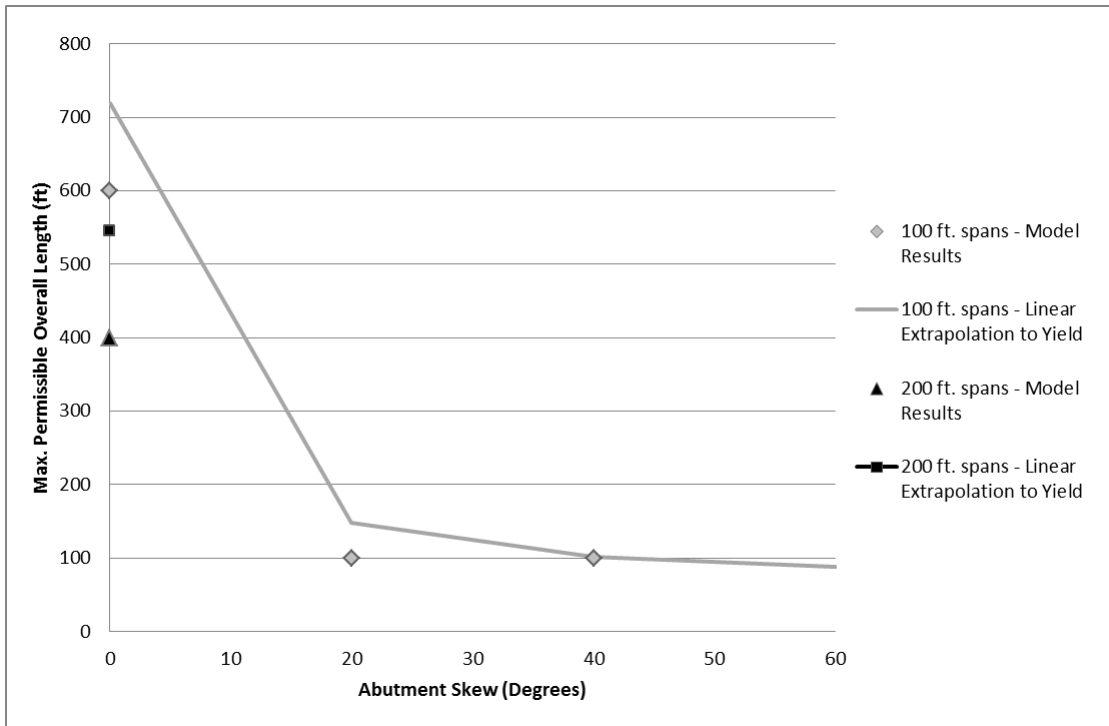


Figure 22. HP 12x74: Permissible IDOT IAB lengths vs. skew.

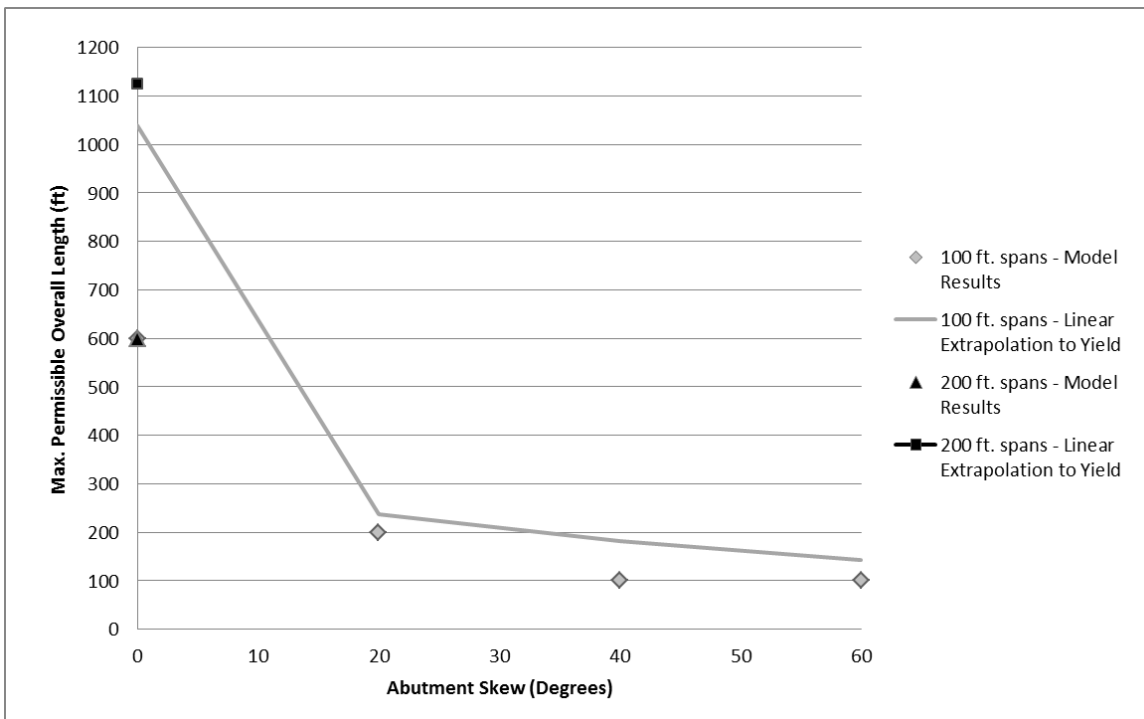


Figure 21. HP 14x89: Permissible IDOT IAB lengths vs. skew.

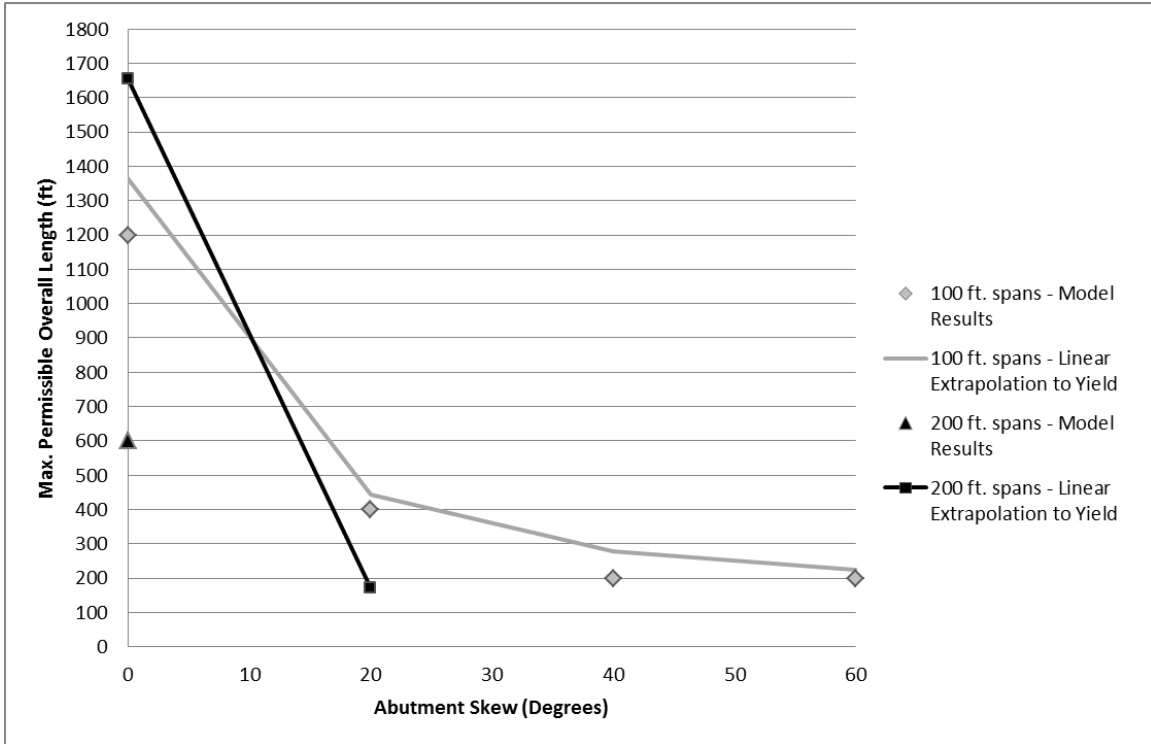


Figure 22. HP 14x117: Permissible IDOT IAB lengths vs. skew.

In zero-skew IABs, the H-piles remain in the elastic range of the steel at such extreme lengths because a great deal of the longitudinal thermal movement, driven by the superstructure, is never directly transmitted to the pile heads. The complex 3-D response of the bridge system absorbs much of the horizontal displacement. Theoretically, for a given temperature change, the composite superstructure will expand or contract an amount directly proportional to its length and effective longitudinal coefficient of thermal expansion, α_{eff} . However, this theoretical value of thermal movement is strictly valid only if the superstructure is completely unrestrained. In an IAB, a number of factors influence how the structure responds to and resists the thermal movement; the end result is that only a fraction of the theoretical horizontal movement of the superstructure affects the pile heads.

For example, the composite 8-in. concrete deck and W36x194 girder superstructure model used in our FE models with 100-ft intermediate spans has an $\alpha_{\text{eff}} = 5.943 \times 10^{-6} / ^\circ\text{F}$. For reference, the values of α_{concrete} and α_{steel} used in the study were $5.5 \times 10^{-6} / ^\circ\text{F}$ and $6.5 \times 10^{-6} / ^\circ\text{F}$, respectively. Accordingly, under the 80°F temperature changes considered in this study, a 600-ft, zero-skew IAB should experience an unrestrained thermal expansion or contraction of 1.712 in. at each abutment. However, in the expansion case, the authors observed that the FE model for the 6 x 100-ft, zero-skew, HP14x117 bridge exhibited only 73% of the unrestrained longitudinal expansion value in the abutment at the elevation of the deck and only 48% of this displacement at the pile heads. As shown in Figure 14, the maximum pile stress observed in this bridge model is 28.9 ksi. Because the amount of longitudinal displacement exerted on the pile head is significantly reduced by the response of the bridge structure, and additionally, abutment rotation reduces the fixity of the pile head, the H-piles remain below first yield at IAB lengths well beyond those anticipated by simpler modeling approaches.

Figure 25 illustrates how the proportion of the theoretical longitudinal thermal expansion actually seen at the deck-abutment interface varies with length in zero-skew IABs. Generally,

the percentage of the theoretical displacement transmitted to the abutments decreases as IAB length increases. Two factors influence this behavior. First, as bridge length increases, the resistance to thermal movement provided by the foundation system and surrounding soils increases, causing internal stresses in the superstructure to increase and restrict a greater portion of the theoretical movement. For very long bridge lengths, even relatively small axial stresses throughout the superstructure can generate a substantial change in length that counters the unrestrained thermal tendencies. Furthermore, significant second-order geometric effects occur in the end bays as thermal load increases, and these effects grow considerably with overall bridge length. Because of the fixity at the connections of the girders and abutments, the foundation and abutment moment-rotation resistance causes additional vertical deflections in the end spans of IABs with increasing thermal load. Uplift of the end bays in expansion and further downward deflection during contraction results in additional reduction of pile longitudinal displacements compared with unrestrained thermal movement of the superstructure in the horizontal plane. Though not explicitly analyzed as part of this study, the authors maintain that it is reasonable to assume that such second-order geometric effects in IABs are strongly affected by both the flexural stiffness of the superstructure and pile size. Both of these parameters would affect the degree to which the moment resistance to thermal load developed in the foundations flexes the superstructure away from the horizontal line of thermal action. The authors generally observed similar reductions in thermal movement in the FE results for the contraction case, but slightly higher percentages of the theoretical displacement are transmitted to the abutments and piles.

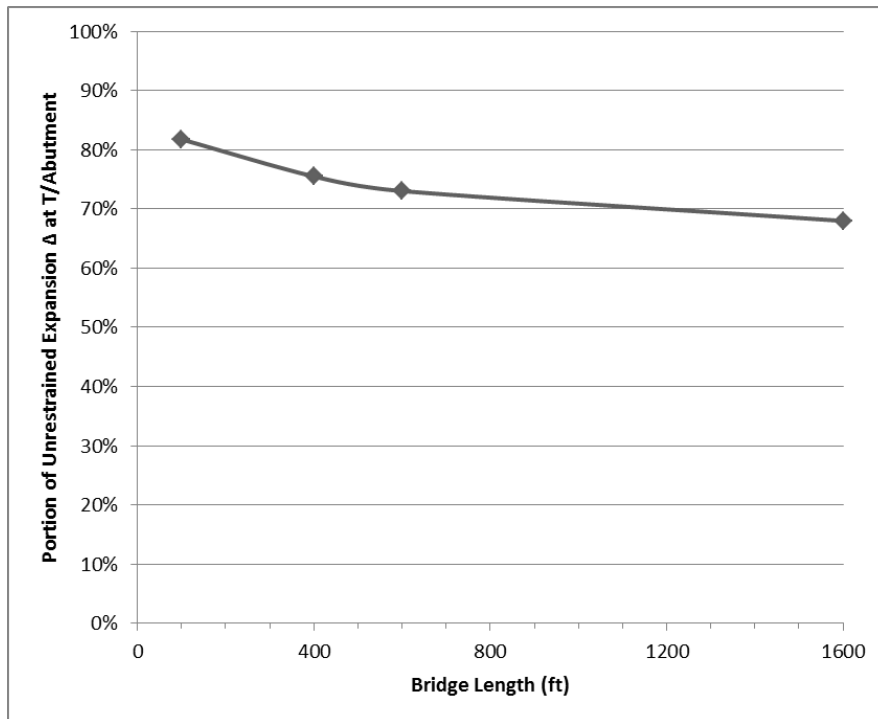


Figure 23. HP14x117, zero-skew FE models: Percentage of unrestrained thermal expansion displacement ($\Delta_{\text{Unrestrained}}$) observed at T/abutment vs. overall bridge length.

Finally, even as the percentage of the theoretical thermal displacement transmitted to the abutments decreases as IAB length increases, the rotations of the abutments continue to increase. The continued rotation of the abutments reduces pile-head fixity in long IABs,

decreasing the stresses in the H-piles. It is the combined effect of all of these parameters on the 3-D response of the bridge that permits H-piles to remain elastic at very long lengths in zero-skew IABs.

3.3.4 Revised H-Pile Orientation

As part of our exploration of IAB behavior beyond the basic parametric scope, we critically examined pile orientation. In our 3-D models, each H-pile in the pile group displaces slightly differently in space under thermal loading because of the differential translation and rotation of the abutment. For each pile, the maximum stress developed in the steel is a non-linear function of its orientation relative to its unique 3-D displacement. Changing an individual pile orientation changes the global stiffness, and in turn, affects the displacement response.

Conceptually, in a given bridge design, a preferred orientation could be selected for each individual pile in the bridge to equalize its share of the thermal loading and minimize the steel stresses. While theoretically interesting, this would require intensive, iterative computations; and it is infeasible from a field constructability standpoint. However, the authors noted that because the primary direction of foundation movement caused by thermal loading is parallel to the longitudinal axis of the bridge, an easily constructible alternate orientation for H-piles in IABs might yield significant benefits in reducing pile stress, particularly in high-skew bridges. Figure 26 illustrates the proposed alternate orientation. Here, the H-pile web remains parallel to the bridge longitudinal axis regardless of skew, ensuring that the primary direction of pile motion aligns with the strong-axis bending of the pile. While the foundation system generates greater resistance to thermal movement (which is likewise transmitted to the abutments and superstructure), the pile steel stresses in skewed bridges are lower than those in the current IDOT orientation because the weak-axis component of the resultant moment is significantly reduced. For comparison, we also examined the use of a weak-axis alternate orientation for H-piles, where the pile web remains perpendicular to the bridge longitudinal axis regardless of skew. Many states that use IABs currently employ a weak-axis H-pile orientation in design; and accordingly, such an orientation is of interest to IDOT.

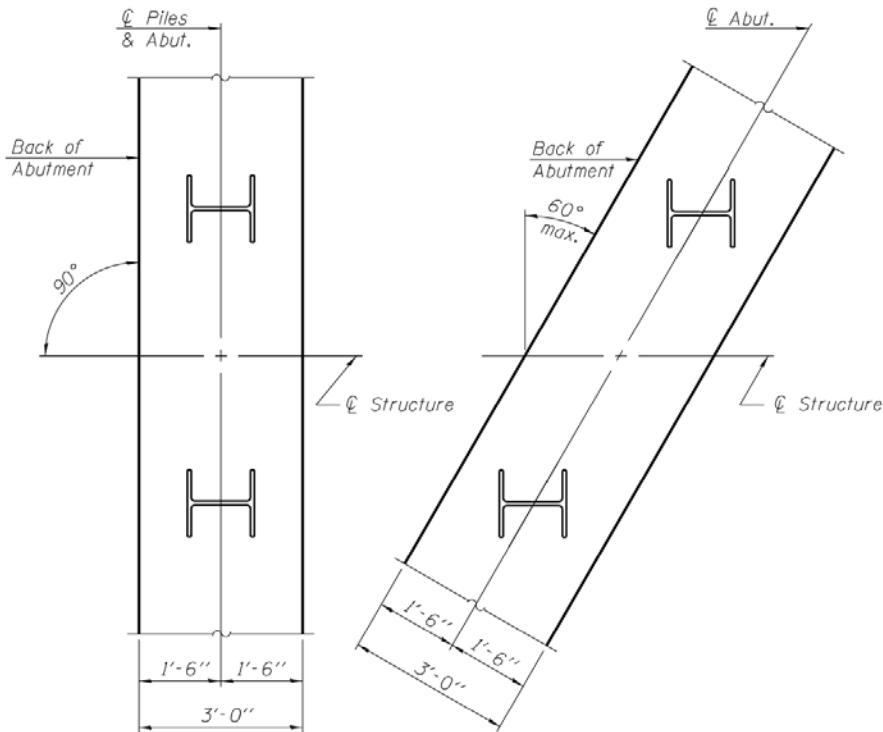


Figure 24. Proposed strong-axis alternative orientation plan for Illinois IABs founded on H-piles.

Figures 27 and 28 compare the moments and corresponding stresses generated in HP14x117 piles supporting 400-foot bridges; based on our observations during the parametric study, we expect similar results in H-pile bridges of varying lengths, intermediate spans, and pile sizes. The figures clearly show that although the strong-axis alternate orientation attracts roughly 20% to 30% additional moment resistance compared with the lower of either the IDOT standard or weak-axis alternate configurations at a given skew, the pile stresses remain considerably lower. Though the additional pile resistance generated will vary depending on other bridge parameters and must be accommodated in the abutments and superstructure, a strong-axis H-pile orientation shows considerable promise for improving feasible overall IAB lengths in skewed configurations.

Figure 27 also illustrates that the stresses in the worst-case pile differ from the average pile stress in the all three orientations. The worst-case pile (typically in the acute corner) in the strong-axis alternate orientation experiences greater localized effects than the corner piles in the IDOT and weak-axis alternate orientations. This is beneficial in IABs that approach the limits of acceptable length and skew because the remaining piles in the group with the strong-axis alternate orientation have more available capacity prior to first yield than the corresponding piles in the IDOT and weak-axis configurations, where the worst-case pile result agrees more closely with the average of the group.

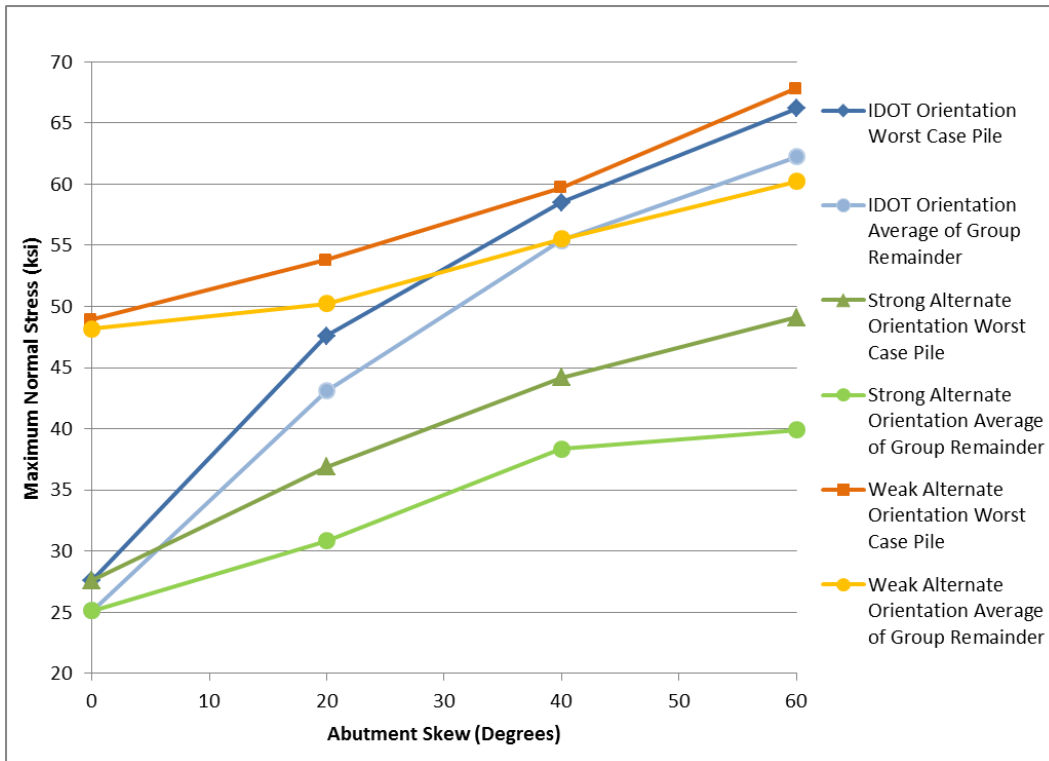


Figure 25. HP14x117, 4 x 100 ft IAB: Variation of pile stress with pile orientation.

In scenarios where yielding initiates in the worst-case pile, more significant load redistribution may occur throughout the pile group with the strong-axis alternate orientation before the worst-case pile begins to experience significant plastic damage. In the current IDOT orientation, soon after the worst-case pile begins to yield, the remaining piles also begin yielding, and the performance of the group as a whole may degrade more rapidly. Though outside the capability of our linear-elastic models to predict, the behavior qualitatively described here is worthy of further research and may afford significant benefits in permissible IAB length and skew if limited plasticity is permitted in pile steel.

Even without allowing for plasticity to develop in the piles, based on these results the authors recommend that IDOT consider changing the standard orientation of its IAB H-piles to align the webs with the longitudinal axis of the bridge, regardless of skew. The increased proportion of strong-axis bending may allow considerable increase in overall IAB lengths, particularly in skewed bridges. Figure 29 demonstrates the length benefits derived at high skews from changing the orientation of HP14x117 piles, where the proposed strong-axis alternate orientation can handle roughly 200 ft of additional IAB length before the onset of yield at a flange tip compared with the current IDOT orientation. At all skews, the strong-axis alternate orientation performs considerably better than its weak-axis counterpart throughout the linear-elastic range of the piles.

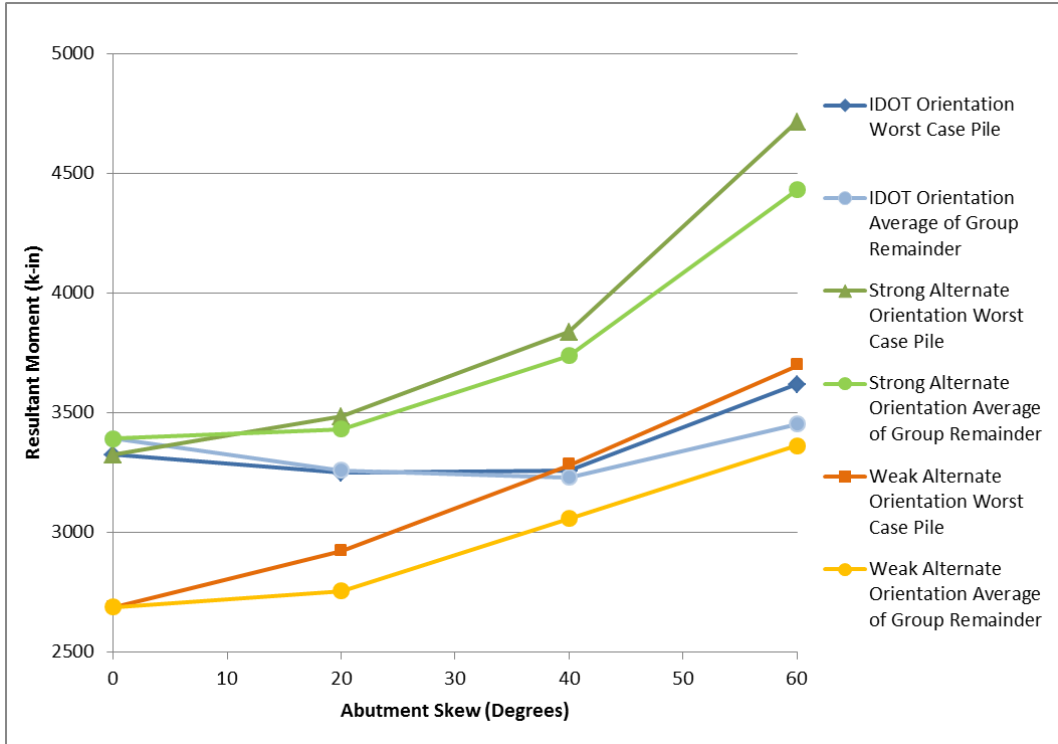


Figure 26. HP14x117, 4 x 100 ft IAB: Variation of pile resultant moment with pile orientation.

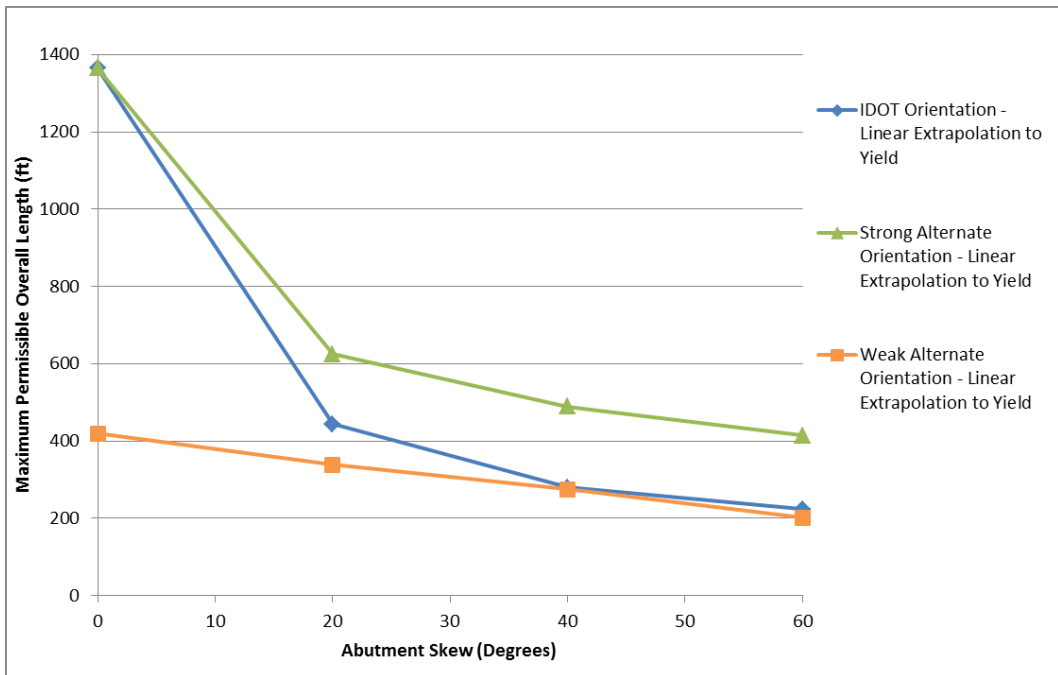


Figure 27. HP 14x117: Effect of orientation on permissible length vs. skew.

3.3.5 Compacted Sand Backfill

Olson et al. (2009) concluded that backfill soil pressures acting on the abutments of an IAB have no significant effect on pile loadings. However, this conclusion was drawn from a handful of 3-D models at moderate skews using a static force modeling technique. In contrast, this study suggests that backfill pressures play a substantial role in the response of IAB piles to thermal expansion.

Using a shell pile-supported IAB, Figure 30 illustrates how pile moments are influenced by compacted granular backfill behind the abutments. In IABs with low or moderate abutment skew, backfill soil passive pressures significantly reduce pile moments compared with an identical bridge without backfill. Surprisingly, as skew increases to approximately 40° , the beneficial effects vanish, and at an extreme skew of 60° , the backfill pressures actually cause an increase in pile moments. The effect of backfill is one reason why without live load, thermal contraction generates higher pile stresses than expansion in low-skew bridges, as seen in Figure 8. Shell piles were chosen to illustrate the Figure 30 results because their uniform stiffness in any direction serves to isolate the backfill effect. In contrast, the changes in pile stress are more pronounced in H-piles where additional transverse abutment drift at high skews is especially punishing on the weak-axis bending mode. The authors define this unusual behavior in terms of deformation of the superstructure in the horizontal plane and the moderating role that friction between the abutment backwall and the compacted backfill soil plays in that movement.

As an IAB expands, it pushes the abutments into the compacted backfill, and passive soil pressures build up on the concrete backwall as displacement increases. The resultant force of the backfill pressure on one abutment forms a couple with its counterpart at the opposite end of the bridge. In IABs with minimal skew, the resultant passive forces serve only to generate additional resistance to the thermal displacement and cause a slight amount of additional abutment rotation, both of which tend to reduce pile loads. At low skews, friction mobilized between the abutment and the backfill is sufficient to resist any eccentricity between the components of the backfill forces normal to the abutment faces, and no net moment is exerted on the superstructure. However, when the abutment skew exceeds the abutment-backfill interface friction angle (i.e., no greater than 30° , and conservatively assumed as 15° in this study), the resultant passive force couple begins to exert a significant moment on the bridge and cause significant global rotation of the superstructure in the horizontal plane. This leads to substantial transverse movements of the abutments (rather than the purely longitudinal movement that occurs when skew is low) which considerably increases bending of the foundation piles. This effect is also enhanced with skew because the area of backfill in contact with the abutment doubles in a 60° skew bridge compared with a zero-skew configuration, which correspondingly increases the magnitude of the passive soil forces.

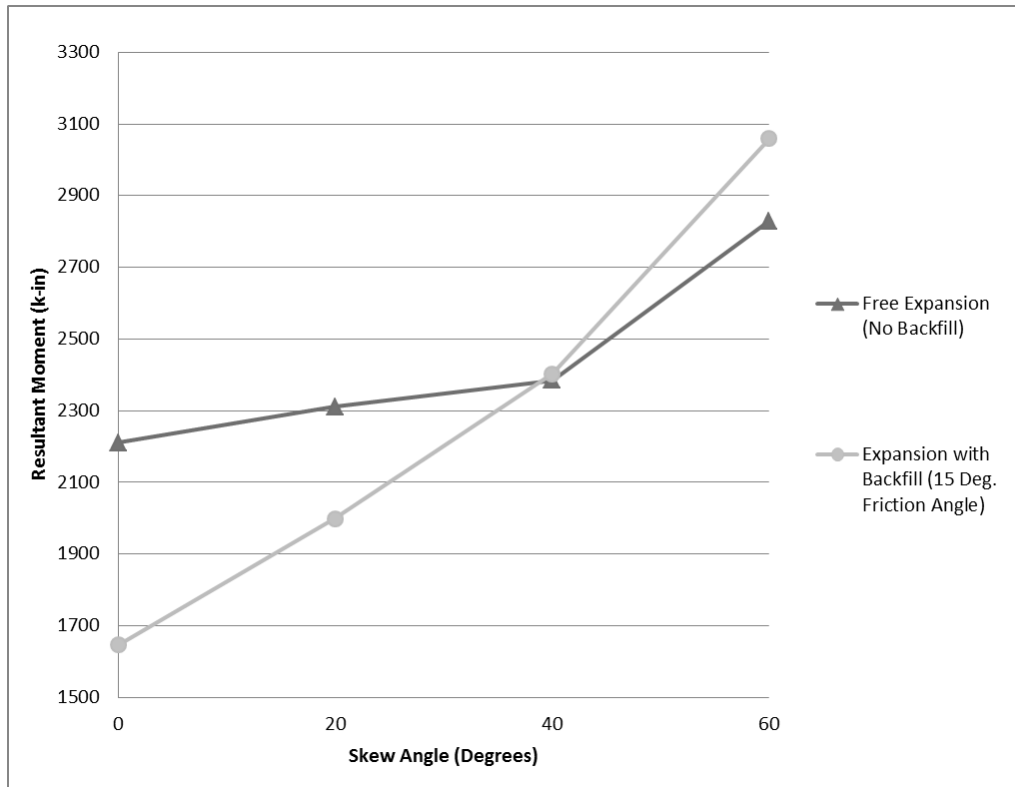


Figure 28. Effect of compacted granular backfill on pile loads. Max. resultant moment vs. skew, MS14x0.25, 4 x 100 ft span bridges.

Therefore, for the vast majority of bridges in Illinois that might be constructed integrally (i.e., skews less than about 40°), backfill passive soil pressures tend to reduce pile loads. Thus, the authors recommend using a compacted backfill behind IAB abutments, both for its beneficial effect on the piles and the superior support it provides to the approach slabs as noted by Olson et al. (2009). However, should IDOT choose to build IABs with abutment skews significantly greater than 45°, caution should be used with regard to backfill design. For example, specific interface details between the abutment and backfill soils could yield significantly greater frictional resistance than the 15° component assumed in our study; this may extend the benefits of compacted backfill to bridges with higher skews on a case-by-case basis.

The authors further suggest that IDOT detail the drainage system and other non-structural components behind the abutment in a way that will not cause an undue reduction in friction between the backfill soil and the abutment. If friction were completely eliminated (in theory) between the abutment and the backfill, the resulting passive pressures normal to the abutment backwall are significantly more problematic for the foundation piles, even at lower skews; the increased transverse abutment movement erases the modest benefits of backfill against thermal expansion of the superstructure.

Finally, we note that significant axial loads were induced in the girders by the backfill, and that they were substantially reduced when backfill was removed. Although this observation was beyond the scope of our current study, it has been observed by a number of researchers and warrants further consideration by IDOT to ensure safe and efficient superstructure design.

The project team also considered the possibility of resistance to global bridge rotation offered by the intermediate piers, in light of the fact that we modeled them as simple roller

supports. However, we concluded that the idealized roller assumption at the intermediate supports is reasonable because the displacements generated by the horizontal rotation of the bridge superstructure at the intermediate supports are too small to argue that the steel girders could significantly restrain them. The flexibility of the girder webs on top of the intermediate bearings, combined with a relative lack of transverse rotational restraint in that connection means that the system is simply not stiff enough to generate much resistance to the rotation of the bridge deck in the horizontal plane. While some additional resistance to horizontal superstructure rotation might be afforded in PPCI girder IABs with continuity diaphragms at the intermediate piers, this was not explored as part of the project scope.

3.3.6 Live Loading

Our parametric study shows that the presence of live loads on an IAB can significantly affect the performance of the pile foundations; in fact, for nearly all of the bridge configurations analyzed, live load effects determined which thermal load case caused the maximum stresses in the piles. The impact of AASHTO HL-93 live loading applied to IABs experiencing extreme thermal displacements is shown for shell pile foundations in Figure 31. Interestingly, live load increases pile moments during thermal expansion and relieves them during thermal contraction. In both cases, the magnitude of the effect decreases with increasing abutment skew.

While contraction frequently causes higher pile loads than expansion in low-skew bridges, the increase in moments caused by the addition of live load is large enough to make expansion the critical loading condition for the IAB foundations at all skews. This behavior results because of the effect that the imposed gravity load has on abutment rotation. The combined (and sometimes competing) effects of abutment rotation and thermal displacement of the pile head dictate the loads developed in the piles. Superstructure deflections related to live load have a secondary effect on the abutment displacement but substantially change their rotation. It is important to recall that thermal expansion causes abutment rotation outward from the center of the bridge, while contraction causes inward abutment rotation relative to the piles. Because live load generally causes the abutment to rotate inward, it directly shifts the pile-head conditions toward fixed-head behavior under thermal expansion, while introducing additional rotational freedom to the pile heads during contraction. As a result, the critical moments at the pile heads are exacerbated by live load in expansion and improved in contraction.

Also notable in Figure 31 is the general decrease in the live load effect on pile loads with increasing skew. Because the effect is driven by the amount of restraint to abutment rotation provided by the superstructure, its magnitude diminishes at higher skews. This is due to the increasing influence of the more flexible torsional and transverse components of the superstructure stiffness on the behavior. Finally, it is important to recall that because the authors modeled the HL-93 load in a single end bay (as opposed to throughout the entire structure), the live load effects on pile loads observed in this study are probable service conditions and are not overly conservative, even under extreme thermal loading.

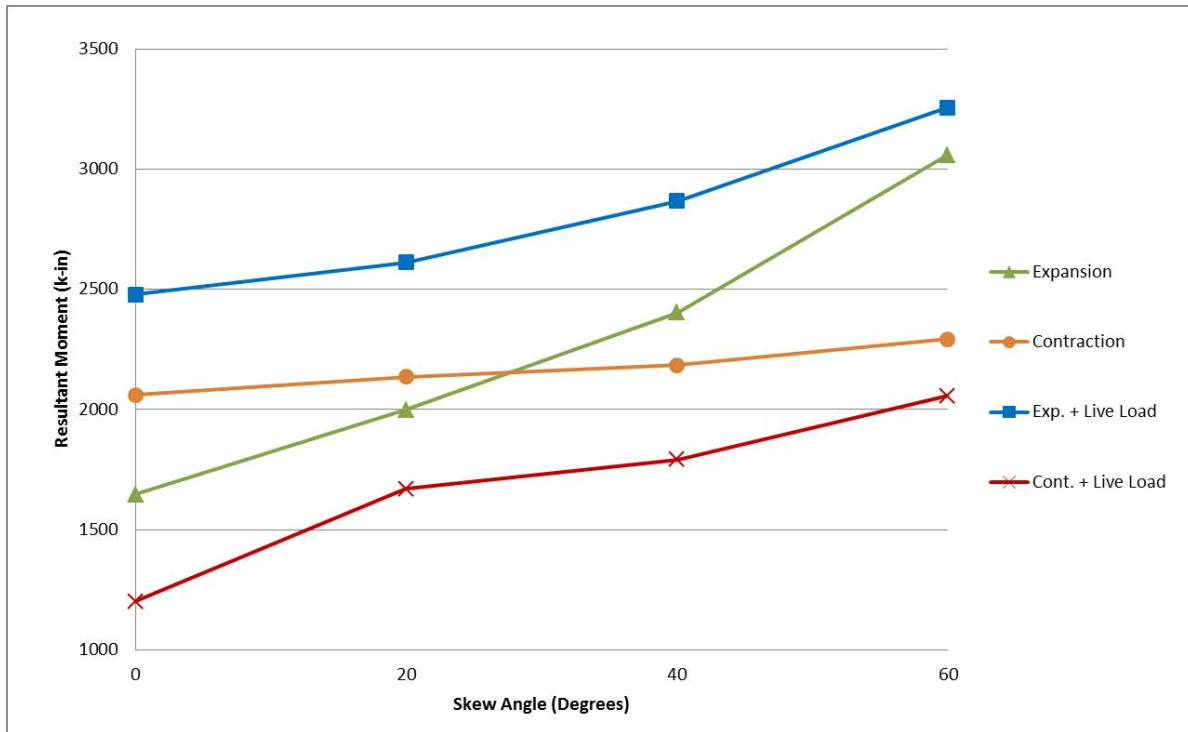


Figure 29. Maximum resultant moment for MS14x0.25 piles vs. skew for 4 x 100 ft span bridges under varying load cases.

3.3.7 Intermediate Span Length

Careful review of Figures 12 and 14 reveals that for bridges of a given length and skew, pile stresses are significantly higher in bridges with longer spans between intermediate supports. While the parametric study generally indicates that this trend holds for the IAB configurations considered, the extent that intermediate span length affects pile behavior depends on a number of other variables. Furthermore, a change in the intermediate span of a bridge requires modification of numerous other design components, each of which uniquely affects IAB behavior. For example, the bridge models with 200-ft spans utilize deep plate girders rather than more compact W36 girders. This directly affects the superstructure stiffness in all directions, and it also requires the height of the abutment backwall to increase significantly. While deeper, stiffer girders might reduce abutment rotation, thereby increasing pile loads, a taller abutment does not need to rotate as much to accommodate a similar magnitude of thermal displacement. The longer intermediate spans also provide greater flexibility, perhaps counteracting some of the additional stiffness imparted to the abutment with a deeper girder cross-section. Thus, the net effect of increasing intermediate span length tends to increase pile stresses, but the magnitude of increase is highly variable with individual bridge geometries.

Also, by extension, these results somewhat qualify the assertion of Olson et al. (2009) that girder type (PPCI or steel) and size play minimal roles on the pile stresses. Olson et al. (2009) concluded that, for the sets of steel and PPCI girders considered, the difference in rotational restraint on the abutments approximately offset the differences in thermal expansion between the two materials. While this is true for the limited subset of girders and 3-D geometries considered in the 2009 study, our expanded 3-D parametric results demonstrate that this conclusion is not generally applicable. Because the stiffness of the superstructure in all

directions (i.e., the design of the girders) can strongly influence abutment rotation, in some configurations, it can far outweigh a corresponding effect on the thermal displacements and be the controlling pile stress parameter.

3.3.8 Time-Dependent Shrinkage Effects

Though it was not originally part of the parametric study, the research team elected to explore the effects of concrete shrinkage on Illinois IABs because of the significant work being conducted on time-dependent IAB behavior by others. This was partially motivated by the assertion by Frosch that shrinkage-induced ratcheting of contraction displacements would typically be the controlling load history for Indiana IABs (Frosch 2011). We executed a series of analyses incorporating shrinkage in both the usual steel girder bridge models and in PPCI bridge models.

The results of these analyses indicate that while shrinkage may not significantly affect pile loads in IABs with steel girders, in PPCI bridges it can potentially result in pile stresses that exceed the expansion plus live load combination (defined as the critical case above). Additionally, we noted that significant axial forces developed in the superstructure because of shrinkage, consistent with the literature. Complete results and discussion of our analyses incorporating shrinkage are provided in Appendix A.

3.3.9 Plasticity in Pile Steel

The authors encountered research and design approaches in a number of leading IAB states that permit significant plastic deformation of pile steel as a matter of practice in order to increase their ability to build bridges integrally (Dunker and Abu-Hawash 2005; Burdette et al. 1999; Frosch 2011). Additionally, in our parametric analyses, we repeatedly observed that the majority of the foundation piles in skewed bridges possessed substantial additional bending capacity when the acute corner pile first yielded. We anticipate that considerable load redistribution likely occurs throughout the pile group in skewed bridges before the onset of significant plastic damage. Though not included in the initial project scope, the research team investigated the performance of plastically deforming piles in IABs. By quantifying the remaining capacity in the piles beyond first yield and generating some additional FE models that incorporate material non-linearity in the pile steel, we identified potential benefits in terms of IAB length and skew by permitting plastic deformation in the foundation pile steel. Appendix B provides details regarding pile steel plasticity.

CHAPTER 4 INSTRUMENTATION AND MONITORING OF TWO ILLINOIS INTEGRAL ABUTMENT BRIDGES

The project scope included instrumenting three integral abutment bridges constructed in Illinois that approached (or exceeded) the current IDOT limitations for length and/or skew. Eventually, the IABs selected for instrumentation were: (1) Illinois State Route 108 over Macoupin Creek (near Carlinville, Illinois); (2) Peoria Airport Road over Kickapoo Creek and Union Pacific Railroad (Peoria, Illinois); and (3) Illinois State Route 16 over the Embarrass River (near Charleston, Illinois). Regrettably, a lack of state and district funding resulted in the third bridge not being let for bid during the project lifetime. Furthermore, contractual issues with ICT resulted in the instrumentation packages for the first two bridges not being completed.

This section summarizes the instrumentation packages intended for the IABs; details the instruments used for each bridge; describes the instrument preparation, calibration, and installation (as appropriate); and summarizes the current status of the first two bridges and the remaining instrumentation that was procured for the third bridge.

4.1 GENERAL INSTRUMENTATION SCHEME

The instrumentation scheme for each of the IABs consisted of five types of instruments used to measure stress in the driven-pile foundation and longitudinal, transverse, and rotational displacement of the integral abutment. The five instruments include vibrating wire (VW) strain gages; vibrating wire (VW) temperature sensors; micro-electro-mechanical systems (MEMS) tiltmeters; string potentiometers; and MEMS biaxial inclinometers. All instrumentation is confined to a single bridge abutment, with instrumentation applied at two driven piles, two reference piles, the backwall of the abutment, and one of the bridge girders. Figure 32 presents a simple schematic of the instrumentation scheme. Regarding the instrumented piles, one was oriented for strong-axis bending while the other was oriented for weak-axis bending, to evaluate the impact of orientation on pile stresses.

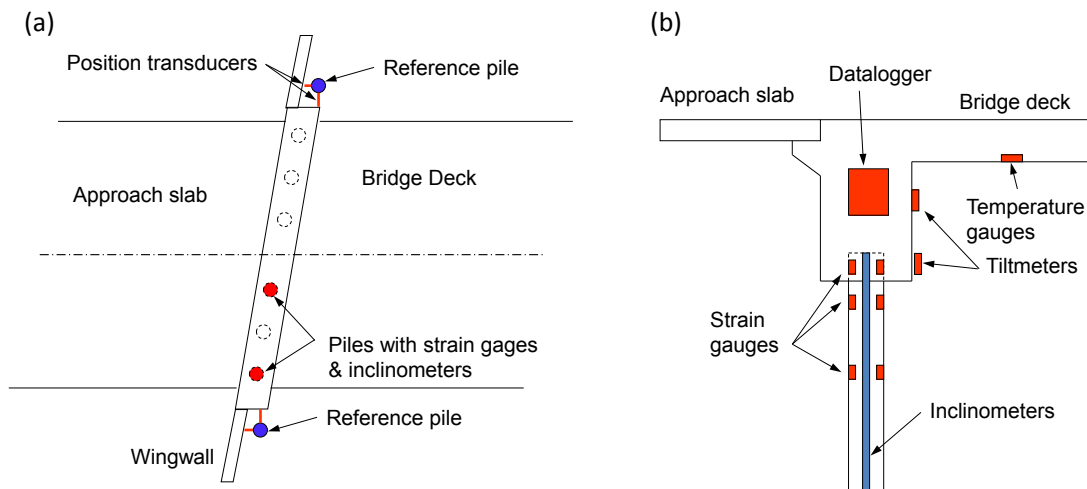


Figure 30. Schematic illustration of instrumentation scheme used at project IABs.

4.2 INSTRUMENTS AND DATA-ACQUISITION SYSTEM COMPONENTS

4.2.1 Vibrating Wire Strain Gages

The strain gages are Geokon model 4000 VW strain gages with built-in thermistors. The gages are durable enough to endure pile driving, yet provide long-term stability, high resistance to water intrusion and unobstructed use over long signal cables. Gage readings output via a 16x4 channel multiplexer over two channels, the first reading micro-strain and the second reading temperature. The Model 4000 cut-sheet is available at <http://www.geokon.com/products/datasheets/4000.pdf>.

As illustrated in Figure 32, two piles were instrumented with strain gages, an exterior and an interior pile. Eight gages per pile flange were distributed longitudinally along the pile, as illustrated in Figure 33a. To protect the gages during pile driving, angle iron acts were welded over them as a protective covering (Figure 33b). Small boxes enclose all loose strain gage wires to prevent shearing during pile movement or excessive water damage. Appendix C provides details of strain gage installation and calibration.

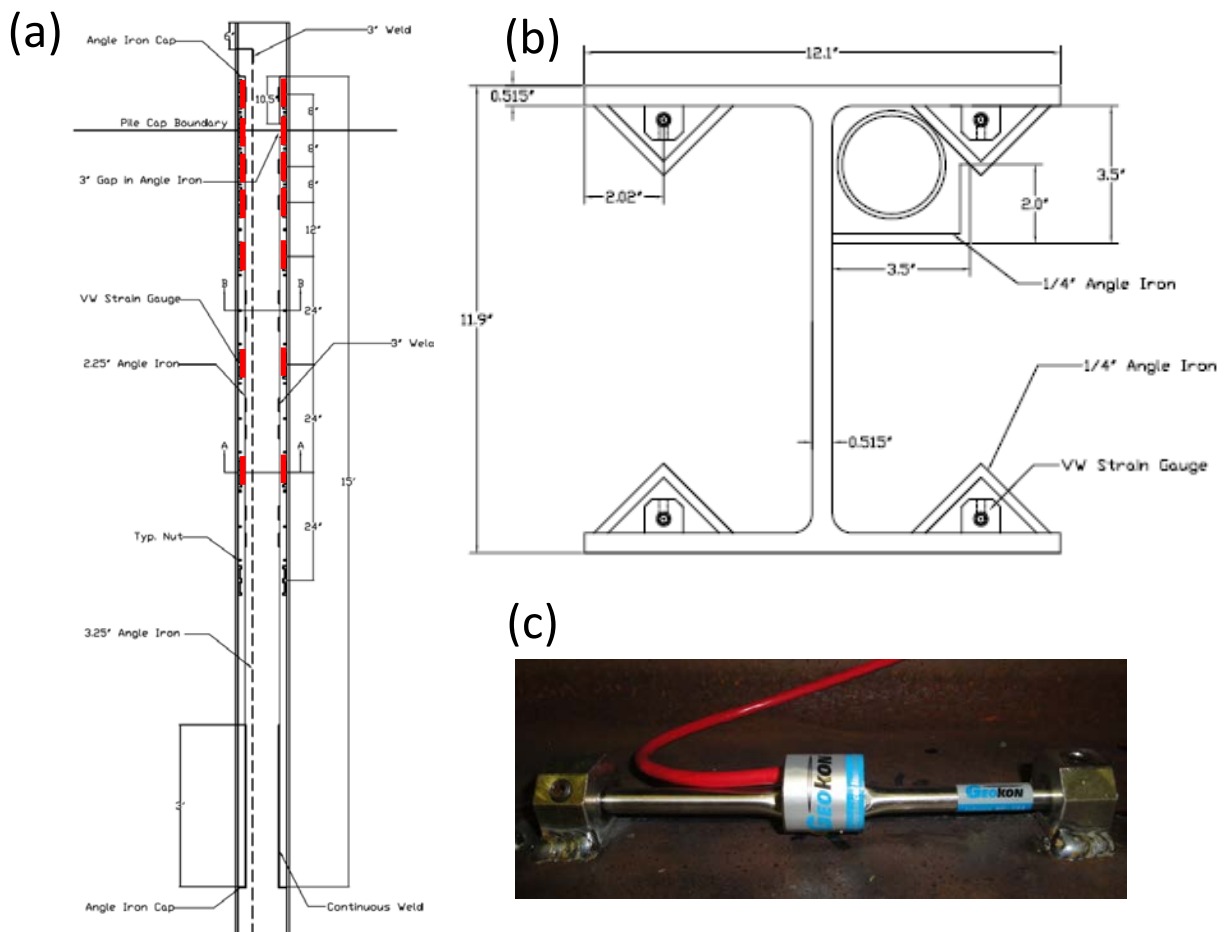


Figure 31. (a) Strain gage distribution on H-pile; (b) cross-section illustration of VW strain gage and inclinometer casing protection scheme; (c) Geokon Model 4000 VW strain gage.

4.2.2 Vibrating Wire Temperature Sensors

Geokon Model 4700 (<http://www.geokon.com/products/datasheets/4700.pdf>) VW temperature sensors (with backup thermistors) were selected for the project. The temperature sensors were installed at the top, middle, and bottom of a selected bridge girder.

4.2.3 Micro-Electro-Mechanical Systems (MEMS) Tiltmeters

Geokon Model 6160 (<http://www.geokon.com/products/datasheets/6160.pdf>) MEMS tiltmeters were installed at two locations on the front face of the abutment above and below the pile cap-abutment cold joint. The sensor is equipped with an internal thermistor. These sensors will monitor tilt of the abutment and determine whether differential tilt occurs at the cold joint.

4.2.4 Linear String Potentiometers

Celesco Model SP2-4 (<http://www.celesco.com/datasheets/sp1.pdf>) compact string potentiometers were attached to the reference piles in two orthogonal directions (at each location) to monitor deflection of the abutment relative to a reasonably isolated position. The reference pile was driven into a 10-ft deep pre-drilled hole, and the upper portion of the hole was backfilled with bentonite to allow the abutment to move independently of the pile.

4.2.5 MEMS Inclinometers

A Geokon Model 6100 (<http://www.geokon.com/products/datasheets/6100.pdf>) biaxial inclinometer was selected to provide redundant (campaign-style) measurements of abutment and pile deformation. Geokon inclinometer casing was installed in the protective channel along each of the instrumented piles (see Figure 32) after driving. The annulus between the casing and the channel was filled with grout. Additional details regarding the installation are provided in Appendix C.

4.2.6 Multiplexers

Multiplexers are used in the data-acquisition system to expand the number of channels that a data logger can read. These were used to provide cost savings, given the large number of instruments used for the project. We selected Geokon Model 8032 16x4 for the VW instruments and MEMS Multiplexers for the MEMS instruments. The 16x4 multiplexers accommodate up to 16 instruments, and the MEMS multiplexers accommodate up to eight instruments.

4.2.7 Data Loggers

Data loggers are the key component of the data-acquisition system. The MICRO-1000 Dataloggers selected for this project consist of a Model CR 1000 Measurement and Control System and AVW200 Vibrating Wire Spectrum Analyzer and are used in conjunction with the Multilogger software, all produced by Campbell Scientific. When coupled with the maximum of six multiplexers, the MICRO-1000 Datalogger may read a maximum of 96 instruments.

4.3 ILLINOIS ROUTE 108 OVER MACOUPIN CREEK

4.3.1 Bridge Details

The first IAB instrumented during the project was IDOT structure number 059-0509 on Illinois State Route 108 over Macoupin Creek, approximately 1.5 miles east of Carlinville, Illinois. Figure 34 provides the bridge plan. The four-span bridge is 320 ft long with no skew. The bridge deck is supported by six, 48-in.-deep pre-cast, pre-stressed concrete I-beams, and each abutment is supported on 6 HP12x63 piles.

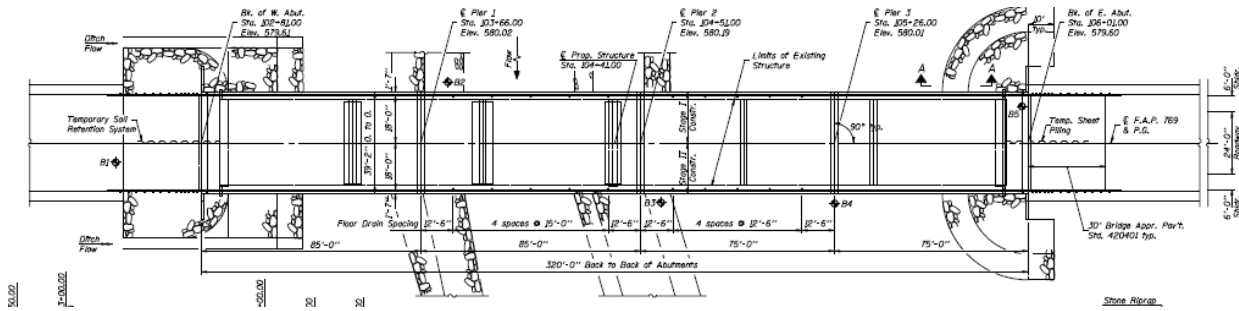


Figure 32. Plan view of IDOT SN 059-0509.

4.3.2 Instrument Installation

Six Phase I production piles were driven in March 2009. Two Phase II production piles (42.5-ft-long HP12x63) were delivered to the project team for instrumentation in April 2009, and these piles were driven in September 2009. In addition, two isolated reference piles were driven at this time. Figure 35 provides a plan and section view of the strain gage cabling.

All remaining instruments (tiltmeters, temperature sensors, and string potentiometers) and data-acquisition system equipment were installed at a later date, as illustrated schematically in Figure 36.

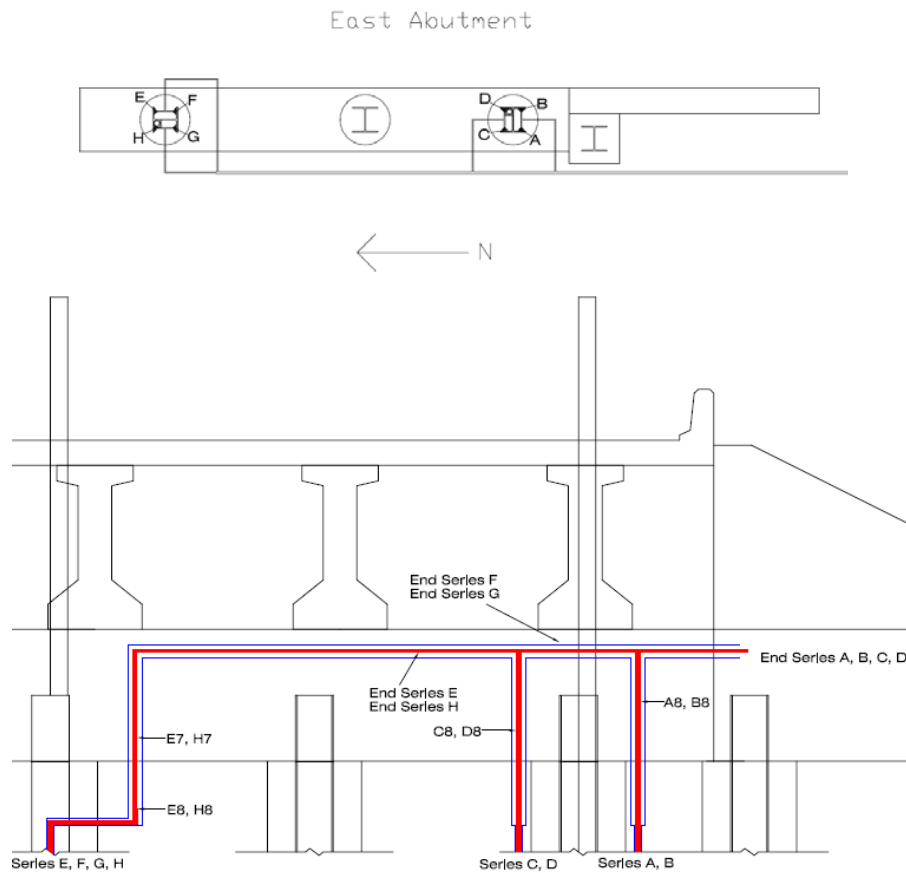


Figure 33. Plan and sectional view of strain gage instrumentation at east abutment.

4.3.3 Current Status

As of August 2011, all instruments are functioning. Because of contractual issues, the instruments were not integrated into the multiplexers and data logger. In addition, a power supply (i.e., solar panels and 12-volt battery system) must be installed at the site to operate the instruments and data-acquisition system.

4.4 PEORIA AIRPORT ROAD OVER KICKAPOO CREEK AND UNION PACIFIC RAILROAD

4.4.1 Bridge Details

The second IAB instrumented during the project was IDOT structure number 072-0201, Peoria Airport Road over Kickapoo Creek and the Union Pacific Railroad in Peoria, Illinois. Figure 37 provides the bridge plan. The three-span bridge is 330 ft long with a 30° skew. The bridge deck is supported by nine, 45-in.-deep plate girders, and each abutment is supported on 17 HP10x42 piles.

4.4.2 Instrumentation Installation

Two Phase II production piles (45-ft-long HP10x42) were delivered to the project team for instrumentation in spring 2010, and these piles were driven in fall 2010. In addition, two isolated reference piles were driven at this time. All remaining instruments (tiltmeters, temperature sensors, and string potentiometers) and data-acquisition system equipment were installed at a later date.

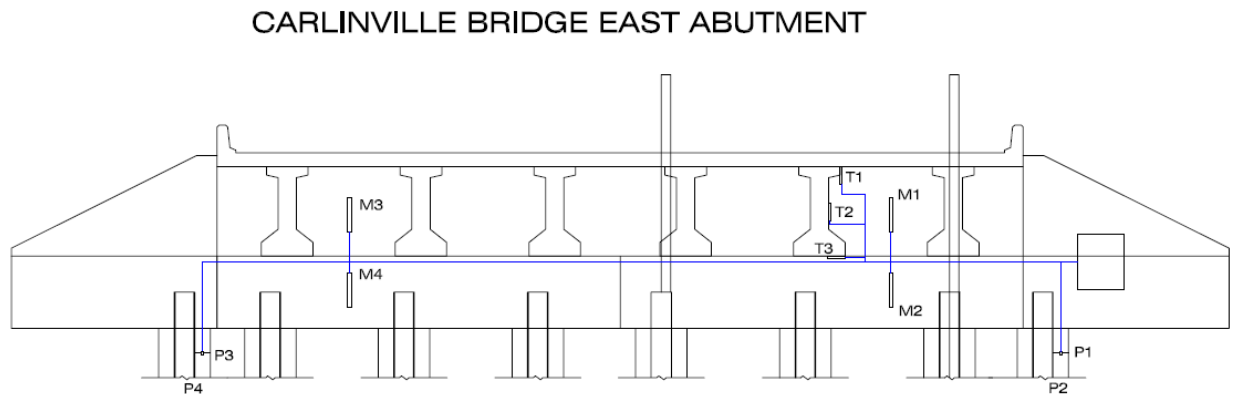


Figure 34. Sectional view of east abutment illustrating locations of instruments.

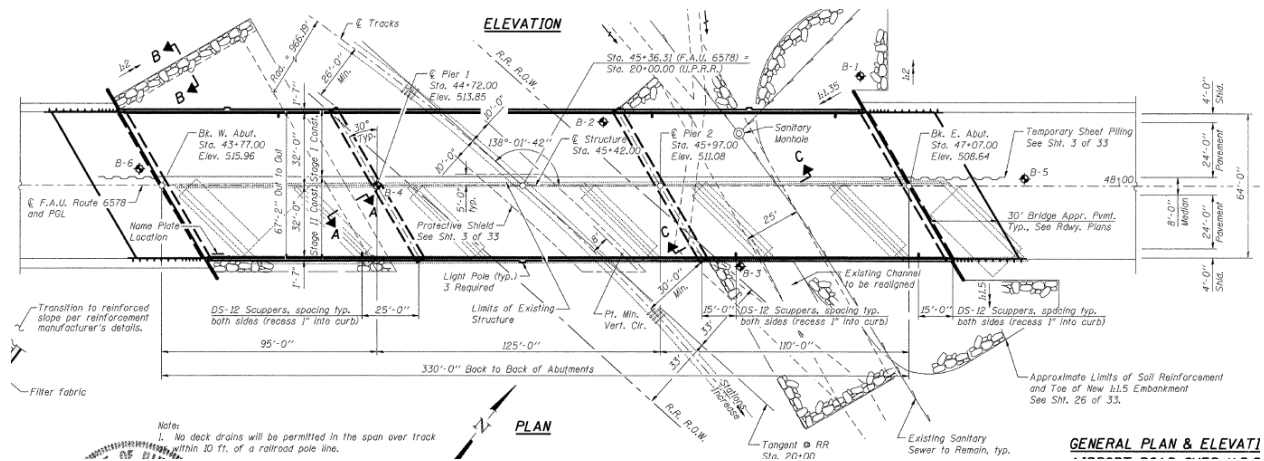


Figure 35. Plan view of IDOT SN 072-0201.

4.4.3 Current Status

As of August 2011, all instruments are functioning. Because of contractual issues, the instruments were not integrated with the multiplexers and data logger. In addition, a power supply (solar panels and 12-volt battery system) must be installed at the site to operate the instruments and data-acquisition system.

CHAPTER 5 CONCLUSIONS AND RECOMMENDATIONS

The considerable advantages of constructing bridges integrally have increased the popularity of these structures throughout the United States, including in Illinois. While IABs are the preferred bridge type in Illinois, current IDOT restrictions on their length and skew are relatively conservative compared with those in other states, and they are based more on engineering experience and judgment than thorough analysis. While a previous study by Olson et al. (2009) highlighted many of the important parameters affecting IAB performance, a more complete investigation of Illinois IAB behavior was needed to fully evaluate these parameters and allow IDOT greater confidence in revising its IAB length and skew limitations.

To establish a more rigorous technical basis for increasing current IDOT IAB length and skew limitations, this study used a suite of 3-D FE models that evaluated parametric variations in Illinois IAB behavior. The analytical research effort was complemented by a review of pertinent IAB literature, discussions with leading IAB researchers and DOT officials from other states, and preparations for acquisition of data from field monitoring of two recently constructed Illinois IABs. While primarily focused on assessing the performance of the pile foundations, the research team also characterized several other important aspects of IAB behavior. The primary objective of this research was to identify, based on pile performance, bridge configurations that would not exceed the pile steel yield stress using typical IDOT construction details. Figures 38 and 39 summarize our predictions of maximum permissible IAB lengths at varying skews for concrete-filled shell piles and H-piles, respectively.

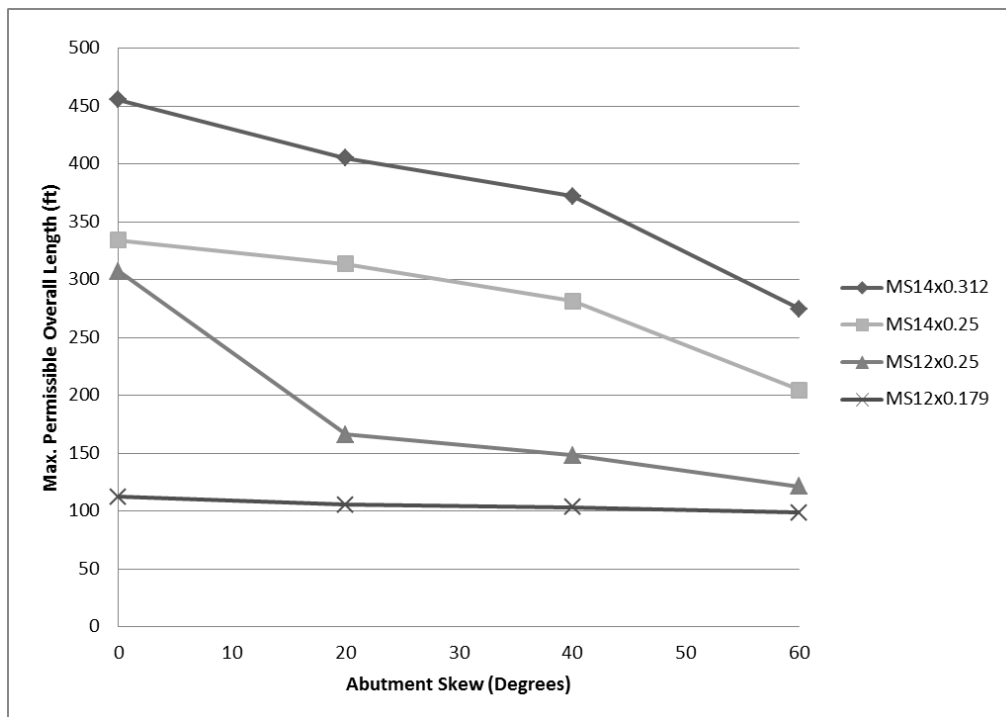


Figure 36. Shell pile summary: Permissible IDOT IAB lengths vs. skew (100-ft intermediate spans).

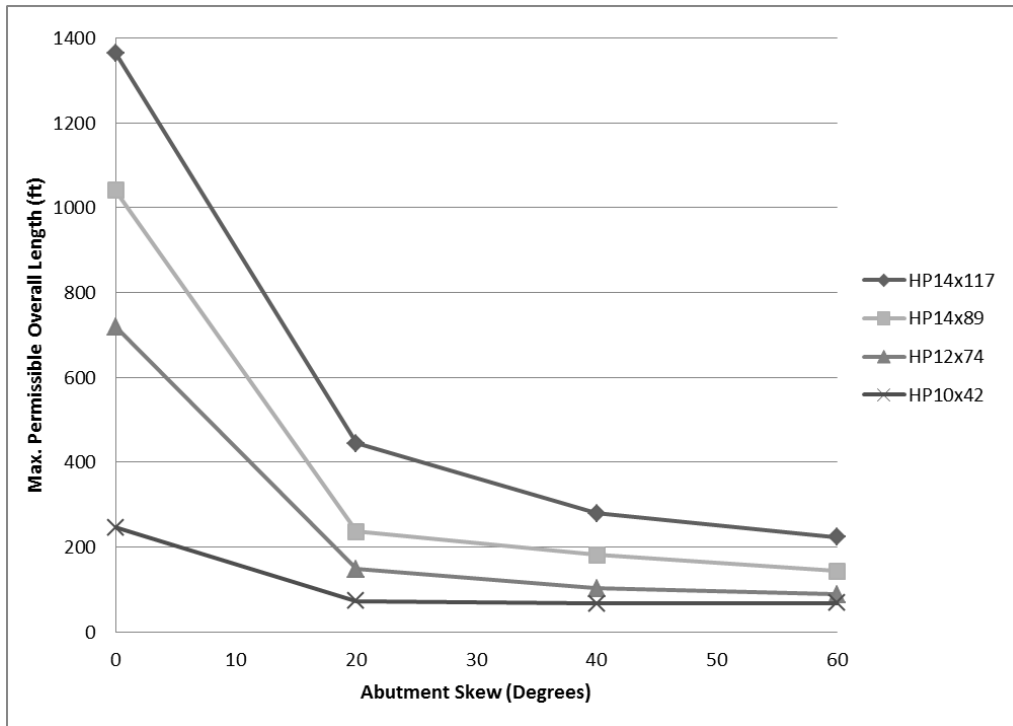


Figure 37. H-pile summary: Permissible IDOT IAB lengths vs. skew (100-ft intermediate spans).

The projected maximum allowable lengths for each pile involve some judgment, particularly for zero-skew bridges founded on HP12x74 and HP14x89 piles. For these two cross sections, the extrapolation to the first-yield condition was significantly beyond the longest bridge model analyzed (i.e., 600 ft). However, the authors have reasonable confidence in these extrapolations based on FE analyses of 1,200-ft and 1,600-ft bridges using HP14x117 piles. Also, a level of uncertainty is present because of the inevitable minor errors introduced by assumptions in the modeling process and other associated limitations, variations of the material properties in actual bridge construction, and most important, the planned and unplanned asymmetries present in any real IAB structure related to soil and other geometric variations at the site. Finally, the maximum allowable IAB lengths summarized here focus on the performance of the pile foundations; the authors acknowledge that other structural and non-structural components (e.g., the superstructure, abutments, approach slabs, or pavement joints) may further restrict thermal movements. However, the authors provide these limitations on pile performance so that IDOT may fully leverage the advantages of integral bridge construction as detailing of other bridge components and appurtenances advances.

The authors have noted in our review of the state of practice and our studies here that IABs display significant tendencies to deform asymmetrically in the field, even when the bridge is nominally symmetric. We have also addressed the possibility that substantial plastic deformation of the piles may occur without degradation of their performance. In light of these two somewhat disparate perspectives, the authors suggest that IDOT's current approach to prescriptive guidelines for IABs may serve the design community fairly well. By nominally permitting IABs up to first-pile steel yield under the somewhat idealized service performance limits examined in our study, IDOT would likely be acknowledging the possibility of a limited amount of pile plasticity in some real IAB designs because of simplifying the assumptions made in the design and asymmetric complexities present in the field. However, this can be done with

relative confidence, given the demonstrated success of plastically deformed piles in numerous tests and completed IABs elsewhere.

In addition to more completely quantifying the current elastic limits of Illinois IAB pile performance, the authors observed a number of structural mechanisms influencing IAB behavior that are of interest to IDOT from a design and detailing perspective. Based on our numerical analyses, the project team offers the following conclusions and recommendations regarding Illinois IAB design and behavior.

- While IABs with extreme abutment skew (e.g., 60°) do exhibit an additional decrease in pile performance compared with bridges with more moderate skews (e.g., 40°), this trend is generally not disproportionately large. With proper design and detailing to account for the 3-D aspects of thermal displacements, even IABs with extreme skew can be effective. Therefore, we recommend that IDOT consider relaxing any strict limitation on IAB skew in favor of provisions that acknowledge the combined effects of length and skew.
- The current IDOT H-pile orientation provisions are disadvantageous in skewed bridges because they permit excessive weak-axis bending. We recommend revising the standard to orient all H-pile webs parallel to the longitudinal axis of the bridge, regardless of skew. Though this revised orientation will increase the resistance in the piles (and the loads transmitted to the abutments and superstructure) in skewed bridges, it substantially reduces weak-axis bending and H-pile stresses correspondingly. With appropriate reevaluation of abutment and superstructure detailing, the end result may be considerably lighter H-pile sections and longer IAB lengths in skewed configurations.
- We recommend the use of compacted granular backfill behind the abutments. Backfill passive pressures are beneficial to piles resisting thermal expansion except in bridges with extreme skews (beyond 45°). Because these skews are relatively unusual (and likely only approved on a case-by-case basis), adequate care could be taken to design the backfill-abutment interface in such high-skew bridges. In all IABs, the authors emphasize the important role of friction between the abutment and backfill in resisting transverse abutment movements that are detrimental to pile performance. We recommend evaluating details of drainage and other non-structural components affecting the abutment-backfill interface to avoid reduction in friction.
- Live loads on IABs primarily affect thermally induced pile stresses by changing the rotation of the abutments. While the displacement of the pile head sees little change, the net increase or decrease in abutment rotation substantially changes the fixity condition at the pile head, increasing loads at the pile head under thermal expansion and relieving them in thermal contraction. As a result of this behavior, thermal expansion combined with live loading typically generates the greatest stresses in the piles of a given bridge. Also, we note that only a single end bay of the structure needs to see the HL-93 loading to generate these effects, making this loading scenario reasonably likely even during an extreme thermal cycle.
- Longer intermediate spans, combined with the effects of other associated parameters such as girder depth and abutment height, affect the stiffness and geometry of the IAB response and, by extension, the piles. While this effect depends on the individual bridge configuration, the increased intermediate span lengths tend to drive pile stresses higher, compared with similar shorter-span geometries.

- Time-dependent behaviors, such as concrete shrinkage, may significantly affect maximum pile stresses in certain IAB configurations. Specifically, IABs using PPCI girders may exhibit unusually high contraction displacements over the life of the bridge caused by shrinkage of the superstructure. In addition to affecting the piles, shrinkage may also induce additional axial loads in the superstructure. Therefore, we suggest IDOT consider incorporating shrinkage and other significant time-dependent behaviors such as concrete creep, pre-stress relaxation in concrete girders, and yearly increases in backfill pressure related to cyclic compaction in any subsequent IAB research.
- In addition to a growing body of research and successful IAB designs in other states utilizing the plastic capacities of foundation pile steel, our parametric study reveals the potential for significant load redistribution across the pile group in skewed bridges where the acute corner pile has reached first yield. We recommend IDOT further consider the potential benefits and risks of accounting for plastic deformation of pile steel in its IAB design methodology; additional Illinois IAB research should devote some effort to exploring pile plasticity as a means for further extending IAB length and skew limitations.

In addition to these findings, the research team also provides IDOT these additional suggestions for subsequent IAB research:

- We modeled the embedded connection of the girder to the abutment in our IAB models as a rigid interface. Because many of our results were strongly linked to the stiffness with which the superstructure restrains abutment rotation, further examination of this connection is recommended. More refined FE models or laboratory testing of the girder-abutment interface may reveal that full fixity is not achieved; this could significantly affect both the loads developed in the piles and the superstructure.
- The bridges modeled in this parametric study were symmetric, two-lane, 36-ft-wide bridges. Because the geometry of the superstructure has a dominant effect on the thermal movements of IABs, we recommend that further IAB research also explore bridges with different roadway widths, numbers of supporting piles, and asymmetries.

REFERENCES

- Abendroth, R. E., Associate Professor of Civil Engineering, Iowa State University. Personal communication, May 2011.
- Abendroth, R. E., and L. F. Greimann. "Field Testing of Integral Abutments," *Final Report*, Iowa Department of Transportation Project HR-399. Ames, Iowa: Center for Transportation Research and Education, Iowa State University, 2005.
- American Association of State Highway and Transportation Officials (AASHTO). *LRFD Bridge Design Specifications*, 5th ed. Washington, D.C.: AASHTO, 2010.
- American Institute of Steel Construction, Inc. (AISC). *Steel Construction Manual*, 13th ed. Chicago: American Institute of Steel Construction, Inc., 2005.
- Burdette, E. G., Professor of Civil Engineering, University of Tennessee, Knoxville. Personal communication, May 2011.
- Burdette, E. G., J. H. Deatherage, and D. W. Goodpasture. "Behavior of Laterally Loaded Piles Supporting Bridge Abutments—Phase I," *Final Report*, Tennessee Department of Transportation Project TNSPR-RES1081. Knoxville: Center for Transportation Research, University of Tennessee, Knoxville, 1999.
- Burdette, E. G., J. H. Deatherage, and D. W. Goodpasture. "Behavior of Laterally Loaded Piles Supporting Bridge Abutments—Phase II," *Final Report*, Tennessee Department of Transportation Project TNSPR-RES1190. Knoxville: Center for Transportation Research, University of Tennessee, Knoxville, 2003.
- Chen, W. F., and S. Santathadaporn. "Review of Column Behavior Under Biaxial Loading," *Journal of the Structural Division*, ASCE, 94, ST12, 1968, pp. 2999–3021.
- Civjan, S. A., C. Bonczar, S. F. Brena, J. DeJong, and D. Crovo. "Integral Abutment Bridge Behavior: Parametric Analysis of a Massachusetts Bridge," *Journal of Bridge Engineering*, ASCE, 12(1), 2007, pp. 64–71.
- Computers and Structures, Inc. (CSI) (2009). *SAP2000 Advanced 14.1.0 Structural Analysis Program*, Berkeley, CA. <<http://www.csiberkeley.com/>>
- Dunker, K. F., Master Engineer, Office of Bridges and Structures, Iowa Department of Transportation. Personal communication, May 2011.
- Dunker, K. F., and A. Abu-Hawash. "Expanding the Use of Integral Abutments in Iowa," *Proc., 2005 Mid-Continent Transportation Research Symposium*. Ames, IA, August 2005.
- Ensoft. *LPILE Plus 5.0 Geotechnical Analysis Program*, 2005. <www.ensoftinc.com>
- Fennema, J. L., J. A. Laman, and D. G. Linzell, "Predicted and Measured Response of an Integral Abutment Bridge," *Journal of Bridge Engineering*, ASCE, 10(6), 2005, pp. 666–677.
- Frosch, R. J., Professor of Civil Engineering, Purdue University. Personal communication, August 2011.

- Hassiotis, S., Y. Khodair, E. Roman, and Y. Dehne. "Evaluation of Integral Abutments," *Final Report*, FHWA-NJ-2005-025. Federal Highway Administration, Washington, D.C., 2006.
- Hassiotis, S., and K. Xiong. "Field Measurements of Passive Pressures Behind an Integral Abutment Bridge," *Proc., Seventh International Symposium on Field Measurements in Geomechanics*. American Society of Civil Engineers, 2007.
- Illinois Department of Transportation (IDOT) Bureau of Bridges and Structures. *Bridge Manual*, Springfield: Illinois Department of Transportation, 2009.
- Kim, W. and J. A. Laman. "Numerical Analysis Method for Long-Term Behavior of Integral Abutment Bridges," *Journal of Engineering Structures*. Elsevier, Vol. 32, 2010, pp. 2247–2257.
- Lukey, A. F., and P. R. Adams. "Rotation Capacity of Wide Flanged Beams Under Moment Gradient," *Journal of the Structural Division*, ASCE, 95 (ST6), 1969, pp. 1173–1188.
- Olson, S. M., J. H. Long, J. R. Hansen, D. Renekis, and J. M. LaFave. *Modification of IDOT Integral Abutment Design Limitations and Details*, Illinois Center for Transportation Research Report, ICT-09-054. Urbana: University of Illinois at Urbana–Champaign, 2009.
- Ribando, R.J., and G. W. O'Leary. "A Teaching Module for One-Dimensional, Transient Conduction," *Computer Applications in Engineering Education*, Vol. 6, 1998, pp. 41–51.
- Rollins, K. M., and T. E. Stenlund. "Laterally Loaded Pile Cap Connections," *Utah Department of Transportation Research Division Report No. UT-10.16*. Provo: Brigham Young University, 2010.
- Wasserman, E. P., Director of Civil Engineering, Structures Division, Tennessee Department of Transportation. Personal communication, May 2011.

APPENDIX A TIME-DEPENDENT EFFECTS OF CONCRETE SHRINKAGE ON IAB BEHAVIOR

The authors constructed a subset of additional 3-D FE models to examine the long-term effects of concrete shrinkage on the performance of Illinois IABs. The bridges modeled to include shrinkage were relatively long (400 ft) with 100-ft intermediate spans and were founded on HP14x89 piles oriented in accordance with the current IDOT standard. In addition to reference models that did not incorporate shrinkage, the shrinkage-model group consisted of two straight bridges and two with significant skews of 40°. We created two sets of models for each geometric configuration that used either W36x194 or 54-in. PPCI girders, respectively. For reference, key section properties of the girders are summarized in Table A-1. By comparing the numerical results of the models incorporating shrinkage for various load combinations with the corresponding shrinkage-free results from the reference models, we more clearly defined the extent that shrinkage affects IAB behavior and the structural mechanisms by which this occurs.

Section Property	Girder Type	
	W36x194	54" PPCI
Elastic Modulus, E (ksi)	29,000	4,769
Area, A (in ²)	57	599
Section Depth, d (in)	36.5	54
Strong-Axis Moment of Inertia, I _x (in ⁴)	12,100	213,721
Weak-Axis Moment of Inertia, I _y (in ⁴)	375	13,673
Torsion Constant, J (in ⁴)	22.2	15,146
Strong-Axis Radius of Gyration, r _x (in)	14.6	18.9
Weak-Axis Radius of Gyration, r _y (in)	2.56	4.78

Table A-1. Comparison of section properties for girders used in FE models considering concrete shrinkage.

In comparing the results of the shrinkage models with those without shrinkage, we observed that, consistent with the findings of Frosch (2011), shrinkage of the concrete deck generally caused pile moments to increase during thermal contraction and to decrease during thermal expansion. Shrinkage causes a net inward displacement of the abutments over the life of the IAB that adds to inward thermal contraction, while during thermal expansion, the net inward movement due to shrinkage must be overcome before net outward thermal displacement begins. Given that shrinkage occurs regardless of IAB temperature and is most rapid early in the structure's life, the relationship observed in our numerical modeling corroborates the field observations and analytical work by Frosch (2011) demonstrating a seasonal "ratcheting" increase in maximum contraction displacements for IABs with PPCI girders.

Figure A-1 compares the worst-case pile stress under varying load conditions for straight 400-ft bridges with W36x194 and 54-in. PPCI girders, respectively. It is apparent that while shrinkage affects both bridges, the magnitude of this effect is not equal. The PPCI bridge sees a more dramatic change in H-pile stresses caused by shrinkage than its steel girder counterpart. In fact, despite significant effects of shrinkage in the absence of thermal loading, the steel girder bridge sees virtually no net change in pile stresses after subsequent expansion or contraction. Of particular interest is the observation that, for the PPCI girder bridge, the typical controlling load combination of thermal expansion and live load (without shrinkage) identified by our main parametric study is surpassed by thermal contraction when shrinkage is also considered. In other words, at least for certain IAB configurations employing concrete girders, analysis of the

bridge for pile design should incorporate time-dependent behaviors such as shrinkage in determining the critical load combination.

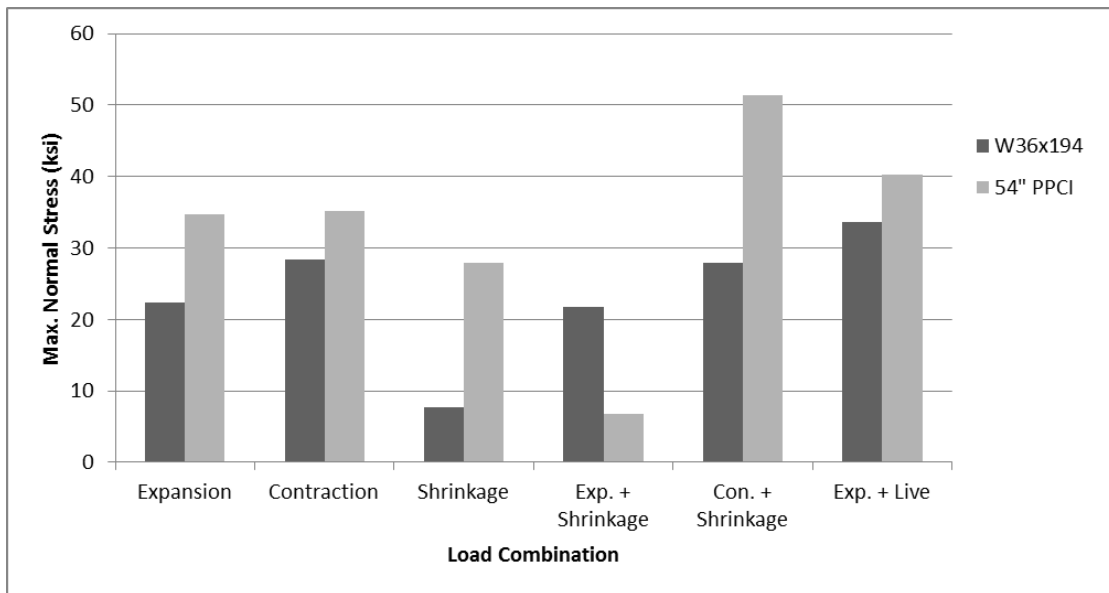


Figure A-1. Worst-case normal stress in HP14x89 piles for varying loading conditions, 4 x 100 ft span, 0°-skew bridge.

There are two factors that contribute to the disparity between the steel bridge and PPCI bridge results. First, in the steel girder bridge, the steel does not shrink. Therefore, axial resistance to deck shrinkage develops in the girders as a result of the composite bond between the two superstructure components. However, in the PPCI girder bridge, the girders shrink with the deck, albeit at slightly different rates. The resistance of the concrete girders to deck shrinkage, therefore, is less, and greater abutment displacements develop. Secondly, the rotational restraint between the abutment and girders impacts the extent that shrinkage displacements at the deck elevation are translated into corresponding displacements at the pile heads. Because the bending stiffness of the PPCI girder is many times higher than that of the W36 girders, the abutment rotates considerably less when undergoing the same shrinkage-driven displacement. This, in turn, results in greater pile-head fixity and higher pile moments.

Figures A-2 and A-3 track how displacement and rotation at the bottom of the bridge abutment vary under differing load combinations; comparing the differences in these values between the PPCI and W36 bridges (along with the changes in stress noted previously) sheds further light on the mechanisms that cause this behavior. With pre-cast girders, abutment rotation caused by shrinkage (and all other loads) is smaller; thus, shrinkage-induced displacements are transmitted more directly to the piles by the relative rigidity of the abutment. Furthermore, the contraction case stresses are larger than expected, while stresses in the expansion case are relieved when the respective rotations and displacements of the two cases are sequentially added together. In steel girder IABs, expansion rotations counteract those induced by shrinkage, leaving very little net rotation at the point of maximum expansion displacement. Thus, despite lower total displacement, the pile-head fixity is very high, and pile stresses are virtually the same. In contraction, the converse is true; despite higher total displacement, the additional rotation (and loss of pile-head fixity) reduces moments at the pile heads.

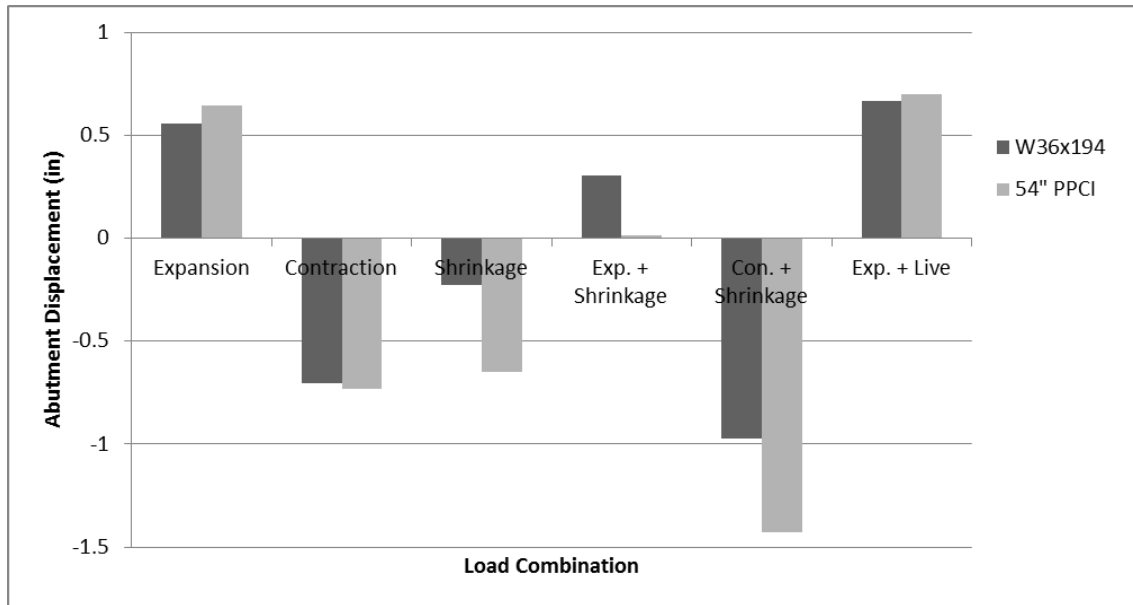


Figure A-2. Centerline longitudinal displacements at bottom of abutment for varying loading conditions, 4 x 100 ft span, 0°-skew bridge with HP14x89 piles.

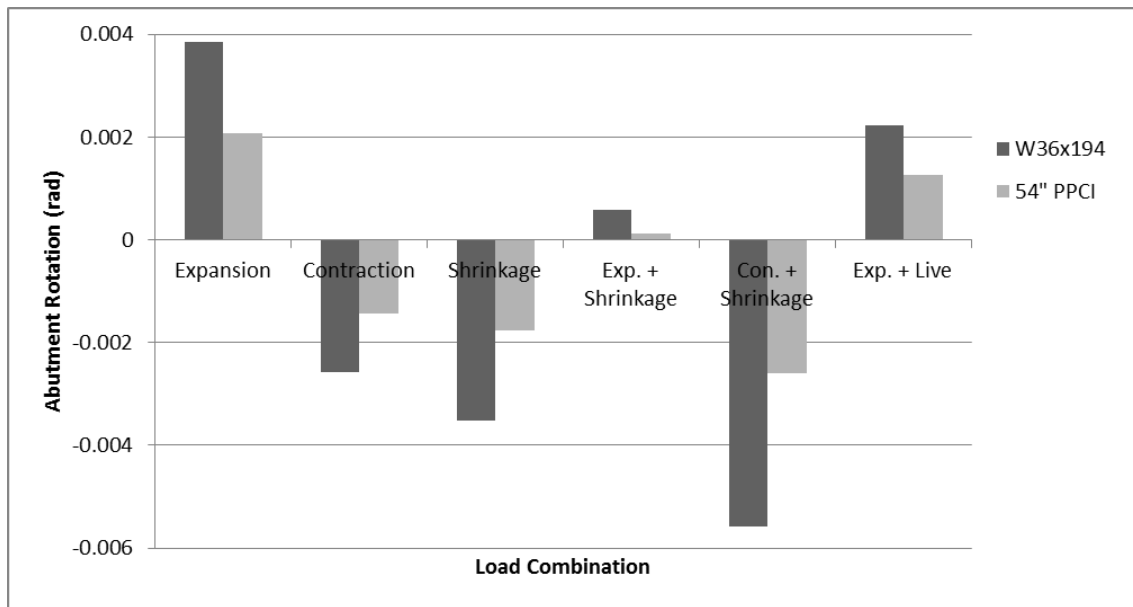


Figure A-3. Centerline primary rotations at bottom of abutment for varying loading conditions, 4 x 100 ft span, 0°-skew bridge with HP14x89 piles.

Figure A-4 demonstrates how pile stresses vary for similar loading combinations in a high-skew bridge. Though the general patterns of behavior are the same, in skewed bridges, shrinkage movements involve strongly 3-D characteristics, similar to thermal displacements. As a result, the rotational flexibility of the abutment-superstructure interface in skewed bridges, particularly for steel girder systems, tends to further dilute the impact of shrinkage displacements on pile loadings. Again, our study assumed a rigid interface between the girders and the abutment; in reality, this connection is semi-rigid. Because the 3-D rotational restraint of

the abutment by the superstructure is the most significant influence on the extent that shrinkage displacements affect the piles, more accurate modeling of the rotational stiffness of this connection may reduce shrinkage effects, especially in PPCI bridges where the girder bending stiffness is very high.

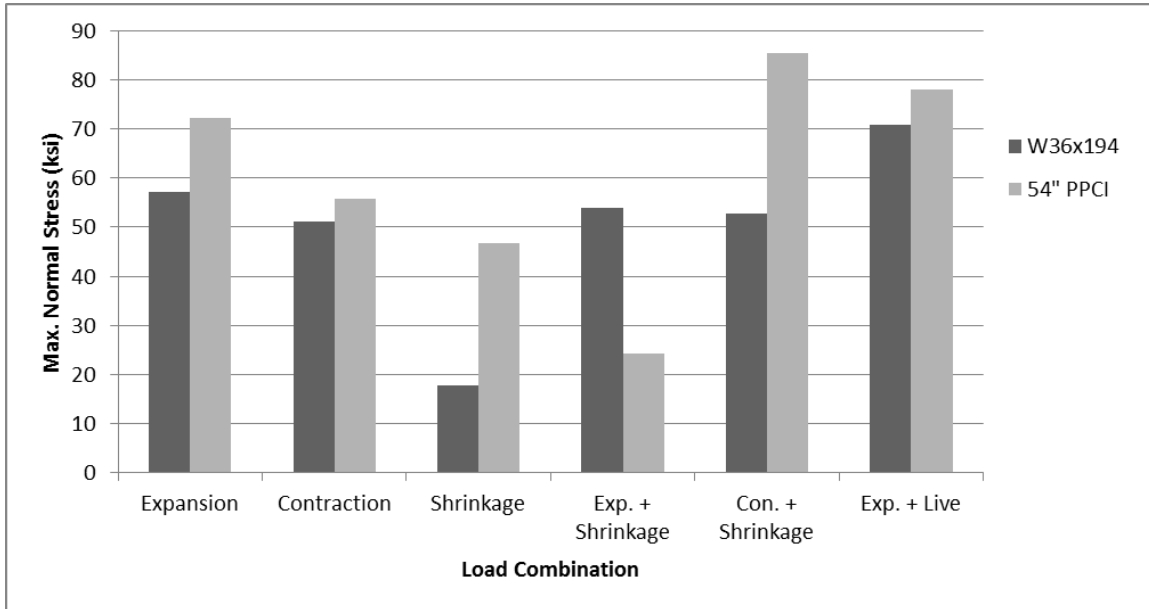
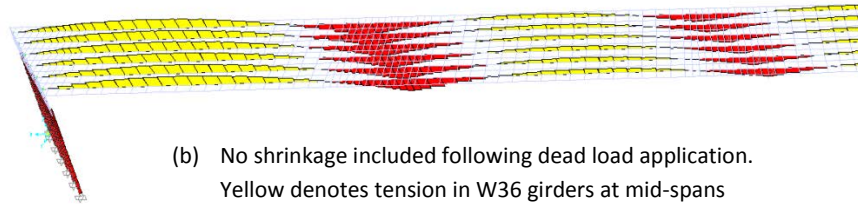


Figure A-4. Worst-case normal stress in HP14x89 piles for varying loading conditions, 4 x 100 ft span, 40°-skew bridge.

We noted one additional significant effect on IABs caused by shrinkage: Significant axial compression is generated in the bridge girders when the deck shrinks, particularly in steel girder systems. Figure A-5 illustrates how, as an IAB shortens from shrinkage of the concrete deck, the axial force distribution in the bridge exhibits a tendency toward net compression throughout the structure. In our relatively simple superstructure models, these forces vary greatly throughout the bridge based on IAB configuration, and they can be on the order of hundreds of kips. Our linear-elastic, fully composite FE superstructures likely incompletely address the issue. A more comprehensive evaluation of axial compression in IAB girders caused by shrinkage should incorporate material non-linearity in the steel and concrete, along with a more realistic approach to modeling the composite interface of the girder and deck system that accounts for deformation of the shear connectors and cracking in the concrete deck. More detailed analyses such as these are beyond this project scope, but they may reveal that a significant portion of the predicted shrinkage-induced axial load in the girders never develops because much of the imposed deformation is absorbed by localized plasticity in the shear connectors and systematic cracking of the surrounding deck concrete.



(b) No shrinkage included following dead load application. Yellow denotes tension in W36 girders at mid-spans with red indicating compression developing over intermediate supports.



(a) Shrinkage included following dead load application. Shrinkage imposes a net compressive force throughout the W36 girders, essentially offsetting the axial force diagram in (a). Largest compression still occurs over the intermediate supports.

Figure A-5. Isometric views of axial force results in 40°-skew steel girder models immediately prior to thermal load initiation.

Even from the limited set of analyses conducted by the project team, it is evident that time-dependent behaviors such as shrinkage are worthy of further consideration in research and design for Illinois IABs. In some bridge configurations, specifically those utilizing PPCI girders, the effects of concrete shrinkage were significant enough to change which thermal loading combination proved most critical for the foundation piles. Additionally, we discovered that significant axial force is induced in the superstructure (namely, the girders) because of concrete shrinkage; this could be a significant concern in the design of steel girders for IABs.

APPENDIX B EFFECTS OF PLASTIC DEFORMATION IN H-PILES ON IAB BEHAVIOR

In an effort to further probe the potential benefits of incorporating plastic deformation of pile steel into Illinois IAB design, the authors conducted a small subset of analyses incorporating material non-linearity (i.e., yielding) of H-piles in the 3-D FE bridge models. Our objectives were to verify that significant load redistribution occurs across the pile group in skewed bridges and to observe whether pile loads are reduced by the decrease in pile stiffness with plastic deformation. We achieved this by comparing the FE results for IAB models accounting for pile steel yielding with results from corresponding linear-elastic models.

B.1 MODELING OF H-PILE PLASTICITY

In order to determine the significance of pile plasticity on skewed IAB behavior, we chose to consider yielding in the diminutive HP10x42 piles, used in 600-ft-long bridges at 0° and 60° skews. By examining these extreme configurations within our modeling scope, we gained a rough sense of the maximum effects of pile plasticity in an IAB. In addition to modeling the H-piles in the standard IDOT orientation, we also considered plasticity for such bridges using strong and weak-axis alternate pile orientations with the webs parallel and perpendicular to the bridge longitudinal axis, respectively.

In SAP 2000, plasticity in frame elements is accommodated by the addition of discrete plastic hinges of a finite length along members or at connections where yielding is expected. We added a series of four, 3 in.-long plastic hinges at the top of each pile. With four hinges in the frame elements through the top 12 in. of the pile, the model can roughly approximate the changing amount of plasticity in the member with depth. The changes in stiffness, deformation, and loading caused by yielding in the hinges are analytically linked with the frame element in the FE model; this permits SAP to track the global effects of yielding in the hinges throughout the bridge at each step in the non-linear loading sequence.

While several types of plastic hinges are available in SAP 2000, we elected to use a discrete fiber hinge in our analyses. In order to numerically simulate H-pile yielding, the fiber hinges rely directly on the non-linear stress-strain relationships of the materials assigned to them and the geometry of the fiber discretization. This offered us several advantages for the approximation of pile plasticity we sought to capture in our modeling effort. First, unlike other SAP 2000 hinges requiring detailed non-linear curves for the interaction of axial load deformation and weak- and strong-axis moment-rotation behavior of the pile cross-section, the fiber approximation of the cross-section automatically accounts for these interacting loads. This is especially beneficial in the case of Illinois IAB piles because the significant change in axial load with temperature variation makes this load interaction path-dependent. Also, the constraint on global and local buckling in the H-piles provided by the surrounding concrete and soil makes empirical equations for predicting biaxial moment-rotation behavior under axial load inapplicable. Additionally, a fiber section model captures results for the average stress in each fiber during the analysis, permitting the user to examine gradients of stress across the section in addition to the global loading, deformation, and rotation of the hinge.

In the case of our HP10x42 piles, the material was represented by SAP 2000's default non-linear tensile and compressive relationships for A992 steel, illustrated in Figure B-1. In the 3-in. hinges, the HP10x42 cross-section was represented by 43 discrete A992 fibers, each with an area and position selected so as to mimic the stiffness and geometry of the actual member as closely as possible. The 43-fiber configuration allowed reasonably close approximation of the

cross-section without undue addition of computation time; it also allowed some examination of stress gradients across the width and through the depth of the H-pile flanges.

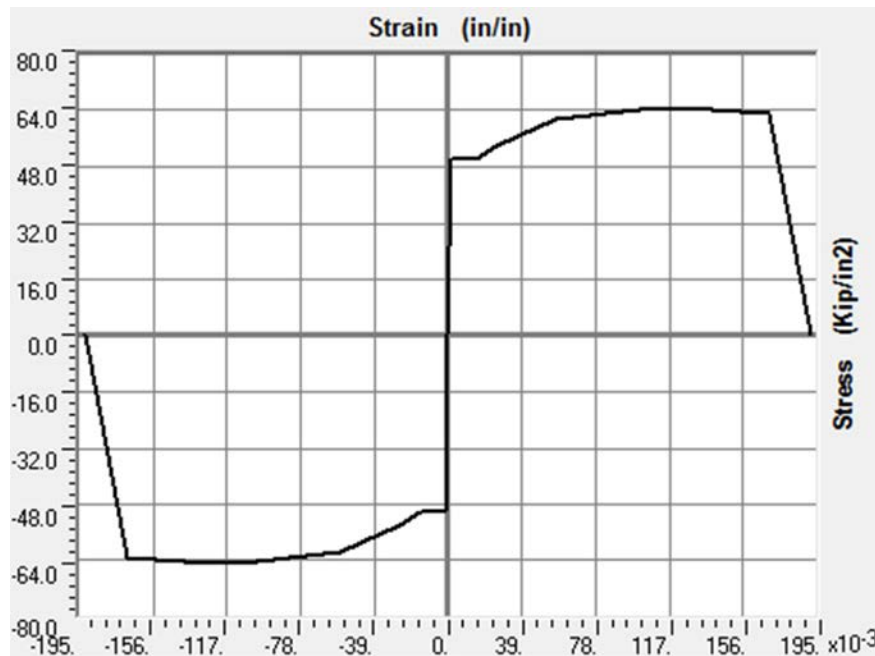


Figure B-1. SAP 2000 plot of axial stress-strain relationship for A992 steel ($F_y = 50$ ksi).

B.2 COMPARISON OF PLASTIC AND ELASTIC RESULTS

The authors analyzed the FE models incorporating H-pile yielding under identical thermal loading conditions to their linear-elastic counterparts. In order to examine the possibility of load redistribution across the pile group in the skewed configurations, we compared the load components induced in each pile of one abutment of the plastic and elastic models at the conclusion of the thermal expansion load case (without live load). The acute corner pile, which in the main parametric study repeatedly tended to attract the worst-case loading, is designated as pile number 1 in the group, with the pile designation increasing as the piles get further from the acute corner. The obtuse corner pile is designated as pile number 6.

We observed two primary effects of pile steel yielding in the analyses. First, the moments in the H-piles were significantly lower in the FE models incorporating plasticity. The decrease in bending load was generally largest in the degree(s) of freedom predominant in the elastic model (e.g., weak-axis bending for the 60° skew IDOT orientation bridge). The overall reduction in bending resistance versus elastic modeling was present in the skewed configuration for all pile orientations. However, only the weak-axis alternate orientation registered significant plasticity (and a corresponding drop in resultant bending resistance) in the non-skew configuration. The 0° skew IDOT/strong-axis orientation model did not pick up the substantial yielding in the flanges predicted by the elastic model.

The second effect we observed in the skewed models was noticeable load redistribution present in all three loading degrees of freedom. Load redistribution occurred in differing amounts depending on H-pile orientation, but in all cases, some of the load typically drawn to the acute corner of the skewed bridges was picked up by the rest of the pile group after the

onset of yield. Figures B-2 through B-4 compare the loading components in the foundation pile group for both the plastic and elastic FE models using the standard IDOT H-pile orientation. Figures B-5 through B-7 provide similar comparisons for models utilizing the strong-axis alternate pile orientation, which has more balanced weak and strong-axis bending components. For reference, it is helpful to recall that the weak and strong-axis yield moments for a HP10x42 pile are 710 k-in and 2,170 k-in, respectively, with $F_y = 50$ ksi and no axial load applied.

In the 60°-skew IDOT orientation model, the greatest difference in the magnitude of the load and largest redistribution across the pile group occurs in the weak-axis bending component. This is reasonable considering the high skew of the bridge. In addition to the roughly 40% decrease in weak-axis moment in the plastic model, we note that the 250 kip-in gradient from the acute to obtuse corner in the elastic model virtually disappears when pile yielding is permitted. Similar load redistribution occurs in the other degrees of freedom; the elastic gradients all shift down in severity to relieve the worst-case pile for the degree of freedom in question. Also, because of the high skew, results for the weak-axis alternate orientation are highly congruent with those of the IDOT orientation; they are therefore omitted.

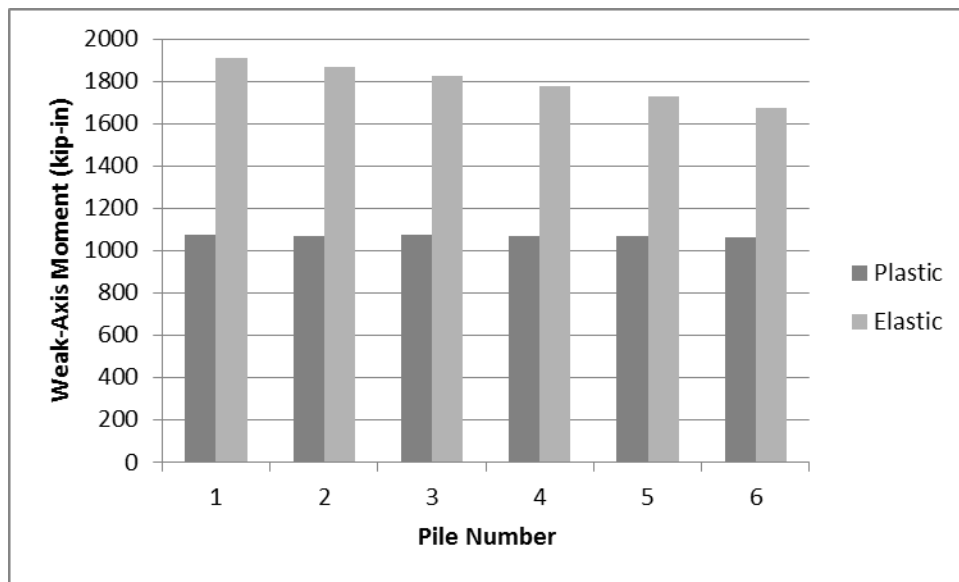


Figure B-2. Comparison of weak-axis moment at top of HP10x42 piles: 6 x100 ft span, 60°-skew IAB, IDOT orientation.

When we revised the pile orientation such that the H-pile webs were parallel to the bridge longitudinal axis (i.e., strong-axis alternate orientation), we observed similar trends in the load components. However, because both bending degrees of freedom were significantly loaded in the alternate orientation, we observed major reductions in weak and strong-axis moments and substantial load redistribution across the pile group.

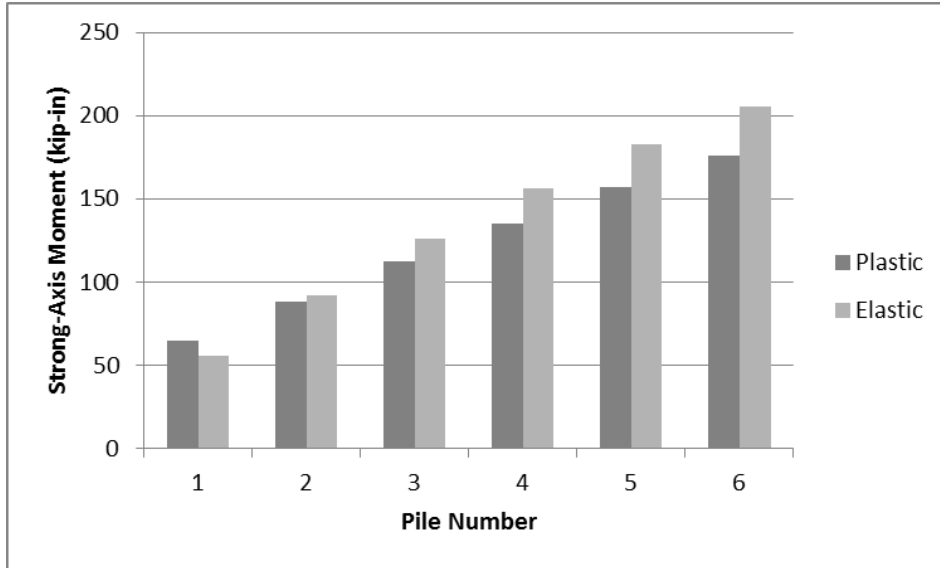


Figure B-3. Comparison of strong-axis moment at top of HP10x42 piles: 6 x100 ft span, 60°-skew IAB, IDOT orientation.

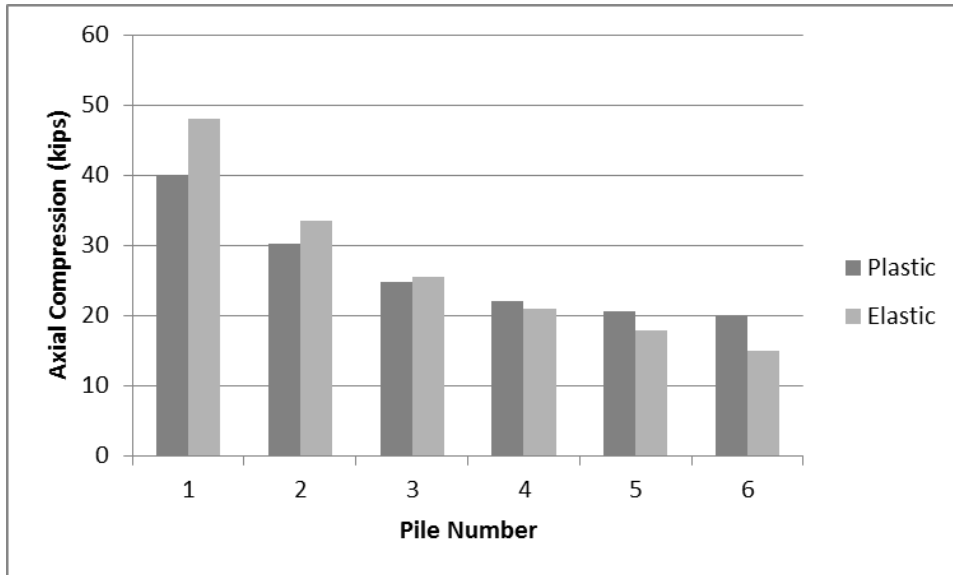


Figure B-4. Comparison of axial compression at top of HP10x42 piles: 6 x100 ft span, 60°-skew IAB, IDOT orientation.

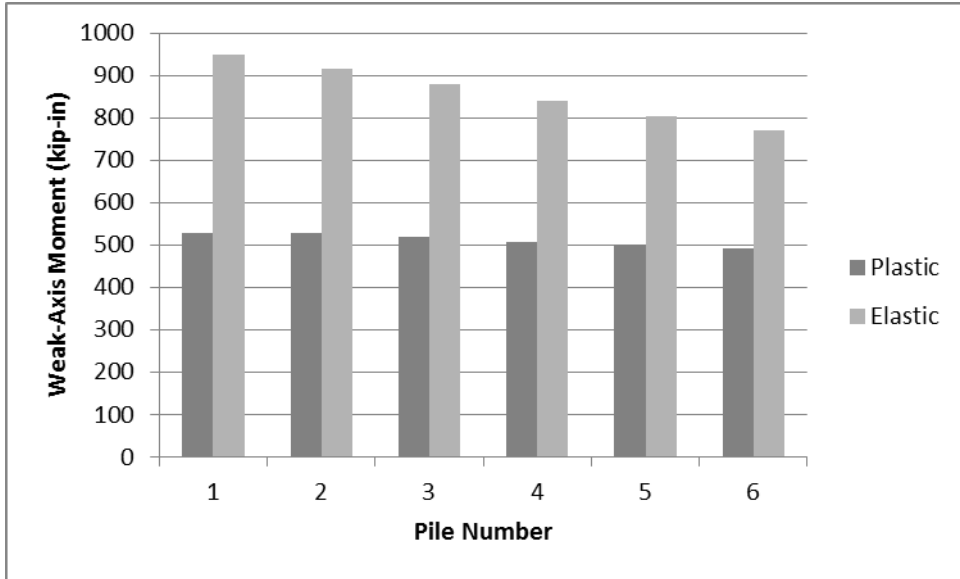


Figure B-5. Comparison of weak-axis moment at top of HP10x42 piles: 6 x100 ft span, 60°-skew IAB, strong-axis alternate orientation.

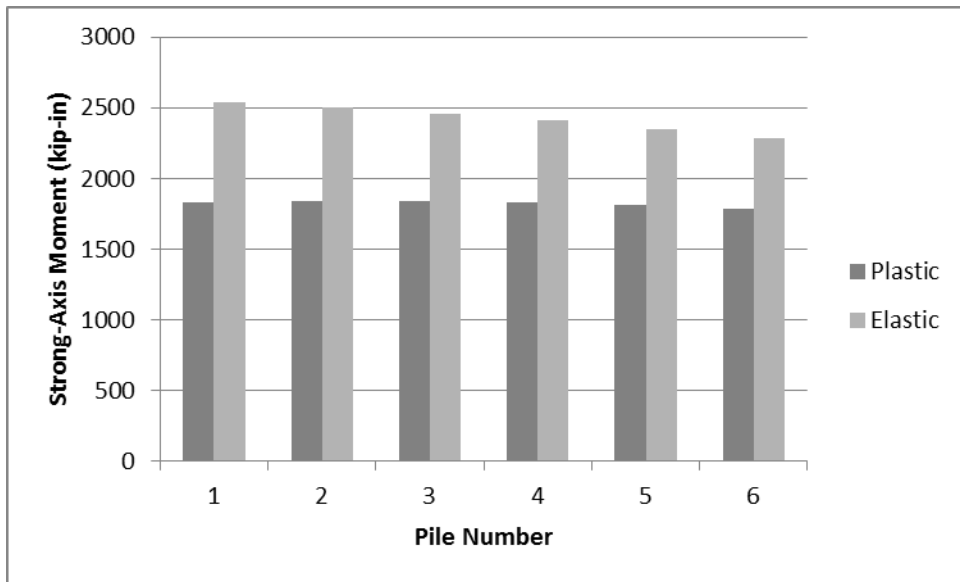


Figure B-6. Comparison of strong-axis moment at top of HP10x42 piles: 6 x100 ft span, 60°-skew IAB, strong-axis alternate orientation.

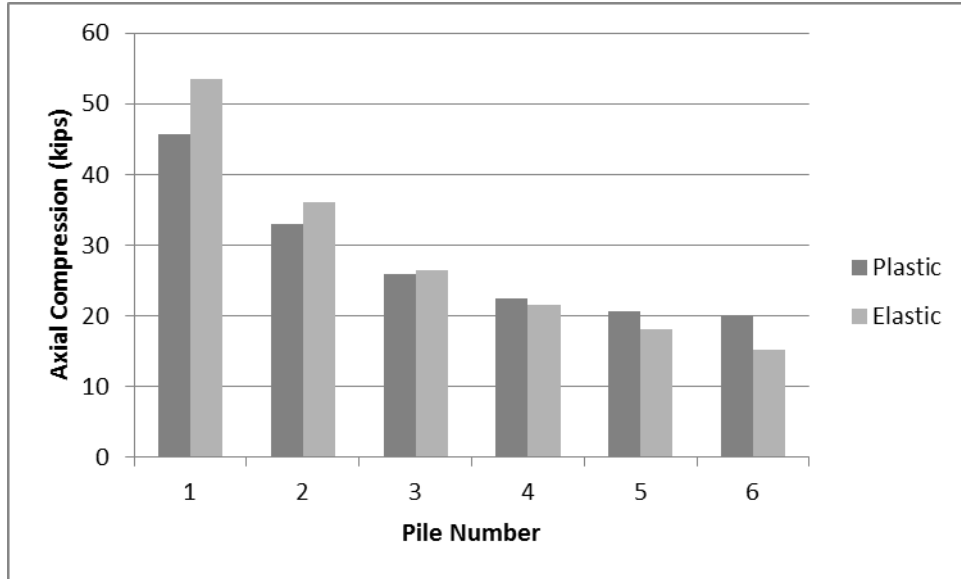


Figure B-7. Comparison of axial compression at top of HP10x42 piles: 6 x100 ft span, 60°-skew IAB, strong-axis alternate orientation.

In general, the observed load redistribution in skewed bridges may be understood as the natural shifting of the foundation system's response to thermal expansion, as the critical pile initiates yielding, to even out the resistance among the piles. However, the substantial overall drop in moment induced in the plastically deforming piles during thermal movement requires additional explanation. Figures B-8 and B-9 provide some helpful insight into the mechanism for this behavior as it is exhibited in the 60°-skew IDOT orientation model; though the displacements of the pile heads are roughly the same with or without yielding, much higher rotation occurs in the plastic model. As the top of the pile begins to yield, its stiffness degrades, and it begins to experience localized inelastic rotation. The plasticity in the H-pile flanges increases the flexibility of the pile-abutment interface as expansion continues, and the result is that the moments attained at the end of the thermal movement are substantially lower. The extra rotation at the pile head caused by plastic deformation essentially degrades the fixity of the connection as loading continues, and the load accumulates at a slower rate than in the elastic model.

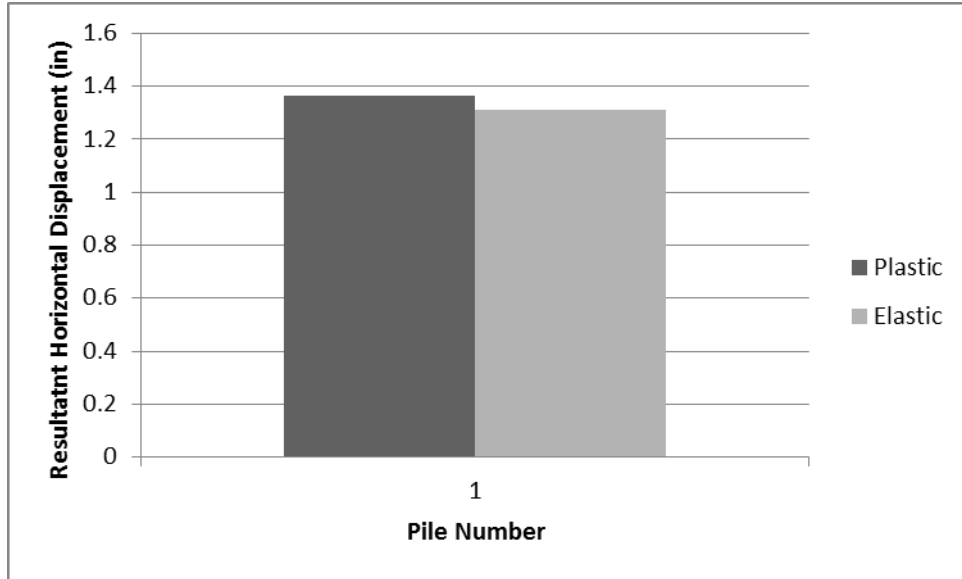


Figure B-8. Comparison of resultant displacement at top of acute pile: 6 x100 ft span, 60°-skew IAB, IDOT orientation.

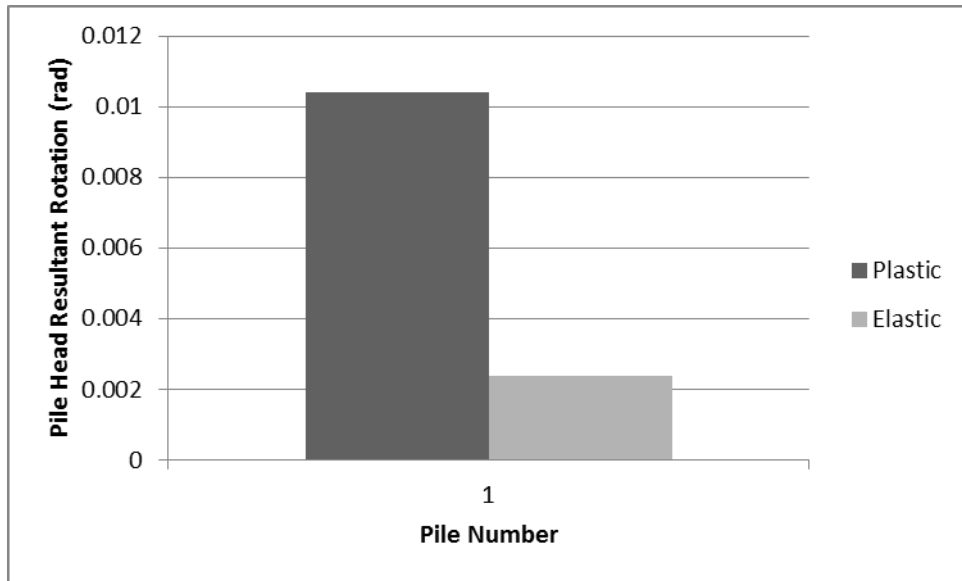


Figure B-9. Comparison of resultant rotation at top of acute pile: 6 x100 ft span, 60°-skew IAB, IDOT orientation.

The fiber discretization of the H-pile cross-section allowed the authors to examine the approximate extents of the plasticity throughout the section, and the series of hinges in the top 12 in. of the pile permitted rough observations of how plastic deformation changed with depth along the pile. We noted that in all three orientations considered in the models, the maximum stress in any fiber was roughly 50 ksi (i.e., F_y). In none of the plastic models did the entire cross-section reach yield, making a full plastic hinge. However, typically only a relatively narrow band of fibers along the effective neutral axis of the section remained in the elastic range; the

piles were stressed very near their plastic capacity. Because full plastic hinging did not occur in any model, the critical A992 steel fibers tended to remain near the yield plateau of the material, and no stress increase caused by strain hardening was observed. In fact, because of load redistribution, it is possible that maximum stresses in IAB piles will remain close to the yield point until the entire pile group has fully yielded. This is promising for IAB design because localized plastic damage in the critical pile(s) under thermal service loads will likely leave plenty of reserve capacity and ductility in the pile group for extreme overload situations.

Figure B-10 illustrates the difference between the elastic and plastic biaxial bending capacities of an HP10x42 under an axial load of 46 kips when buckling failure modes are neglected. This axial load corresponds to the maximum axial compression force observed in our 6 x 100 ft. span, 60°-skew IAB model in the strong-axis alternate pile orientation. The bounding elastic and plastic moment capacities are based on the yield stress for A992 steel ($F_y = 50$ ksi). A simple linear interaction suffices to identify the biaxial yield capacity, but the plastic capacity of a beam-column in biaxial bending is considerably more complicated. For a beam-column without the possibility of local instability (such as our well-confined H-piles), a 3-D non-linear interaction surface, manifested as a biaxial moment interaction curve for a given axial load, describes the plastic strength of the member (Chen and Santathadaporn 1968). Figure B-10 includes an approximation of such a curve for the HP10x42 section; as axial load increases, the plastic moment capacity in each direction decreases. This causes the area beneath the interaction curve to diminish and its shape to change. Also plotted on this chart is the maximum loading combination in the acute pile of our inelastic model. Though the piles in this model significantly yielded, the stresses in our fiber hinge model closely align with the interaction curve's prediction that only slightly more strength remains before the full plastic hinge forms. Interestingly, according to Burdette et al. (1999), even if the bounds of the plastic strength curve were reached, axial and moment resistance in the piles would not drop. Any further thermal displacement would be handled by additional inelastic rotation at the full plastic hinge and strain hardening in the steel, leaving significant remaining ductility to address overload scenarios.

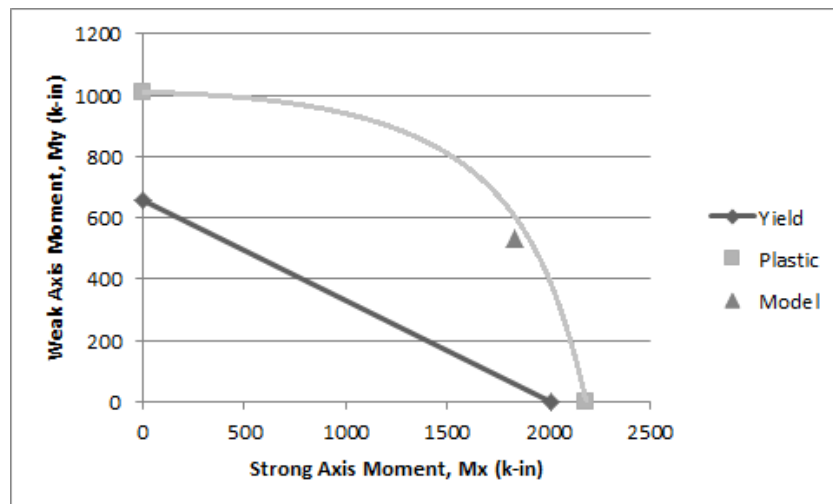


Figure B-10. Biaxial moment strength capacity interaction diagrams for HP10x42 subjected to 46 kips of axial compression and acute pile load combination result from 6 x 100 ft span, 60°-skew IAB, strong-axis alternate orientation model.

The distribution of yielding throughout the cross-section varied between the IDOT orientation and the strong-axis alternate orientation in the 60°-skew models. In the IDOT orientation, the predominance of weak-axis bending resulted in yielding of virtually all fibers in the flanges of the HP10x42, while the web generally remained well below yield. Yielding initiated in the tips of the flanges; and as thermal expansion increased, it spread toward the centerline of the section. Depending on the location of the pile in the group and the corresponding degree of eccentricity in the interaction of the axial force and biaxial moment components, the ends of the web also began to yield on some piles. In the strong-axis alternate case, where the H-pile webs were oriented parallel to the bridge longitudinal axis, the yielding distribution was much different. Owing to the more balanced levels of strong- and weak-axis bending, yielding did not necessarily initiate at all four flange tips, often occurring only in two flanges. As a result of the greater biaxial nature of the load, yielding often spread well into portions of the web, while parts of two flanges remained in the elastic range. In short, the section remained elastic in a diagonal band parallel to its effective neutral axis under the biaxial bending. The angle of this effective neutral axis varied considerably depending on the position of the pile along the highly skewed abutment.

The authors also observed that, consistent with the nearly fixed-head pile conditions, yielding in the piles was concentrated near the abutment-pile interface where moments were greatest for all cases considered. However, as yielding began spreading throughout the cross-section in the top 3 in. of the pile with increasing thermal displacement, it also began to spread further down the pile away from the abutment connection. We also recorded significant yielding in each pile from 3 in. to 6 in. below the abutment, but the yielding in this region initiated later in the load history and was less extensive than at the top of the pile, as we expected. Beyond 6" below the abutment, the authors observed little to no yielding in the plastic hinge fibers in the IDOT and strong-axis alternate orientations, and only minor yielding in the weak-axis alternate orientation models up to about 12 in. below the abutment.

Based on our limited analyses, the continuous structural nature of Illinois IABs seems to promote well-behaved plastic deformation in H-piles. Because 3 ft of concrete encasement and the embankment soils substantially restrict buckling failures at the tops of the piles, inelastic deformation to the H-piles tends to have the opportunity to redistribute itself. The plasticity may initiate at the acute corner pile in a skewed bridge, but the IAB continues to gradually shift its response to the increasing thermal load such that the plasticity is shared across the pile group and down the length of the piles instead of concentrating itself in the form of excessive damage and buckling at the top of the acute corner pile. Additionally, by spreading the plasticity across the whole foundation group, the added inelastic rotation permitted in the system reduces the overall resistance developed in not only the piles, but the loads induced throughout the rest of the structure as well (e.g., the axial compressive forces in the superstructure). This effect is significant in both skewed and non-skewed IAB configurations. So long as yielding in the foundation piles is controlled, intentionally permitting some plasticity in IAB design may facilitate improved bridge length and skew limitations.

B.3 INCORPORATING PILE PLASTICITY IN IAB RESEARCH AND DESIGN: CONCLUSIONS AND RECOMMENDATIONS

From our limited subset of FE analyses incorporating yielding of the HP10x42 piles on straight and highly skewed IABs of significant length, we developed some quantitative evidence of behaviors suspected during our linear-elastic parametric study. In bridges where significant yielding occurs at the tops of the foundation piles, a portion of the load predicted by elastic analysis never develops because the plastic deformation permits additional rotation near the pile-abutment interface, reducing the effective stiffness of that connection. Also, in skewed IABs,

plasticity beginning in the acute corner pile causes some redistribution of the load throughout the pile group as the thermal displacements continue to increase. This limits the extent of localized damage on the critical pile; the IAB's response adjusts to more evenly load the foundation.

Given the inherent eccentricities and asymmetries in the responses of real IABs, it is likely that some pile yielding already may occur in some Illinois IABs based on our elastic parametric study. Our current analyses show that this fact should cause minimal concern for IDOT. Any minor yielding that occurs in existing Illinois IABs likely follows the well-controlled behaviors and mechanisms outlined above. The author's analyses exploring non-linearity in the pile steel should add confidence in the performance of the existing stock of IABs in the state.

Though our rudimentary plastic analyses in SAP 2000 are adequate to illustrate and provide some evidence of the potential effects and benefits of permitting yielding in IAB pile steel, they are limited in their accuracy and scope. While our models with small piles, high skews, and long superstructures produced reasonable results in line with the authors' expectations, other IAB geometries modeled using a similar approach failed to yield meaningful results. Specifically, the coarse mesh of fiber hinges used may not have been appropriate to pick up yielding in other bridge configurations, even if the corresponding elastic model predicted stresses well beyond yield. A more fundamental issue is that exploring the 3-D complexities of non-linear plastic pile deformation in skewed IABs stretches the abilities of the models created in this project scope. Our SAP 2000 models of the IAB superstructures, abutments, piles, and their connections simplify the structure as a system of rigidly joined frame and shell elements, and consequently, they are capable of only a rough approximation of localized plastic deformation in the bridge piles. A more detailed exploration of pile plasticity, load redistribution, and connection fixity at the pile-abutment interface may require a more appropriate tool, such as FE continuum modeling. The authors recommend that such models be incorporated into subsequent Illinois IAB research.

In short, our analyses demonstrate that by permitting considerable plasticity in the foundation piles of very long IABs, the piles used in the design of such bridges may be appreciably smaller than those required to ensure linear-elastic behavior in the pile steel. As long as the plastic deformation is limited such that a full plastic hinge does not develop, the pile stresses should remain close to F_y , and most of the plastic capacity and ductility will remain available for other extreme load events.

A better understanding of how yielding affects Illinois IABs may increase confidence in plastic design, permitting even more extensive variation in the configurations of bridges that may be constructed integrally in Illinois and across the country. Given that several other states already account for pile yielding in design, and some full-scale tests have successfully demonstrated that the vertical load capacity of H-piles confined by soil is undiminished even after significant plastic hinging caused by lateral loading (Burdette et al. 1999), the benefits of plastic design in Illinois IABs may be considerable.

APPENDIX C STRAIN GAGE INSTALLATION AND CALIBRATION DETAILS

C.1 INSTRUMENT CALIBRATION

All Geokon instruments were calibrated at the factory prior to shipment. Technicians calibrate strain gages in pre-production annually indicating that individual calibrations vary only by a nominal batch factor. Technicians calibrate vibrating wire temperature sensors and MEMS tiltmeters fully in the laboratory and ship each instrument with a calibration report, including several factors that are later programmed into the data logger or data readout box.

C.2 STRAIN GAGE WELDING PROCEDURES

Each strain gage includes mounting blocks, set screws, the instrument, and the coil housing. Mounting blocks securely hold the gage to the H-pile flange. Set screws, located in the mounting blocks, secure the instrument to the mounting blocks. The instrument is a thin cylindrical tube that contains the tensioned vibrating wire. The coil housing is a slotted cylindrical mold that fits securely over part of the instrument. The coil housing transmits the “plucking” voltage to the instrument and relays the vibrating wire frequency back to the data-acquisition system.

The mounting blocks are installed first by welding the blocks to the H-pile flange. This process is facilitated with a prefabricated welding jig and a spacer bar. A certified welder arc-welded the mounting blocks in place with three welding passes (to minimize temperature-induced strains in the flange): one pass on the block side facing the beam web, one pass opposite the web, and one pass on the outer face of the mounting block. No welding takes place at the interior face of the mounting block per Geokon recommendations. In addition, ¼-in. square nuts were welded to the flanges at regular intervals to act as guides for the strain gage cables.

Following the welding process, the strain gage instruments are installed into the mounting blocks, and the set screws are used to secure the instruments in place. The set screws are then epoxied to prevent loosening. Following this process, the coil housings are epoxied in place and further secured with a hose clamp. All strain gage wiring was zip-tied to the ¼-in. nuts as a bundle to protect the wiring during additional installation. A completed installation is illustrated in Figure C-1.

To prevent damage during pile driving, L2.5x2.5 angle irons were welded along a 16-ft length of the instrumented flanges. One-in.-long spot welds were placed every 10 in. in the strain gaged portion of the flange, and these spot welds were increased to 3”-long below the strain gages. All welds were staggered to minimize temperature-induced straining in the piles. Exit slots were cut into the angle irons 2 ft below the top to allow strain gage cables to exit. Finally, a tapered end-cap was installed at the bottom of the angle iron to prevent soil plugging during pile driving. Figure C-2 illustrates the angle iron installation.

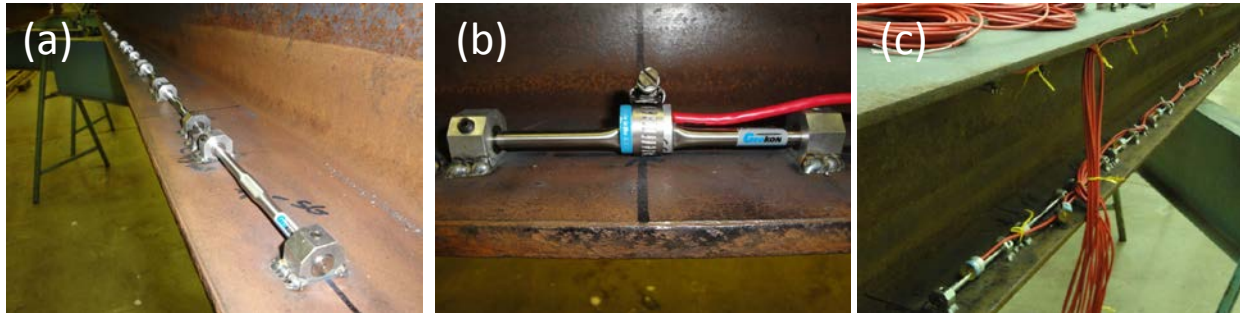


Figure C-1. (a) Strain gages installed in mounting blocks. (b) Coil housing installed on strain gage. (c) Completed strain gages along H-pile flange.

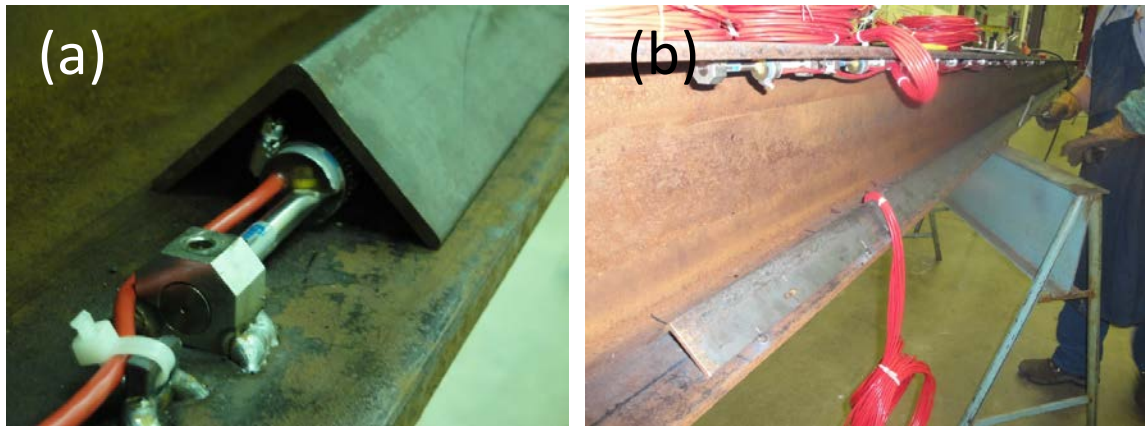


Figure C-2. (a) Angle iron installed over strain gages. (b) Cables extending out of angle iron.

C.3 INCLINOMETER HOUSING INSTALLATION

A protective L3.5xL3.5 angle iron was welded to the full length of the pile to house the plastic inclinometer casing (2.75-in. OD). This angle iron housing is illustrated schematically in Figure 33. Approximately 2 in. of angle iron was cut from one side (over the upper 16 ft where the strain gage protection is located) to facilitate installation. The inclinometer housing angle iron then was welded to the pile flange and web using 3-in.-long spot welds every 10 in. Near the strain gages, the spot welds were decreased to 1-in. long.

After pile driving, the inclinometer casing was installed and the casing was grouted in place.

C.4 LABORATORY LOAD TESTING

Laboratory tests were performed on the instrumented piles following strain gage installation to “exercise” the strain gages and remove any residual stresses induced during installation by high welding temperatures. Further, the addition of angle iron to the foundation pile to protect strain gages and house the inclinometer casing inevitably affected the properties of the pile. Particularly, the pile moment of inertia increased significantly. To quantify the increase, an adjusted moment of inertia was calculated for the pile from strain readings in the strain gages during testing.

